

# The Radio and Electronic Engineer

The Journal of the Institution of Electronic and Radio Engineers

## Millimetric Waveguides for Telecommunications

THE recent announcement that the British Post Office is to install, as part of its public trunk network, a millimetric waveguide link between Bristol and Reading (a distance of about 130 km) is a significant technological milestone. For it is almost exactly thirty years since, at the 1947 Radio Convention of this Institution in Bournemouth, Professor H. M. Barlow read a paper entitled 'The exploitation of microwaves for trunk waveguide multichannel communications': the Bristol-Reading link, to be in service in the early 1980s, will be the first commercially practical realization, certainly in this country if not in the world. The phrase 'commercially practical' reflects the view of the Post Office that this £7M scheme is virtually a 'no-risk' enterprise, and although the necessary economic and technological assessment has certainly not taken three decades, this confidence in the undertaking justifies the careful process of assessment during the past 10-15 years.

It is interesting today to read Professor Barlow's original paper (published in the Journal for October 1947) and to note how clearly important features of the Post Office's project were forecast and analysed. Recalling that he was writing in the pre-transistor era—and the present day scheme has largely been brought to fruition by many new advances in semiconductor techniques—even the basic 'block diagram' is a good prediction of today's accomplishment. Much basic work on millimetric waveguides was subsequently directed by Professor Barlow under a Post Office contract given to his Department at University College London to investigate techniques in the laboratory and using an experimental link at what is now the Post Office's Research Centre at Martlesham.

As a result of this UCL work, described in a series of papers which appeared in the 'sixties, extensive development work was started at the new Centre. This has included a field trial, to gain experience of how such a system operates in typical conditions, over a 14 km link from Martlesham to Wickham Market, and industry has been closely involved in the necessary development of suitable waveguide, sharp bends, joints and termination techniques, as well as the terminal and repeater equipment. The concept of a 50 mm diameter circular guide, operating in the 'fast' wave  $TE_{01}$  mode in the region 35 to 110 GHz, and with 80 multiplexed channels, each of capacity of about 500 Mbit/s, indicates the magnitude of some of the technical problems which have been solved.

Inevitably, in any discussion of the technological options in establishing a high capacity telecommunication network, both multiplex 'conventional' coaxial cables and optical fibres must also be considered. Only this month the final stage was announced of a £9M project for a 383 km London-Reading-Birmingham-Manchester link using what is claimed to be the world's largest cable with eighteen 2.6 mm/9.5 mm coaxial pairs, each carrying a 60 MHz system of 10,800 telephone circuits potential.

Optical fibre communication is a technique which is barely ten years from its conception, and it has already made impressive progress. The achievement of fibres with attenuations that can be realistically coped with in a communication system has confounded many of those who doubted whether the almost astronomical attenuation figures of the early fibres could be overcome. Termination and jointing problems have been largely solved but it is still preferable to avoid joints—hence relatively short, single-fibre links, avoiding joints and repeaters, are desirable. Present indications are that well within the next decade optical fibres will have found their most widespread practical role in linking adjacent telephone exchanges with enormously large numbers of circuits within a single thin cable.

All three of these transmission techniques, and microwave radio links too, ought thus to be regarded as complementary rather than competitive: each has its particular role to play in establishing a countrywide 'grid' with sufficient capacity to meet the bandwidth needs of the many systems of communication which are or may be envisaged.

F. W. S.

## Contributors to this issue\*



**Kamilo Feher**, Associate Professor Electrical Engineering at Concordia University, is the author of a large number of publications in the fields of microwave, cable and satellite transmission and signal processing. His background includes many years of experience with RCA Limited in industrial applications of digital communication, and he remains active in this field as a consultant to the Company. Dr. Feher has

long been involved in the research and development of new digital communications techniques and his 1.5 Mbit/s p.s.k. data above f.d.m. voice/video design efforts resulted in the first Canadian d.a.v. systems. He is the Editor of Radio Communications for the *IEEE Transactions on Communications*.



**John Huang** received his B.S. from the National Taiwan University in 1968 and the M.S. from the University of Massachusetts in 1971, both in electrical engineering. At present he is working for a doctorate in engineering at Concordia University, Montreal, his research interests being in digital communication.



**Michel Hanaut** graduated from the Ecole Polytechnique, Paris, in 1964 and received the M.S. degree in electrical engineering from the University of California, Berkeley, in 1966. He joined Texas Instruments, France, in 1967 as an industrial engineer and was promoted to integrated circuit manufacturing manager in 1969. Since 1971 Mr. Hanaut has been engaged in a domain tip memory program in TECSI and Crouzet.

He is currently manager of this development in the aerospace division of Crouzet, France. He has written several papers on the applications of MOD domain tip memories.



**Claude Battarel** graduated from the Ecole Supérieure d'Electricité, Paris, in 1953 and received a M.S. degree in applied mathematics from Harvard University in 1956. He joined IBM France in 1955 where he took part in the development of experimental computers using magnetic amplifiers and diode transistor logic schemes. In 1959 he took up an appointment with LFE in Boston as a senior engineer concerned with the use of incremental digital computers and later worked on the development and applications of domain tip memories. Mr. Battarel returned to France in 1968 as a manager in the Technology Research Department, concerned with the development of new hybrid circuitry and magnetic film memories. In 1970 he was co-founder of the TECSI Company devoted to the development of the MOD domain tip memories which is now a joint venture with the Crouzet Company where he is an advisor to the technical director of the Aerospace Division. Mr. Battarel is the author of numerous papers and patent disclosures concerning mostly magnetic memory devices.



**Geoff Hobson** received a B.A. degree in physics from the University of Oxford in 1961. He was employed at the Royal Radar Establishment from 1961 to 1967, where he worked on laboratory simulation of ionospheric transport properties of germanium and silicon and device aspects of the Gunn effect. In 1968 he joined the Department of Electronic and Electrical Engineering of the University of Sheffield where he continued his work on Gunn effect and avalanche devices, becoming a Senior Lecturer in 1971 and a Reader in 1974. His Ph.D. was awarded by the University of Sheffield in 1971. Dr. Hobson was joint author of a book on 'Transferred Electron Devices' and author of 'The Gunn Effect', in addition to publishing many papers on his research work. Since 1974 his main research interests have turned to applications of charge transfer devices.



**Ron Teperek** went to the Department of Electronic and Electrical Engineering at the University of Sheffield in 1966 and remained with this department for eight years during the course of which he obtained the degree of Bachelor of Engineering in 1969 and his doctorate in 1972 for research on microwave losses in braided coaxial cables. In 1972 he was awarded a two-year research fellowship by the British Steel Corporation to carry out work at the University of Sheffield on microwave instrumentation for the steel industry. On leaving Sheffield in 1974, he moved to Siemens AG of Munich to take up work on satellite communication components in general, and low-noise microwave f.e.t. amplifiers in particular.

\* See also pages 156 and 176.

# Practical realization of superdirective arrays

H. SALT, B.Sc., Ph.D.\*

## SUMMARY

Developments in experimental active and passive superdirective antennas are reviewed. Particular attention is given to the author's work on a two wavelength passive array consisting of nine open-ended waveguide radiators spaced one quarter-wavelength apart. The broadside superdirective patterns for this array are shown and the unnecessary restrictions on the bandwidth, due to the feeding system and the measuring site, are discussed. A new family of superdirective patterns is reported and it is shown that the far-field of a superdirective antenna starts at a distance which is no further from the antenna than that for the equivalent non-superdirective antenna. It is also shown that the high reactive field associated with superdirective arrays is confined to the immediate vicinity of the antenna.

\* Formerly with Admiralty Surface Weapons Establishment, England. Now with Commonwealth Scientific and Industrial Research Organization, Solar Energy Studies Unit, P.O. Box 89, East Melbourne, Australia 3002.

## 1 Introduction

The power gain and directivity of an antenna are terms associated with an antenna's capability to direct the power radiating from it in a specific direction in space. Directivity is formally defined as the ratio of the maximum radiation intensity (which will be in a particular direction) to the average radiation intensity, and the power gain can be defined as the ratio of the maximum radiation intensity to the radiation intensity due to a lossless isotropic radiator, when both antennas are fed with the same input power. The ratio of the directivity to the power gain of an antenna is clearly a measure of efficiency of the antenna, which is less than 100% due to conduction and dielectric losses, mismatches, or even by design as may be the case on some occasions with multiple beam antennas. Since with any directive antenna the object is to concentrate the radiated power within a given range of angles, constituting a beam, and to have only a small amount of power distributed elsewhere, one can associate a beamwidth with the directivity of an antenna since a significant increase in the directivity can only arise by decreasing the width of the beam. Whilst it is not strictly true for small end-fire arrays, it is common experience and generally accepted that the maximum gain or directivity that can be achieved practically, whether the antenna be a continuous aperture or an array of discrete elements, is that obtained by exciting the antenna uniformly, thus giving a practical upper limit to the gain of an antenna. A superdirective antenna is generally taken to be one that has a higher directivity than a similar one excited uniformly, and a supergain antenna is one that has a higher power gain.

The first realization of the possibility of superdirectivity appears to have been made by Oseen<sup>1</sup> but the first feasible theoretical approach appears to have been developed by Schelkunoff.<sup>2</sup> The improvement in directivity is obtained by exciting the radiating antenna in such a way that parts that are separated by less than a half wavelength are excited in phase opposition (if the beam is being formed normal to the plane of the antenna). Hence, superdirective and supergain antennas are array antennas and since there is no direction in real space in which the radiated waves from the elements can add in phase, these antennas have a very severe mismatch with free space. If the antenna is then matched and forced to radiate the power fed to it from a transmitter, a very strong reactive field is developed in the vicinity of the antenna<sup>3</sup> and very large currents, flowing on the elements, are necessary to support it. The degree of supergain that one might expect to achieve is limited by the ohmic losses due to these large currents, and the presence of the very large reactive field imposes severe bandwidth limitations on passive supergain arrays. A consequence of the fact that the elements of the array are excited in phase opposition, for both supergain and superdirective antennas, is that the beam formed normal to the array is due to the differences in the amplitudes of excitation of the elements, and the tolerances required for the element excitations are therefore very much more severe than for antennas in which the elements are excited in-phase. Furthermore, as the size of the antenna is increased, the tolerances required for each element

excitation become higher, and the reactive field increases rapidly.<sup>4</sup>

## 2 Supergain Antennas

The theoretical demonstrations of the possibility of superdirective and supergain antennas were not accompanied by large numbers of practical demonstrations of their feasibility. In fact, the literature would lead one to believe that very few attempts have been made to produce this type of antenna, presumably because of the expected difficulties and very narrow bandwidth. However, Bloch, Medhurst and Pool<sup>5</sup> made a supergain end-fire array consisting of four parallel, half-wave dipoles, where centres were equally spaced along a line  $0.6\lambda$  long, and which operated at a frequency of 75 MHz. The measured gain was 8.7 dB relative to a similar single dipole, as opposed to a calculated value of 10.1 dB, whereas if the array had been fed with equal-amplitude currents phased for maximum field strength in the end-fire direction, then the gain would have been 4.6 dB. The bandwidth was  $\pm 0.5$  MHz for a drop in gain of  $\pm 0.5$  dB. Their technique for determining the current distribution is to calculate a 'resistance voltage' across the terminals of the elements from the self and mutual resistances of the elements, and to make this voltage vary from element-to-element in the same way as the instantaneous local values of a sinusoidal disturbance travelling across the array, in the direction under consideration, with the velocity of an electromagnetic wave. Their procedure leads, therefore, to the uniform distribution for broadside arrays, but it clearly gave a significant increase in gain for their end-fire array.

This work was continued by Bacon and Medhurst<sup>6</sup> with a four-dipole end-fire array operating at 275 MHz. In this case, however, a non-uniform spacing of the elements was used and only one dipole was excited, the other three being parasites. The array length was  $0.6\lambda$  and one made with thin elements had a gain of almost 9 dB and a bandwidth of 5.5 MHz for a drop in gain of 0.5 dB, whereas one made using thick elements had a gain of about 8.8 dB and a bandwidth of 6.5 MHz. The theoretical maximum gain for the arrays was about 10 dB and an orthodox end-fire array, in which the elements are excited with equal amplitude, would have a gain of 5.5 dB less.

The only other work on experimental supergain antennas, known to the author, is unpublished, but a report is available through recognized channels.<sup>7</sup>

## 3 Superdirective Antennas

It has been argued by Tucker<sup>8</sup> that the high  $Q$ -value and very narrow bandwidth normally associated with superdirective arrays is not inherent, because it arises from tuning out the large reactance, and this is done to improve the power transfer between the antenna system and space. It is easier to see how the low radiation resistance and large reactance arise when the antenna is transmitting and to invoke the principle of reciprocity for reception. The elements are closely spaced and

therefore have high mutual coupling, and, consequently, the almost complete phase reversal between adjacent elements of a superdirective array means that the resultant in-phase component of the field, in the vicinity of an element, is small relative to the current on the element. However, if one were to consider the antenna for reception only, then buffer amplifiers could be interposed between the elements and the network connecting them and in this case, since it is the outputs of the amplifiers that are being added together, the radiation impedances of the elements are independent of the far-field pattern seen at the output of the antenna system. Accordingly, the bandwidth of the superdirective array should be the same as the bandwidth of the array without superdirectivity. The power coupled from space to the receiver would of course be very low, so that although it may be possible to construct a superdirective antenna in this way, it would not be a supergain antenna. The function of the buffer amplifiers is to decouple the elements of the array from the receiving system and so improve the bandwidth, but since it is still the small differences (due to the phase reversals) between large quantities that are being used to obtain a superdirective pattern, the tolerance problems normally associated with superdirectivity are not eased. The suggestion that the proposed decoupling should improve the bandwidth appears to agree with Chu's comment<sup>4</sup> that the conduction losses of the antenna decrease the  $Q$ -value. As a result of Professor Tucker's paper, several letters<sup>9, 10, 11, 12</sup> were written agreeing with his arguments and suggesting alternative ways of decoupling the elements from the receiver using passive networks. The difficulties of trying to produce a superdirective array were recognized but it was felt that further investigations would be worthwhile, particularly for small antennas for use at the lower-frequency end of the electromagnetic spectrum, where the noise limitations of systems are due to external sources and where a significant reduction in array size would be welcome.

In his paper, Professor Tucker described an experimental array which consisted of seven half-wave dipoles, backed by a groundplane, but only the three central elements were connected via baluns, buffer amplifiers and hybrid arrangements, the two outer elements on each side being terminated in dummy loads. The array was operated at a frequency of 420 MHz and the element spacing was one quarter-wavelength. The three active elements had equal gains in the amplifier and hybrid systems so that when their outputs were connected in phase, a uniform array was produced; the measured pattern in this mode of operation agreed very well with the theoretical one. When the phase of the central element was reversed, a simple superdirective array was produced and its measured pattern had a beamwidth, at the  $-3$  dB level, of approximately  $\frac{2}{3}$  of the theoretical uniform distribution pattern and about  $\frac{2}{3}$  of the measured uniform distribution pattern. Although the side-lobe level of the superdirective pattern was about  $-8$  dB, the results demonstrated the feasibility of using buffer amplifiers to achieve superdirectivity with receiving arrays.

Whereas Tucker's work was concerned with receiving arrays, Dawoud and Anderson<sup>13</sup> have shown that the integration of active devices with radiating elements is a practical approach to superdirective transmitting arrays. In this case, each element is independently excited by its own transistor and this effectively isolates the feeding network from the radiators and the mutual coupling effects between the radiators. Hence one can expect the bandwidth of such a superdirective transmitting array to be very much greater than an array which is fed by a network which does not isolate the elements from each other. Expressed in another way, one can say that if a superdirective array is fed with a network which allows loop coupling between the elements, that is, the network allows power which has been coupled through space from a first element into a second to be fed back to the first element through the network, then the bandwidth will be much more restricted than it would be if the network prevented loop coupling. A four-element end-fire array was constructed so that its total length was  $3\lambda/8$ , and each element was  $\lambda/4$  long. The array was mounted over a ground plane and the beamwidth at the  $-3$  dB level was about  $40-45^\circ$  as compared with a theoretical beamwidth of  $60^\circ$  for the non-superdirective array. Although the measured side-lobe level was about  $-8$  dB, which was due in part to the characteristics of their anechoic chamber,<sup>13</sup> the authors stated that the pattern was substantially unaltered for a frequency deviation of 5%.

A two-wavelength superdirective broadside array has been constructed by the author<sup>14</sup> and the remainder of this paper is concerned with reporting that work. The array consisted of nine open-ended, reduced-height waveguides as shown in Fig. 1. The operating frequency was 9.4 GHz and the elements were mounted broad-face to broad-face in order to achieve one quarter-wavelength separation between their centres, and the plane of polarization for the array was therefore horizontal. The array was fed from standard size 16 X-band waveguide through tapered sections as shown in Fig. 2.

**4 Superdirective Pattern Synthesis**

The technique developed by Schelkunoff<sup>2</sup> can be used to obtain a distribution that will produce a superdirective pattern. This theoretical technique consists of compressing the null points of the array in the complex plane, to be equi-spaced on that part of the unit circle which corresponds to the range of real angles in space about the array, and a superdirective pattern can certainly be

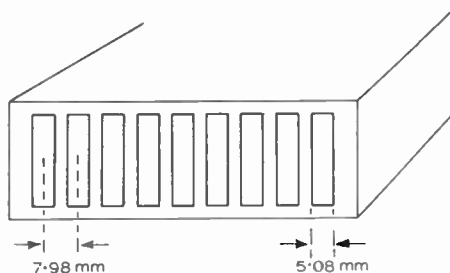


Fig. 1. The nine open-ended waveguide radiators.

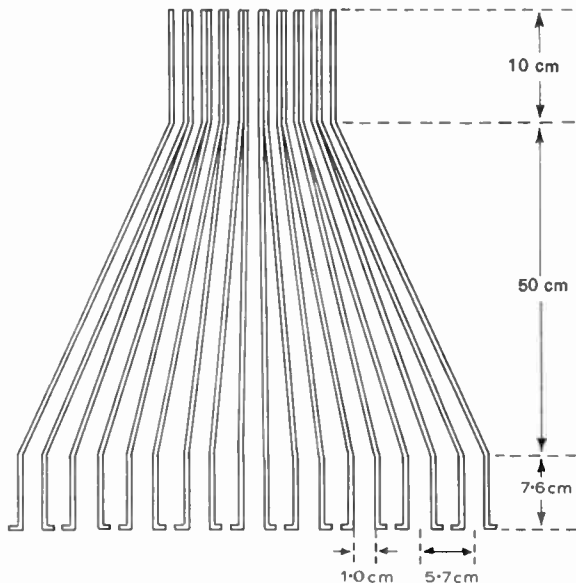


Fig. 2. The transition from the W.G.16 feeds to the nine radiators.

obtained in this way but it does not give any direct control over the side-lobe level. As was stated earlier, the approach used by Bloch, Medhurst and Poole is not suitable for broadside arrays. However, the original work by Dolph<sup>15</sup> on non-superdirective broadside arrays showed that one of the properties of a Chebyshev array is that it has the minimum beamwidth for a given side-lobe level, and Dolph's work was later extended by Riblet<sup>16</sup> to cover superdirective arrays containing an odd number of elements.

Another possible way of obtaining a superdirective pattern is to use the Woodward method<sup>17</sup> of pattern synthesis. Woodward's procedure is to specify the required far-field pattern at those points corresponding to the directions in space of a set of linearly independent synthesizing patterns, whose amplitudes would thus be determined, and the synthesizing patterns can then be added together to give a resultant pattern. The resultant pattern must pass through the original fixed points but its value elsewhere can only be determined by carrying out the summation. Obviously, the synthesized pattern can be more tightly specified if the orthogonal synthesizing patterns are closely spaced. The orthogonal set used by Woodward were the  $\sin x/x$  patterns due to illuminating a continuous aperture with a uniform amplitude and different phase tilts. However, since we are concerned with arrays of elements, the technique will be developed here for these rather than a continuous aperture.

The normalized far-field radiation pattern of an array of  $2N+1$  elements, which all have the same phase and amplitude, is

$$G(\sin \theta) = \frac{1}{2N+1} \sum_{n=-N}^N 1 \cdot \exp(jnkd \sin \theta) \quad (1)$$

where  $\theta$  is the angle from the normal to the array, and this gives:

$$G(\sin \theta) = \frac{\sin((2N+1) \frac{1}{2}kd \sin \theta)}{(2N+1) \sin(\frac{1}{2}kd \sin \theta)} \quad (2)$$

If the elements are excited such that the main beam lies in the direction  $\theta_1$  then equation (2) becomes:

$$G(\sin \theta) = \frac{\sin ((2N+1)\frac{1}{2}kd(\sin \theta - \sin \theta_1))}{(2N+1) \sin (\frac{1}{2}kd(\sin \theta - \sin \theta_1))} \quad (3)$$

and if we represent the expression  $\frac{1}{2}kd \sin \theta$  as  $u$  and  $\frac{1}{2}kd \sin \theta_1$  as  $u_1$ , then equation (3) becomes:

$$G(u) = \frac{\sin ((2N+1)(u-u_1))}{(2N+1) \sin (u-u_1)} \quad (4)$$

We now wish to consider any two of these patterns and determine the conditions that makes them orthogonal. If we consider one pattern to have its main beam lying in the direction  $\theta_1$ , and the other in the direction  $\theta_2$ , then the two far-field patterns can be expressed as:

$$G_1(u) = \sum_{n=-N}^N \exp(jn2(u-u_1)) \quad (5)$$

and

$$G_2(u) = \sum_{n=-N}^N \exp(jn2(u-u_2)) \quad (6)$$

The two functions  $G_1$  and  $G_2$  are said to be orthogonal if the integral, over their whole range, of the product of one function and the conjugate of the other, is zero. Since the far-field pattern of an array antenna is a periodic function, and the period in  $u$ -space is  $\pi$ , the orthogonality integral in this case is:

$$\int_0^\pi G_1(u)G_2^*(u) du = 0. \quad (7)$$

Inserting equations (5) and (6) into equation (7) give

$$\int_0^\pi \sum_{n=-N}^N \exp(jn2(u-u_1)) \times \sum_{m=-N}^N \exp(-jm2(u-u_2)) du = 0 \quad (8)$$

and interchanging the order of integration and summation, we have

$$\sum_{n=-N}^N \exp(-jn2u_1) \sum_{m=-N}^N \exp(jm2u_2) \times \int_0^\pi \exp(j2u(n-m)) du = 0. \quad (9)$$

The integral in equation (9) has the value  $\pi$  when  $n = m$  and is zero when  $n \neq m$  so that equation (9) reduces to

$$\sum_{n=-N}^N \exp(j2n(u_2-u_1)) = 0 \quad (10)$$

and this gives

$$\frac{\sin ((2N+1)(u_2-u_1))}{(2N+1) \sin (u_2-u_1)} = 0. \quad (11)$$

Equation (11) is satisfied when

$$u_2-u_1 = \frac{p\pi}{2N+1}; p=1, 2, \dots, 2N. \quad (12)$$

and we can therefore say that a set of

$$\frac{\sin ((2N+1)(u-u_p))}{(2N+1) \sin (u-u_p)}$$

patterns are all linearly independent if each one is

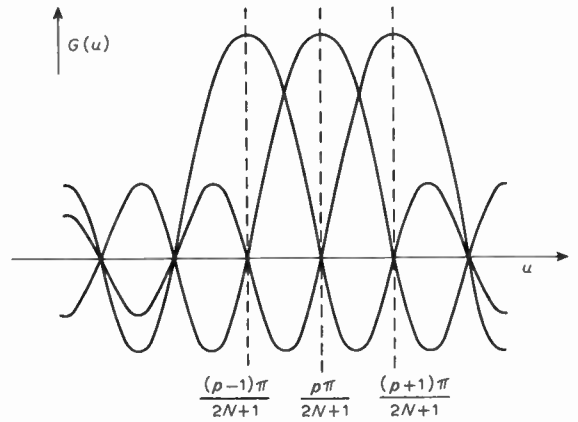


Fig. 3. Adjacent members of an orthogonal set.

separated from the others by an integral number of  $\pi/(2N+1)$  parts in  $u$ -space. Since this is also the separation of the zeros of a single pattern of the set, we can say that the patterns are orthogonal if the maxima of all the patterns lie over the zeros of all the other patterns, as shown in Fig. 3. Each of the patterns repeats itself when  $u-u_p = p\pi$ , or when  $\sin \theta - \sin \theta_p = p\lambda/d$ , so that an array of  $2N+1$  elements can only produce  $2N+1$  orthogonal patterns; the complete set will repeat within the range  $|\sin \theta| < 1$  if  $d > \lambda/2$ , it will cover this range if  $d = \lambda/2$ , and some members of the set will have their main beams outside the range and in imaginary space if  $d < \lambda/2$ .

The Woodward procedure gives a good pictorial insight into the nature of the synthesis of a superdirective pattern. If one considers the broadside

$$\frac{\sin (2N+1)u}{(2N+1) \sin u}$$

pattern, and considers how the other members of the orthogonal set may be combined with it to reduce its beamwidth, then it is evident that if this is to be done without introducing second-order main beams in the real-space part of the resultant pattern, then the beamwidth control must come from the side-lobes of those members of the orthogonal set whose beams lie in imaginary space, as shown in Fig. 4. Since it is only the side-lobes of the imaginary beams that are being used,

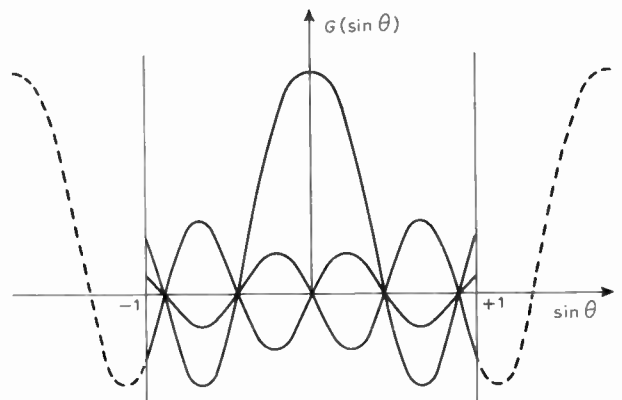


Fig. 4. Real and imaginary beams.

and indeed only the difference in the levels of adjacent side lobes of opposite synthesizing patterns for a symmetrical resultant pattern, then the imaginary beams have to assume very large amplitudes in order to significantly affect the broadside beam. Furthermore, as the overall size of the array and the number of elements is increased, the side lobes affecting the beamwidth become progressively smaller, so the amplitudes of the imaginary beams have to be made progressively larger. The area under a pattern over the imaginary space part gives a measure of the reactive power associated with the pattern, and the area over the real space part gives a measure of the radiated power, so the  $Q$  of a superdirective pattern is high, and increases as the antenna size is increased.

If one wishes to halve the beamwidth normally associated with a  $2\lambda$  array of nine elements spaced  $\lambda/4$  apart, then the most obvious pattern to try to synthesize is

$$G_d(\sin \theta) = \frac{\sin(9\pi/2 \sin \theta)}{9 \sin(\pi/2 \sin \theta)} \quad (13)$$

which is the pattern resulting from feeding nine radiators spaced one half-wavelength apart (a four-wavelength array) with a co-phased uniform amplitude distribution. The nine orthogonal beams associated with the nine quarter-wave-spaced radiators are the set:

$$G_n(\sin \theta) = \frac{\sin(9\pi/4(\sin \theta - 4n/9))}{9 \sin(\pi/4(\sin \theta - 4n/9))} \quad (14)$$

where  $n = -4, \dots, 0, \dots, +4$ .

The mechanics of the Woodward technique in this case are to choose nine values of  $\sin \theta$  within the range  $-1 \leq \sin \theta \leq +1$  and the corresponding values of  $G_d(\sin \theta)$ , and to set these equal to the sum of the products of the values of the nine synthesizing beams, evaluated at these values of  $\sin \theta$ , and their unknown amplitudes. A symmetric synthesized pattern is required and therefore the values of  $\sin \theta$  are chosen symmetrically about zero. Expressed in matrix form, we have:

$$[A_n][G_n(\sin \theta)_p] = [G_d(\sin \theta)_p] \quad (15)$$

where the  $A_n$  are the unknown amplitudes of the synthesizing beams.

When this equation has been solved to give the values  $A_n$ , the resultant synthesized pattern  $G_R$  can be found using

$$G_R(\sin \theta) = \sum_{n=-4}^4 A_n G_n(\sin \theta). \quad (16)$$

For the first attempt to synthesize a superdirective pattern, the angular directions in space were chosen as those making the numerator in equation (13) either unity or zero, the directions being centred about broadside. These values are shown below:

$$\sin \theta = 0$$

$$\text{when } G_R(0) = G_d(0) = 1.0$$

$$\sin \theta = \pm 0.1111$$

$$\text{when } G_R(\pm 0.1111) = G_d(\pm 0.1111) = 0.64$$

$$\sin \theta = \pm 0.2222$$

$$\text{when } G_R(\pm 0.2222) = G_d(\pm 0.2222) = 0.0$$

$$\sin \theta = \pm 0.3333$$

$$\text{when } G_R(\pm 0.3333) = G_d(\pm 0.3333) = -0.2222$$

$$\sin \theta = \pm 0.5556$$

$$\text{when } G_R(\pm 0.5556) = G_d(\pm 0.5556) = 0.1451$$

This selection has five points controlling what will hopefully be the main beam in the resultant pattern, namely, the values at  $\sin \theta = 0, \pm 0.1111, \pm 0.2222$ , and the values at  $\sin \theta = \pm 0.3333, \pm 0.5556$  do of course correspond with the values for the first two side-lobes on either side of the main beam for the pattern  $G_d(\sin \theta)$ . The calculated beam amplitudes for this case are:

$$A_{-4} = A_4 = 5960.568$$

$$A_{-3} = A_3 = 1818.138$$

$$A_{-2} = A_2 = 88.53062$$

$$A_{-1} = A_1 = 0.0845526$$

$$A_0 = 1.0$$

and the resultant pattern is shown as curve (1) in Fig. 5. The next trial released the control over the pattern at the zeros of the main beam and used the values of the next side-lobe of the  $G_d(\sin \theta)$  pattern.

The control points in this case are:

$$\sin \theta = 0$$

$$\text{when } G_R(0) = G_d(0) = 1.0$$

$$\sin \theta = \pm 0.1111$$

$$\text{when } G_R(\pm 0.1111) = G_d(\pm 0.1111) = 0.64$$

$$\sin \theta = \pm 0.3333$$

$$\text{when } G_R(\pm 0.3333) = G_d(\pm 0.3333) = -0.2222$$

$$\sin \theta = \pm 0.5556$$

$$\text{when } G_R(\pm 0.5556) = G_d(\pm 0.5556) = 0.1451$$

$$\sin \theta = \pm 0.7778$$

$$\text{when } G_R(\pm 0.7778) = G_d(\pm 0.7778) = -0.1182$$

The calculated beam amplitudes are:

$$A_{-4} = A_4 = 2198.108$$

$$A_{-3} = A_3 = 591.8014$$

$$A_{-2} = A_2 = 11.74$$

$$A_{-1} = A_1 = 0.1376804$$

$$A_0 = 1.0$$

and the resultant pattern is shown as curve (2) in Fig. 5. Whilst this is an improvement over curve (1) it is clearly still unacceptable and since with nine elements it is only possible to have eight controlling parameters relative to one other (chosen as unity for the broadside pattern value), then further control over the synthesized pattern towards end-fire can only be obtained by relinquishing all direct control over the required main beam about broadside. The pattern control points shown below for the synthesized pattern are the values of the main beam and all the side-lobes of the  $G_d(\sin \theta)$  pattern, when

$$\sin \theta = 0$$

$$\text{and } G_R(0) = G_d(0) = 1.0$$

$$\sin \theta = \pm 0.3333$$

$$\text{and } G_R(\pm 0.3333) = G_d(\pm 0.3333) = -0.2222$$

$$\begin{aligned} \sin \theta &= \pm 0.5556 \\ \text{and } G_R(\pm 0.5556) &= G_d(\pm 0.5556) = 0.1451 \\ \sin \theta &= \pm 0.7778 \\ \text{and } G_R(\pm 0.7778) &= G_d(\pm 0.7778) = -0.1182 \\ \sin \theta &= \pm 1.0 \\ \text{and } G_R(\pm 1.0) &= G_d(\pm 1.0) = 0.1111 \end{aligned}$$

The calculated beam amplitudes in this case are:

$$\begin{aligned} A_{-4} &= A_4 = 231.0341 \\ A_{-3} &= A_3 = 45.85951 \\ A_{-2} &= A_2 = -0.7735809 \\ A_{-1} &= A_1 = -0.2008985 \\ A_0 &= 1.0 \end{aligned}$$

and the resultant pattern is shown as curve (3) in Fig. 5, its value at  $\sin \theta = \pm 2.0$  being 275.

These three curves are interesting in that curve (2) is specified on the main beam only at  $\sin \theta = \pm 0.1111$ , and yet it virtually lies on top of the main beam of curve (1) which is specified at the zeros as well. Curve (3) is not specified at all over the main beam (apart from the normalizing value at broadside) and yet the  $-3$  dB points only increase from  $\sin \theta = \pm 0.096$  ( $11^\circ$  beamwidth) to  $\sin \theta = \pm 0.12$  ( $14^\circ$  beamwidth), whilst the pattern within the visible region becomes much more acceptable in that it has a main beam in the accepted sense, even though there is a very high side-lobe at  $\sin \theta = \pm 0.91$  (it should be remembered that these

curves take no account of an element pattern for the elements of the array, which would reduce this high side-lobe).

The other notable feature when comparing these three results is the dramatic decrease in the values of  $A_{\pm 4}$  and  $A_{\pm 3}$ , which go from 5961 and 1818 to 231 and 46 respectively, when going from curve (1) to curve (3). Since these are the amplitudes of the synthesizing patterns whose main beams lie in imaginary space, and are therefore associated with the energy stored within the aperture, the stored energy for curve (3) is very much less than the stored energy for curve (1). These three results show that in trying to synthesize a pattern having the approximate beamwidth of the pattern formed by the uniform excitation of a  $4\lambda$ -array of nine equi-spaced elements, by using the nine orthogonal patterns associated with uniform amplitude excitations of a  $2\lambda$ -array of nine equi-spaced elements, then it is not necessary to specify the main beam in the synthesis procedure. However, in order to form a main beam at broadside with only side-lobes extending out to end-fire, it is necessary to extend the control parameters throughout the whole of real space; this does not increase the beamwidth very much even though the main beam is not controlled, and it greatly reduces the stored energy.

Whilst curve (3) is a big improvement over curves (1) and (2), it is not wholly satisfactory, and it was decided to try to synthesize the  $G_a(\sin \theta)$  pattern associated with the uniform excitation of a continuous  $4\lambda$ -aperture.

This pattern passes through zero at  $\sin \theta = \pm 1.0$  so that using these two points ought to lower the level of the synthesized pattern towards end-fire. The normalized far-field pattern arising from a co-phased uniform amplitude illumination of a  $4\lambda$  continuous aperture is

$$G_a(\sin \theta) = \frac{\sin(4\lambda a)}{a} \tag{17}$$

where

$$a = \frac{\pi}{\lambda} \sin \theta \tag{18}$$

and the numerator in equation (17) is unity when

$$\sin \theta = \pm 0.125, 0.375, 0.625, 0.875, \dots$$

and is zero when

$$\sin \theta = \pm 0, 0.25, 0.5, 0.75, 1.0, \dots$$

The first points taken from this pattern, to control the synthesized pattern are:

$$\begin{aligned} \sin \theta &= 0 \\ \text{when } G_R(0) &= G_a(0) = 1.0 \\ \sin \theta &= \pm 0.375 \\ \text{when } G_R(\pm 0.375) &= G_a(\pm 0.375) = -0.2122 \\ \sin \theta &= \pm 0.625 \\ \text{when } G_R(\pm 0.625) &= G_a(\pm 0.625) = 0.1273 \\ \sin \theta &= \pm 0.875 \\ \text{when } G_R(\pm 0.875) &= G_a(\pm 0.875) = 0.0909 \\ \sin \theta &= \pm 1.0 \\ \text{when } G_R(\pm 1.0) &= G_a(\pm 1.0) = 0.0 \end{aligned}$$

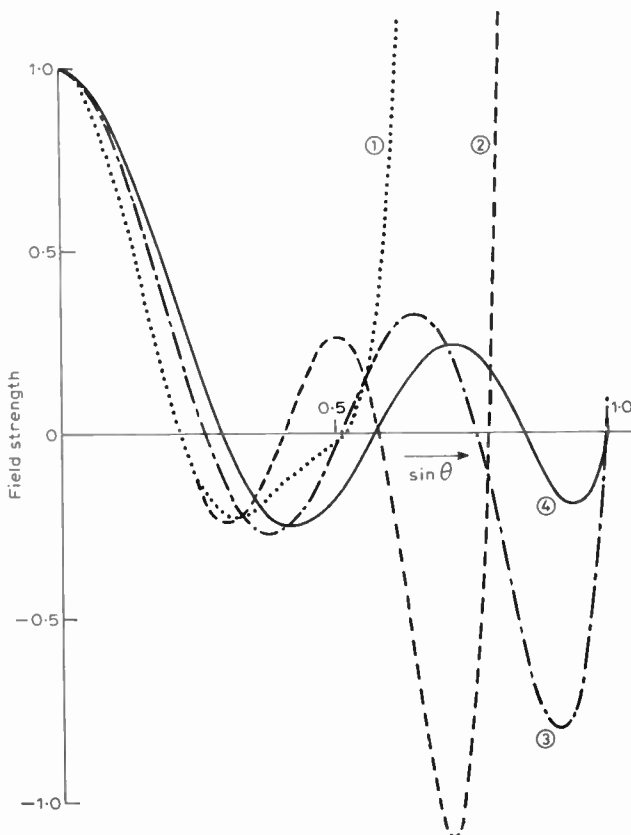


Fig. 5. Resultant far-field patterns for selections 1-4.

The calculated beam amplitudes with these controlling points are

$$\begin{aligned}
 A_{-4} = A_4 &= 104.6898 \\
 A_{-3} = A_3 &= 19.10645 \\
 A_{-2} = A_2 &= -0.1271143 \\
 A_{-1} = A_1 &= -0.2447246 \\
 A_0 &= 1.0
 \end{aligned}$$

and the resultant pattern is shown as curve (4) in Fig. 5. The side-lobe level in this case is clearly satisfactory, although the -3 dB points have moved out to  $\sin \theta = \pm 0.135$  ( $16^\circ$  beamwidth), and the values of  $A_{\pm 4}$  and  $A_{\pm 3}$  have been decreased further to 105 and 19 respectively.

A family of superdirective patterns can be generated by using the Woodward method to try to synthesize the  $G_a(\sin \theta)$  pattern associated with the  $4\lambda$ -aperture. The broadside and end-fire values of the synthesized pattern are controlled to be 1.0 and 0.0 respectively, and the three other control points, allowed by the synthesis technique, are firstly chosen to correspond with the zeros of the  $G_a(\sin \theta)$  pattern, that is, at values of  $\sin \theta = 0.25, 0.5$  and  $0.75$ , and then further selections are made by increasing the value of  $\sin \theta$  by 0.5 for each of these three control points simultaneously. These selections are shown in Table 1, which also shows the amplitudes of the nine synthesizing beams in order that the resultant pattern  $G_R(\sin \theta)$  should pass through the nine points chosen on the pattern  $G_a(\sin \theta)$ , for that particular selection. It should be noted that choosing the zeros of the  $G_a(\sin \theta)$  pattern as the control points for the

**Table 1.** Amplitudes of the synthesizing beams for points selected from  $\sin(4\lambda u)/u$  pattern for  $4\lambda$ -continuous aperture

Selection number	Selected values of		Synthesizing beam numbers $n$	Amplitudes $A_{\pm n}$ of the synthesizing beams for the set of selected points
	$\sin \theta$	$G_R = G_a$		
5	0.00	1.0	0	1.0
	0.25	0.0	1	-0.1984913
	0.50	0.0	2	-1.055520
	0.75	0.0	3	55.11569
	1.00	0.0	4	277.0824
6	0.00	1.0	0	1.0
	0.30	-0.15591	1	-0.2521745
	0.55	0.08504	2	-0.5404281
	0.80	-0.05847	3	37.95343
	1.00	0.0	4	196.8623
7	0.00	1.0	0	1.0
	0.35	-0.21624	1	-0.2616943
	0.60	0.12614	2	-0.2238245
	0.85	-0.08904	3	24.49797
	1.00	0.0	4	131.6698
8	0.00	1.0	0	1.0
	0.40	-0.18921	1	-0.2119096
	0.65	0.11643	2	0.06360102
	0.90	-0.08409	3	14.55277
	1.00	0.0	4	81.34606
9	0.00	1.0	0	1.0
	0.45	-0.10394	1	-0.09976794
	0.70	0.06682	2	-0.01098561
	0.95	-0.04924	3	7.693895
	1.00	0.0	4	44.74107
10	0.00	1.0	0	1.0
	0.49	-0.02036	1	0.02795144
	0.74	0.01348	2	-0.01456099
	0.99	-0.01007	3	4.048729
	1.00	0.0	4	24.08217

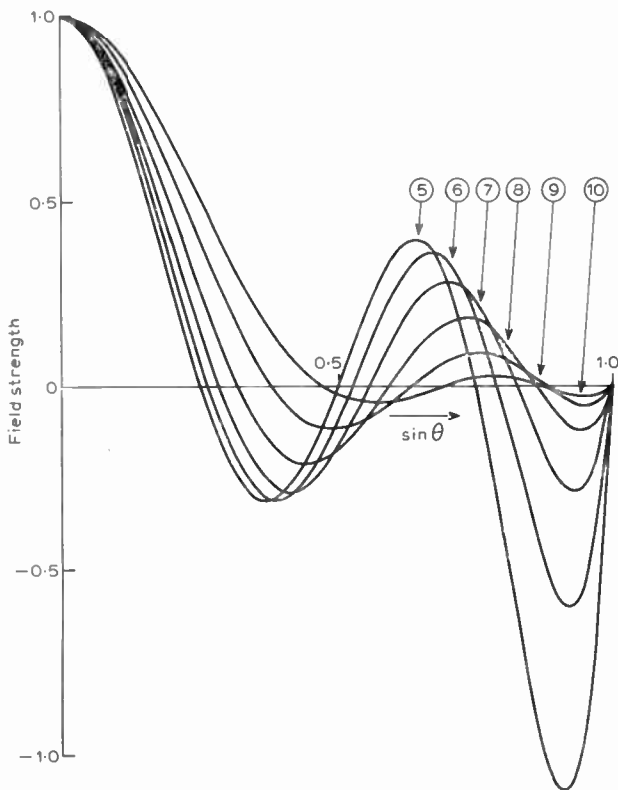


**Fig. 6.** Resultant far-field patterns for selection 5-10.

synthesized pattern, is equivalent to using Schelkunoff's technique of spacing the null points on the complex plane equally over the part of the unit circle corresponding to the range of real angles for the radiation.

The resultant patterns are plotted in Figs. 6 and 7. Considering the patterns as shown in Fig. 6, they clearly represent a family of patterns whose beamwidths steadily increase as the side-lobe levels decrease. Figure 7 shows the main beams of this family of patterns together with the main beams of  $\sin 4\lambda u/u$  and  $\sin 2\lambda u/u$  patterns for the  $4\lambda$  and  $2\lambda$  continuous apertures, and the  $\sin 9v/9 \sin v$  patterns for the arrays of nine elements at half-wavelength ( $v = \pi/2 \sin \theta$ ) and quarter-wavelength ( $v = \pi/4 \sin \theta$ ) spacings, which cover a total length of four and two wavelengths respectively. It is clearly seen in this figure that the main beams of the synthesized family of patterns are bounded by these non-superdirective main beams. However, the side-lobes for the superdirective and non-superdirective patterns are quite different as can be seen from Fig. 6: pattern 5, which has the same beamwidth between its zeros as the  $4\lambda$ -aperture  $\sin 4\lambda u/u$  pattern,

has a second main beam of amplitude 1.1 at  $\sin \theta = 0.91$ , whereas pattern 10, which has the zeros of its main beam  $\sin \theta = \pm 0.47$  as against 0.5 for the  $2\lambda$  aperture  $\sin 2\lambda u/u$  pattern, has a maximum side-lobe level of 0.05 (-27 dB) at  $\sin \theta = 0.56$  as against the value of 0.22 (-13 dB) at  $\sin \theta = 0.72$  in the  $2\lambda$ -aperture case. It is interesting to observe the patterns in Fig. 6 together with Table 1. Patterns 5 and 6 have side lobes which increase towards  $\sin \theta = 1.0$ , pattern 7 has side-lobes which are nearly equal, and patterns 8, 9 and 10 have side-lobes which decrease in value towards end-fire. It can be seen that the three selected points used for controlling the synthesized pattern for patterns 5 and 6 all lie towards  $\sin \theta = 0.0$  of the peaks of their respective side-lobes on the  $4\lambda$ -aperture  $\sin 4\lambda u/u$  patterns, for pattern 7 the selected points lie almost on the peaks of the side-lobes, and for patterns 8, 9 and 10 they all lie towards  $\sin \theta = 1.0$  of the peaks of the side-lobes. Although pattern 7 is very similar to a Chebyshev pattern, the reactive power associated with pattern 7 is higher than with the equivalent Chebyshev pattern.<sup>14</sup>

Rather than using buffer amplifiers to decouple the elements of a receiving array from the antenna system output port, an alternative is to use a multiple-beam antenna to generate the Woodward synthesizing beams and then to add together, in the correct ratio, the outputs of these ports to give a superdirective pattern.<sup>12</sup> One of the principal reasons for this approach is that the difficulties associated with superdirective arrays are primarily associated with the beams formed in imaginary

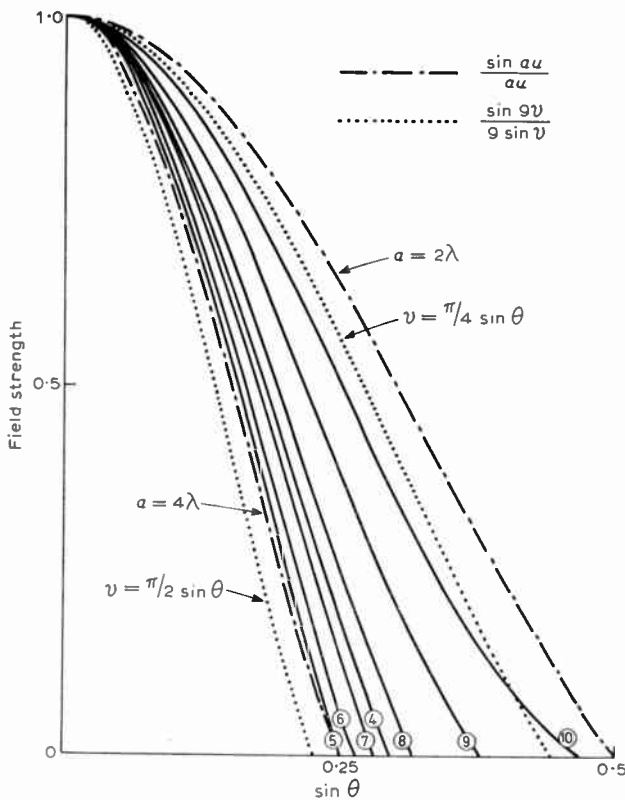


Fig. 7. Main beams for selection 4-10, of  $\sin(au)/au$  for  $a = 2\lambda$  and  $a = 4\lambda$ , and of  $\sin 9v/9 \sin v$  for  $\frac{1}{4}\lambda$  ( $v = \pi/4 \sin \theta$ ) and  $\frac{1}{2}\lambda$  ( $v = \pi/2 \sin \theta$ ) spaced elements.

space, and these can be dealt with independently by a multiple-beam network. However, it has been shown<sup>14</sup> that it is unlikely that superdirectivity can be achieved in this way because of the phase and amplitude accuracies required within the network.

### 5 Experimental Approach

In order to determine the effects of cross-coupling between the elements of the array, the far-field pattern of each of the elements was measured in both phase and amplitude, with all the other elements being terminated in matched loads; these initial measurements were not very accurate and the experimental details are given fully in Ref. 14. The required element excitation was then calculated such that the element patterns should add together to give a resultant pattern that lies on the  $\sin 4\lambda u/u$  pattern at the angles corresponding to selection 4 in the previous section, that is, the resultant pattern  $G_R$  had to pass through the points:

- $G_R = 1.0$  (0 dB) when  $\sin \theta = 0$  ( $\theta = 0^\circ$ )
- $G_R = -0.2122$  (-13.47 dB) when  $\sin \theta = \pm 0.375$  ( $\theta = \pm 22^\circ$ )
- $G_R = 0.1273$  (-17.90 dB) when  $\sin \theta = \pm 0.625$  ( $\theta = \pm 39^\circ$ )
- $G_R = 0.0909$  (-20.83 dB) when  $\sin \theta = \pm 0.875$  ( $\theta = \pm 61^\circ$ )
- $G_R = 0.0$  when  $\sin \theta = \pm 1.0$  ( $\theta = \pm 90^\circ$ )

The required excitation for the elements in order to produce these values in the far-field is given in Table 2.

Table 2. The required element excitation for the approximate element patterns

Element No.	Amplitude	Phase	dB
1	0.2542	-90.1°	-11.90
2	0.5356	+125.1°	-5.42
3	0.5032	-87.5°	-5.97
4	0.4398	+55.1°	-7.13
5	0.8074	+171.7°	-1.86
6	1.0000	0.0°	0
7	0.9566	+162.5°	-0.39
8	0.3485	-17.3°	-9.16
9	0.0604	+78.9°	-24.38

If the effects of cross-coupling between the elements were ignored, then the required excitation would be as shown in Table 3.

Table 3

Element No.	Amplitude	Phase	dB
5	1.0000	0.0°	0
4 and 6	0.8686	180.0°	-1.22
3 and 7	0.5747	0.0	-4.81
2 and 8	0.2627	180.0°	-11.61
1 and 9	0.0747	0.0°	-22.53

These two distributions are quite different, although the total range of the excitations is similar ( $-22.5$  dB as against  $-24.4$  dB), and it is clearly necessary to take into account the effects of mutual coupling on the patterns of the individual elements of the array, if one wishes to generate a superdirective pattern. When the element patterns were multiplied by the calculated excitations shown in Table 2 and then added together, the resultant computed pattern  $G_R$  was superdirective with a width between the nulls of the main beam of  $35^\circ$ , compared with a zeros beamwidth of  $60^\circ$  for a  $2\lambda$  aperture. This shows that the effects of mutual coupling on the element patterns does not prevent superdirectivity being achieved.

The required accuracy for the excitation of the elements was found by calculating the upper envelope of all the superdirective patterns computed for many trials, when a Gaussian error distribution is applied individually to the calculated values of amplitude and phase for the excitation of the elements. It was found that thirty trials were sufficient for the upper envelope to remain sensibly invariant. Several values were used for the standard deviations of the amplitudes and phases applied to each element, and the conclusion drawn was that one could expect to measure a satisfactory superdirective pattern if a phase accuracy of about  $2^\circ$ , and an amplitude accuracy of about  $0.2$  dB, could be achieved.

In order to meet the accurate measurement requirements, the array was mounted on a bench in the laboratory and an anechoic chamber built around it and the transmitting horn, whose phase centre was  $50$  cm from the centre of the array. This pattern measuring site then formed one arm of a microwave bridge so that accurate measurements could be made. The array and the transmitting horn, which is mounted at the end of a rotating arm with the centre of rotation being immediately beneath the centre of the centre element of the array, are shown in Fig. 8. The complete bridge is shown in

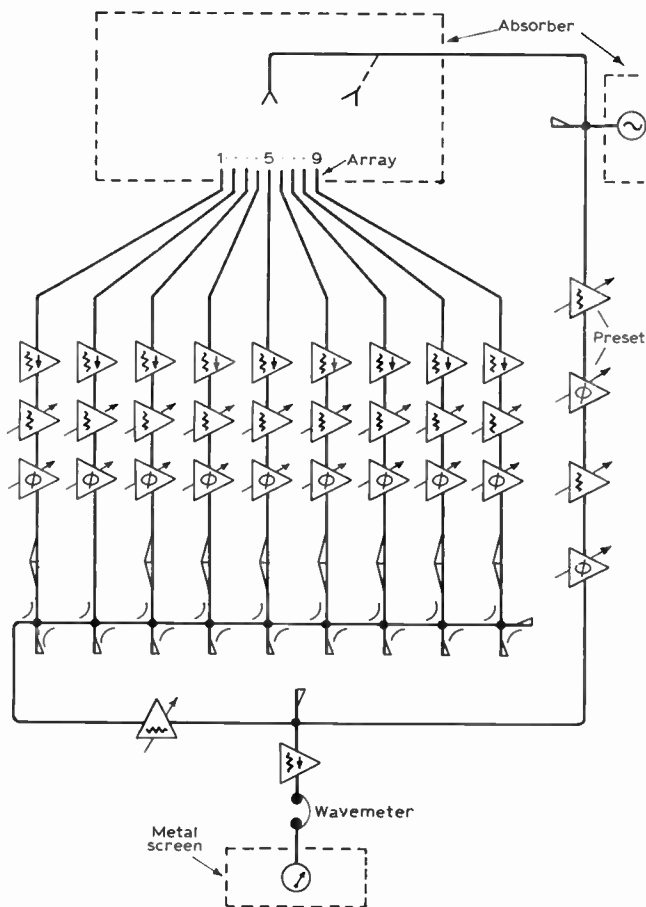
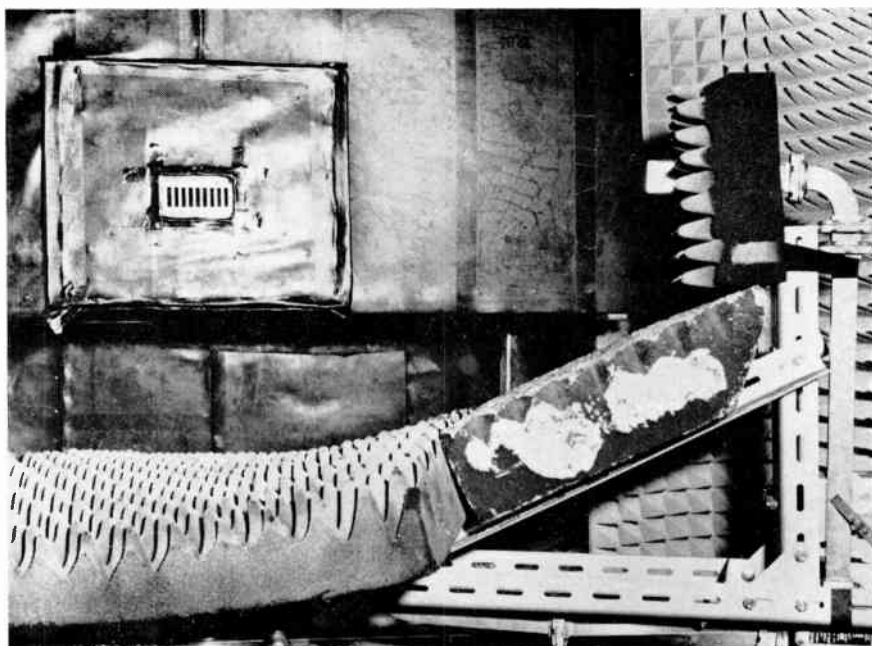


Fig. 9. Measurement of element pattern values and setting the distribution.

Fig. 9, which is drawn so as to indicate a measurement being made on element 2. Loop coupling between the elements is prevented by the serially-fed array of nine directional cross-couplers and the computed distribution

Fig. 8. Laboratory measurement apparatus within anechoic chamber. Nine-element array (top left). Transmitting horn, elevated on rotating arm, is seen near end of travel (top right).



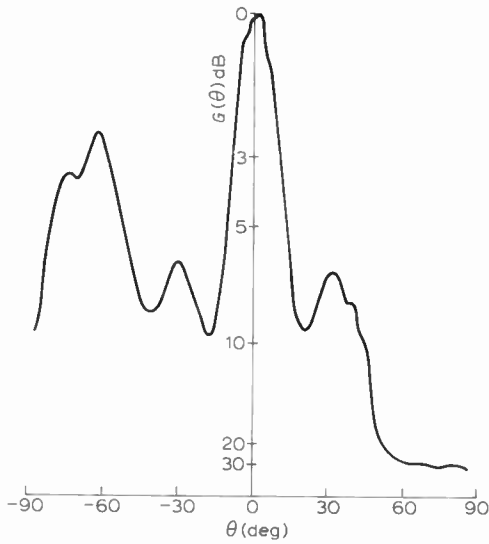


Fig. 10. The first superdirective pattern.

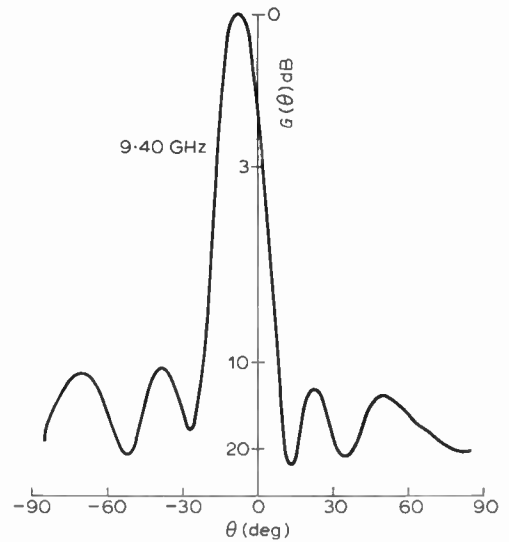


Fig. 11. The final pattern 9.40 GHz.

is applied by using the nine attenuators and nine phase shifters in the feeder arms to the elements. The function of the nine isolators is to prevent the change in mismatch, as the attenuators and phase changers are adjusted, from affecting the elements of the array. The double-ended loads absorb the power flowing along the feeder arms of all the elements other than the one being measured. The nine-element pattern values were measured at nine angles, namely,  $0^\circ$ ,  $\pm 22^\circ$ ,  $\pm 39^\circ$ ,  $\pm 61^\circ$  and  $\pm 80^\circ$ , and the necessary element excitation was computed such that a resultant array far-field pattern would have the same values as the  $\sin 4\lambda u/u$  pattern at these points. The distribution was set up using the same circuit as shown in Fig. 9, and then the double-ended loads were removed so that the array pattern could be measured.

The computed superdirective distribution is shown in Table 4 and the measured far-field pattern is shown in Fig. 10.

This superdirective pattern was steadily improved by careful adjustment of the attenuators and phase shifters in the element feeds and the final superdirective pattern is shown in Fig. 11: the beamwidth at the  $-3$  dB level for this pattern is  $17^\circ$  and the side-lobe level is  $-11$  dB;

the power of the received signal at broadside was  $-10.4$  dB relative to that due to the centre element alone, so that, allowing for the power loss in the attenuators, the relative gain of this superdirective pattern is  $-28.4$  dB. (The power associated with this loss of gain is absorbed by the nine loads terminating the element arms behind the nine directional cross-couplers.) The experimental adjustment of the eighteen controlling attenuators and phase shifters is not as difficult a task as it first appears, because it was found that at any particular state of the pattern, there would be one element that would have a marked effect on the pattern and the other eight would only have a small effect. The variation of the pattern over the frequency range 9.36 GHz to 9.44 GHz is shown in Figs. 12 (a) to (d). For comparison, Fig. 13 shows the measured pattern for a uniform distribution at 9.4 GHz. The beamwidth of this pattern is  $24^\circ$  and the pattern did not significantly change from 9.34 to 9.46 GHz. The measured values of the received signal at broadside, from each element, is shown in Table 5. The figures shown within the brackets in this Table are the corresponding values for the distribution shown in Table 4 and they have been compiled by multiplying the distribution in that Table by the broadside values of the element patterns.

Table 4. The initial superdirective distribution

Element No.	Amplitude in dB	Phase in degrees
1	-20.7	+178
2	-10.9	-164
3	-5.0	+181
4	-1.4	-185
5	0	0
6	-0.8	-191
7	-4.6	+128
8	-10.4	-84
9	-19.1	+146

Table 5. The ratios of the element signals for the superdirective patterns

Element No.	Amplitude in dB	Phase in degrees
1	-16.5 (-19.3)	-41 (+19)
2	-12.8 (-11.8)	-201 (-157)
3	-5.3 (-5.0)	-5 (+24)
4	-1.9 (-1.1)	-182 (-164)
5	0 (0)	0 (0)
6	-1.5 (-1.7)	-169 (-188)
7	-3.0 (-5.0)	+26 (-12)
8	-8.3 (-10.4)	-143 (-202)
9	-14.1 (-19.7)	+29 (-49)

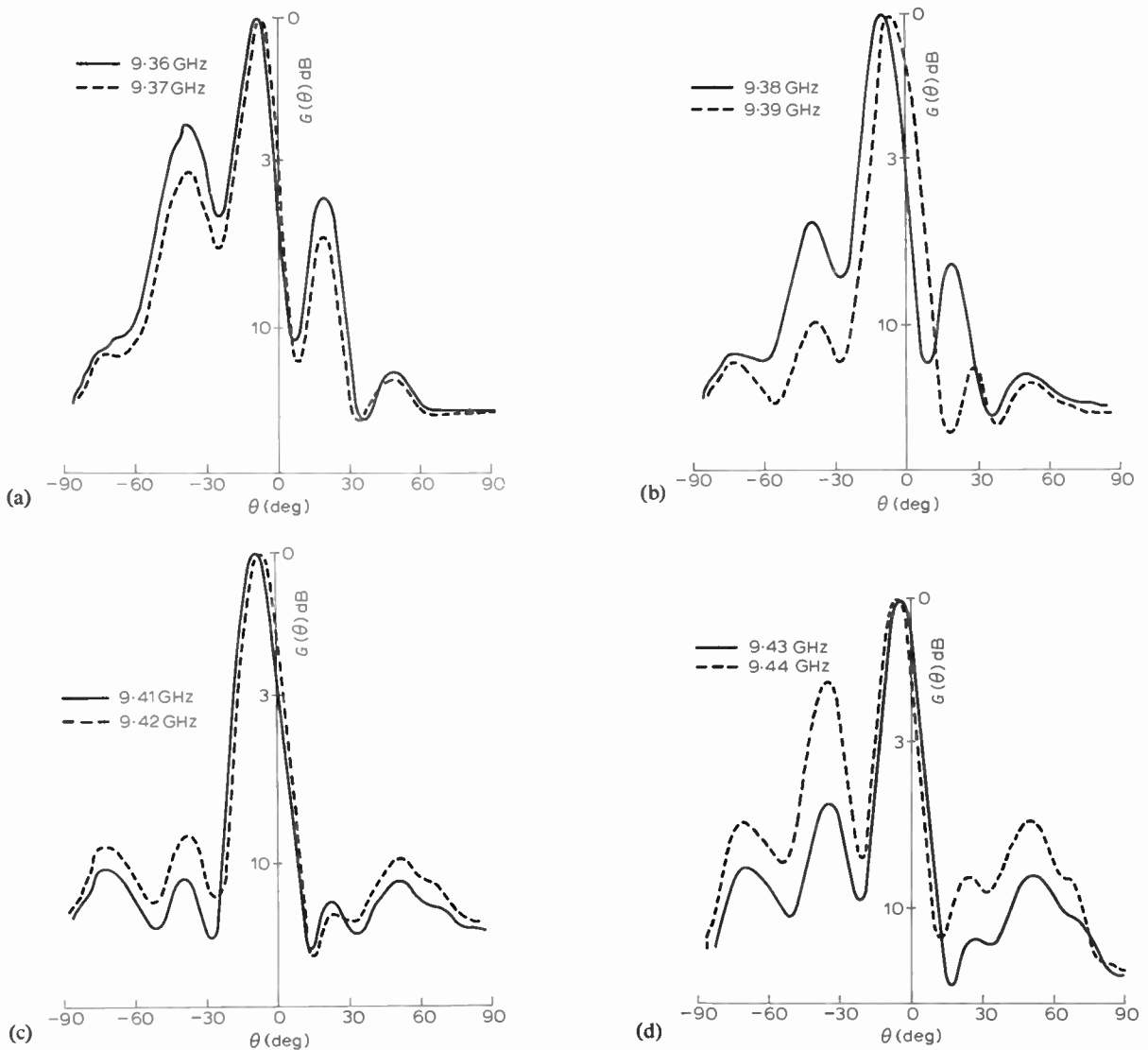


Fig. 12. The final patterns

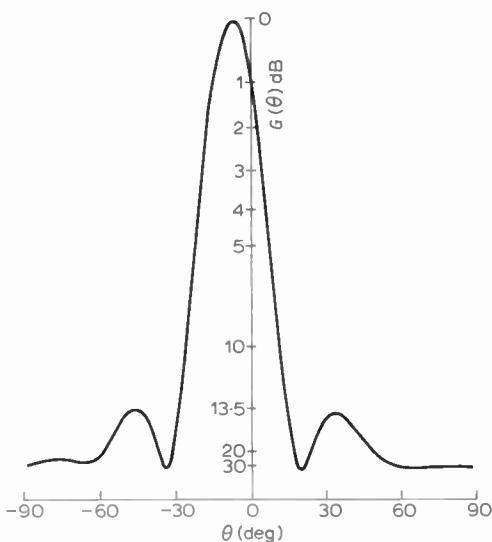


Fig. 13. The pattern for a uniform distribution.

Figures 12 and 13 show that the bandwidth for the superdirective pattern is limited to about 0.4% by the degradation of the side-lobes rather than an increase in the beamwidth. However, the feed system used for this experimental array is frequency sensitive and therefore limits the bandwidth of the superdirective antenna, and the performance of the anechoic chamber will also limit the bandwidth, particularly since reflections from the walls travel over long path lengths and the phase variations over the array from this cause will be particularly frequency sensitive.

### 6 The Reactive Field

A possible limitation on the use of a superdirective array is the associated reactive field. An indication of the variation of the field around the array can be obtained by calculating the variation in the electric field moving out from the array in both the broadside and end-fire directions. Calculations have been performed, in conjunction with Mr. B. R. Gladman of A.S.W.E., for

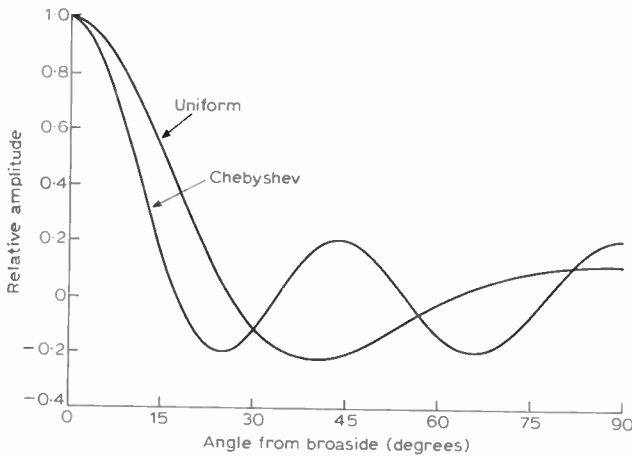


Fig. 14. Patterns for uniform and Chebyshev arrays of nine elements spaced  $0.25\lambda$  apart.

arrays of small dipole elements.<sup>14</sup> The electric field parallel to the dipole and at a distance  $r$  along the normal from the centre of the dipole, can be expressed as<sup>18</sup>

$$E_z = C \left( \frac{1}{kr} - \frac{j}{(kr)^2} - \frac{1}{(kr)^3} \right) \exp(-jkr) \quad (19)$$

where  $C$  is a constant and  $k = 2\pi/\lambda$ .

A  $2\lambda$  nine-element array was considered, with an element spacing of  $\lambda/4$ , for the uniform amplitude distribution case and for a superdirective Chebyshev pattern with a side-lobe ratio of 0.2 (side-lobes about  $-14$  dB). These two far-field patterns are shown in Fig. 14. The relative values of  $E_z$  were calculated using

equation (19) and the results are shown in Fig. 15(a) for the broadside direction, and in Fig. 15(b) for the end-fire direction. The far-field is usually taken as starting at a distance of  $2D^2/\lambda$  from the antenna and it can be seen for the uniformly excited antenna that the field is in fact decreasing by  $1/r$  at the distance of  $8\lambda$  from the antenna. The beamwidth of the superdirective array is approximately equal to that of a  $3\lambda$  uniformly excited array, and it is clear from Fig. 15(a) that its field is certainly decreasing by  $1/r$  at a distance of  $17\lambda$  from the array. It is also clear from this figure that the large reactive field associated with the  $2\lambda$  superdirective antenna does not extend beyond  $0.25\lambda$  in front of the antenna, and that over the region  $0.01\lambda$  to  $0.1\lambda$ , the field due to the superdirective distribution is two orders of magnitude greater than that due to the uniform distribution. Figure 15(b) shows the relative field strengths in the end-fire direction for the two cases and taking the relative field value of 1 as a guide, since this would appear reasonable from Fig. 15(a), then the field for the superdirective distribution falls to this value at a distance of  $1.115\lambda$  from the centre of the array, or  $0.115\lambda$  outside the end element, and for the uniform distribution, the distance is  $1.107\lambda$  or  $0.107\lambda$  outside the end element. Clearly, the field in the end-fire direction for the superdirective distribution is not significantly different in practical terms from the fields for a uniform distribution.

The effect of a quadratic phase error in the distribution on a superdirective pattern has been looked at in more detail by calculating the electric field  $E_z$  at  $1^\circ$  intervals between  $0^\circ$  and  $50^\circ$  at several distances from an array of nine dipoles spaced  $0.25\lambda$  apart. The value of  $E_z$  for each dipole was calculated using equation (19) and the

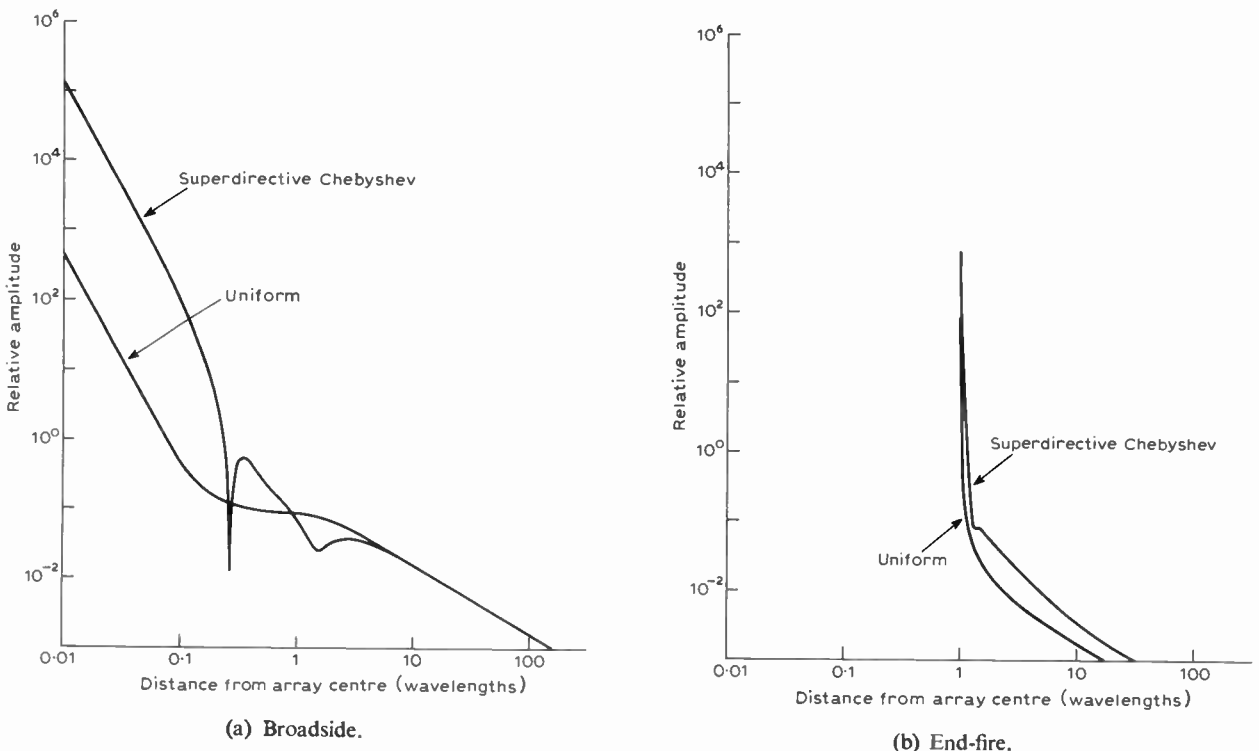


Fig. 15. Variation of  $E_z$  for uniform and Chebyshev arrays of nine dipoles spaced  $0.25\lambda$  apart.

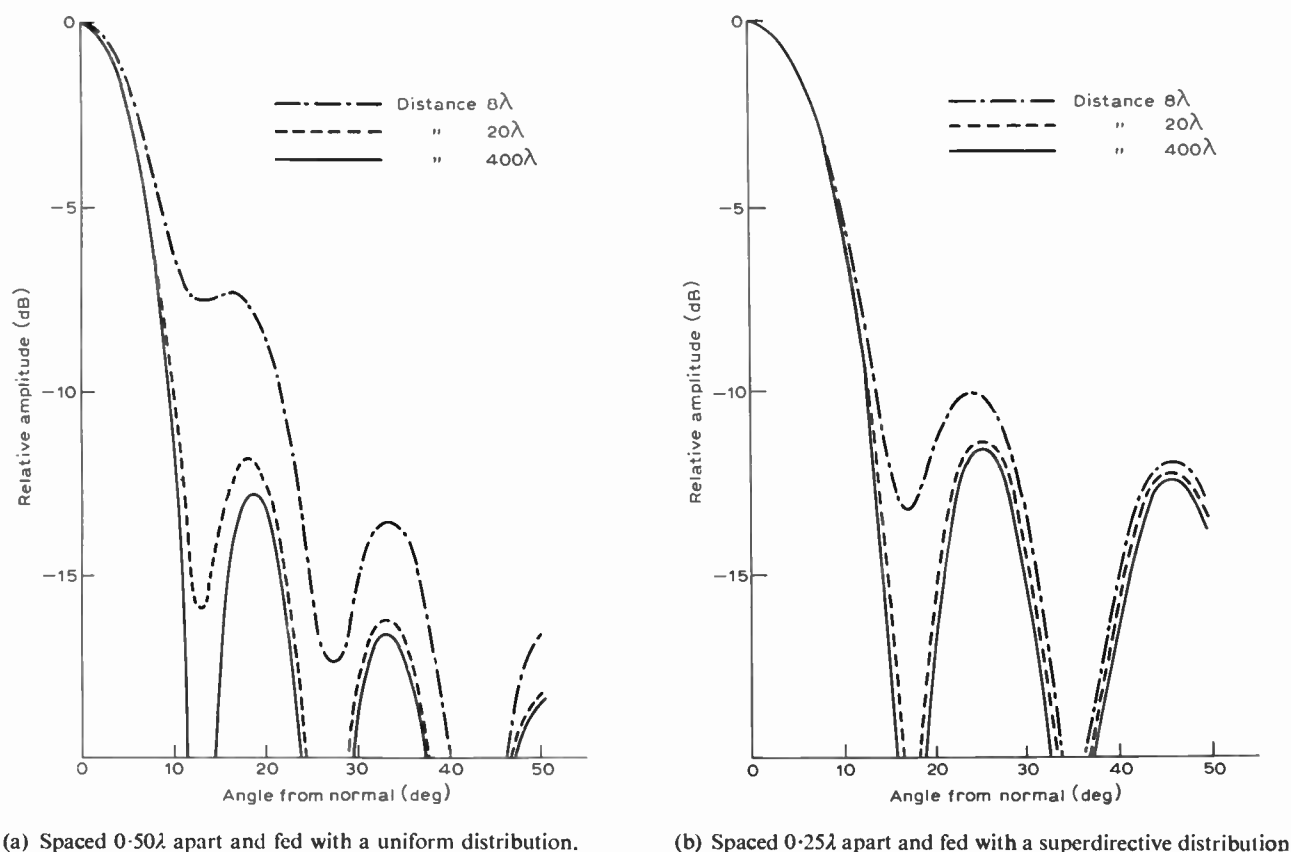


Fig. 16. Variation of radiated field pattern with distance for nine dipoles.

superdirective distribution used was that required to give curve 4 in Fig. 5. For comparison, the calculations were also done for the case when the array is excited uniformly, but with the dipoles  $0.5\lambda$  apart giving an array length of  $4\lambda$ . The patterns at the distances of  $8\lambda$ ,  $20\lambda$  and  $400\lambda$  are shown for the uniform and superdirective distributions in Figs. 16(a) and (b) respectively. These two figures clearly show that the superdirective pattern is no more sensitive to quadratic phase error than is the uniform distribution pattern. However, a superdirective pattern is much more sensitive to random errors in the distribution than is a non-superdirective pattern.

## 7 Conclusions

Small superdirective antennas have been made to work in recent years by overcoming one of the biggest problems associated with mutual coupling between the elements, namely, that of loop-coupling through the feed network. The bandwidths achieved have been usable but very much smaller than that obtainable for non-superdirective antennas. However, certainly in the case of the antenna constructed by the author, the measured bandwidth is restricted more by the radiator feeding system and the measuring site than by the fundamental bandwidth restrictions of superdirective antennas. This limitation stems from the necessary accuracy with which the element signals have to be added together in order to achieve superdirectivity, and this requires that the element signals change very slightly with frequency which in turn requires

that the impedance seen by the elements does not change with frequency. As far as the instantaneous bandwidth is concerned, one cannot overcome the change in the element spacing with frequency, in terms of wavelengths, and one can only use very small elements in order to very severely suppress the higher order modes of excitation, which may be induced by mutual coupling, but one would expect to be able to construct a two- or three-wavelength superdirective antenna with a bandwidth of a few percent and with a beamwidth equal to that of a non-superdirective antenna about twice the size. The tolerance problems would probably be too severe if the degree of superdirectivity or the antenna size were increased beyond this.

The reactive field associated with superdirectivity is confined to the immediate vicinity of the antenna and the far-field of the antenna starts at a distance which is no further from the antenna than the far-field of the equivalent non-superdirective antenna.

## 8 Acknowledgments

I would like to thank Professor J. Brown and Mr. H. Page of Imperial College, London University, for their help and encouragement, Miss E. A. Killick of the Admiralty Underwater Weapons Establishment, who originally aroused my interest in superdirectivity and multiple beam networks, and Professor J. Crony and Mr. B. R. Gladman of the Admiralty Surface Weapons Establishment for their many very useful discussions and

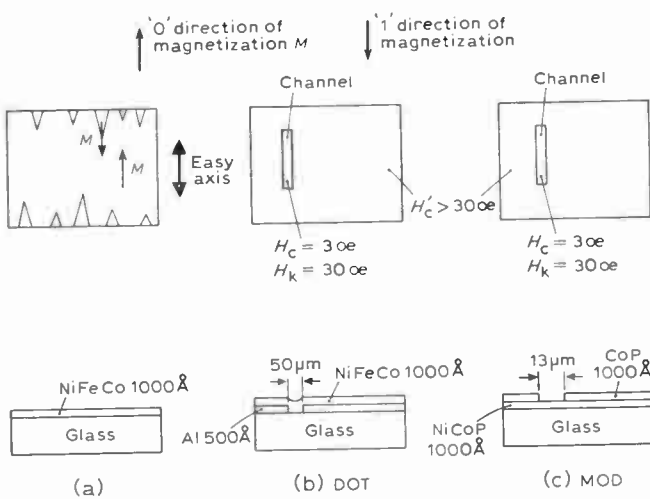


Fig. 1. Magnetic film structure for domain tip memories.

cost to become competitive with fixed head disks with improved performances. Bit densities of 14 000 bits/cm<sup>2</sup> are obtained in the new MOD design which are sufficient to fabricate products comparing advantageously with equivalent bubble or semiconductor memories.

2 Basic Principles

A magnetic thin film suitable for domain propagation must have a uniaxial anisotropy field  $H_k$  several times larger than the coercive force or the threshold for domain wall motion  $H_c$ . Thus a field  $H_a$  applied on a large area of the substrate along the easy axis in order to propagate a domain will not nucleate other domains in low coercivity channels when the expression  $H_c < H_a < H_k$  is satisfied with some tolerances.

For example, in the MOD,  $H_c = 3$  Oe,  $H_a = 13$  Oe,  $H_k = 30$  Oe. When such a film is deposited on a glass substrate without channel as illustrated on Fig. 1(a), nucleation of unwanted domain occurs on the edges of the substrate, because of strong demagnetizing fields.

Figure 1(b) shows how nucleation in the channels of an evaporated structure may be avoided; the coercive force of the magnetic film  $H'_c > H_k$  wherever it is evaporated on top of an aluminium film of high roughness raising the coercivity through short period variations in the magnetic film thickness.<sup>2</sup>

Another means of avoiding nucleation in the channels is illustrated by Fig. 1(c) in which a hard magnetic layer is deposited by a wet chemical process on top of a continuous soft magnetic layer where the channel pattern has been protected from this hard magnetic layer by a photoresist.

Under the hard layer, the soft layer is exchange coupled and if the hard layer is initially magnetized along the zero or no domain easy axis direction, the coupled soft layer will not switch toward the one direction or a domain extend before a large field  $H'_c > H_k$  is applied. In the MOD structure the hard layer has a coercive force of 600 Oe and  $H'_c = 50$  Oe.

The write function is performed through the application of a local magnetic field preferably at 45° off the

'1' direction of magnetization and usually by the coincidence between a current in the advance conductor and another current in a 'write' conductor orthogonal to the advance conductor.

Read-out is much more efficient than in former random access high-speed thin film memories because of two basic properties of domain tip shift registers. The domain tip velocity is limited to about 10<sup>5</sup> cm/s and because the signal sensing conductor is usually placed at a distance of at least 100 µm from the step before the last domain tip location, a delay of at least 100 ns exists between the start of the domain propagation and the beginning of the read-out signal.

Thus the current transition stray pick-up falls outside the signal which can be easily strobed devoid of system noise. The second property refers to the splitting of domain in branching channels as schematically shown in Fig. 2(a). This allows, within a limited number of steps, the sensing of several domains simultaneously for one incoming domain at the branching entry. The multiplying factor will result from a compromise between space taken on the substrate and signal amplitude. The signal lasts for several hundreds of nanoseconds and being devoid of system noise, an amplitude of 0.5 mV is sufficient for a safe detection with a signal-to-noise ratio larger than 20 dB. An amplitude up to 4 mV has been used in the DOT. The electrical signal will result from a flux variation when the magnetic charge carried by the domain tip crosses the flat coil conductors as shown on Fig. 2(b). Such a read-out station is space-consuming and restricted to large registers, 4.352 bits in the MOD, or is shared by a set of recirculating register loops as in the DOT. Another sensing scheme makes use

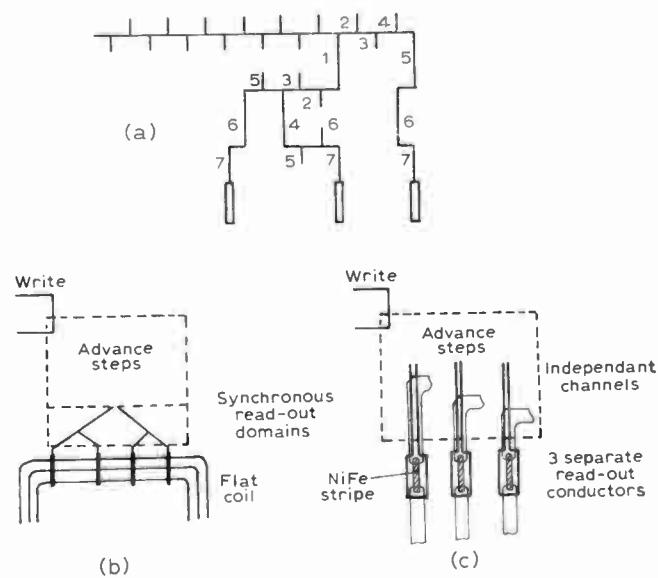


Fig. 2. Signal enhancement in inductive pick-up read-out and magnetoresistive read-out disposition.

- (a) A domain present in 1 at time T1 arrives in the three read-out enlarged channels in 7 synchronously at time T7.
- (b) Inductive pick-up read-out.
- (c) Magneto esistive read-out.

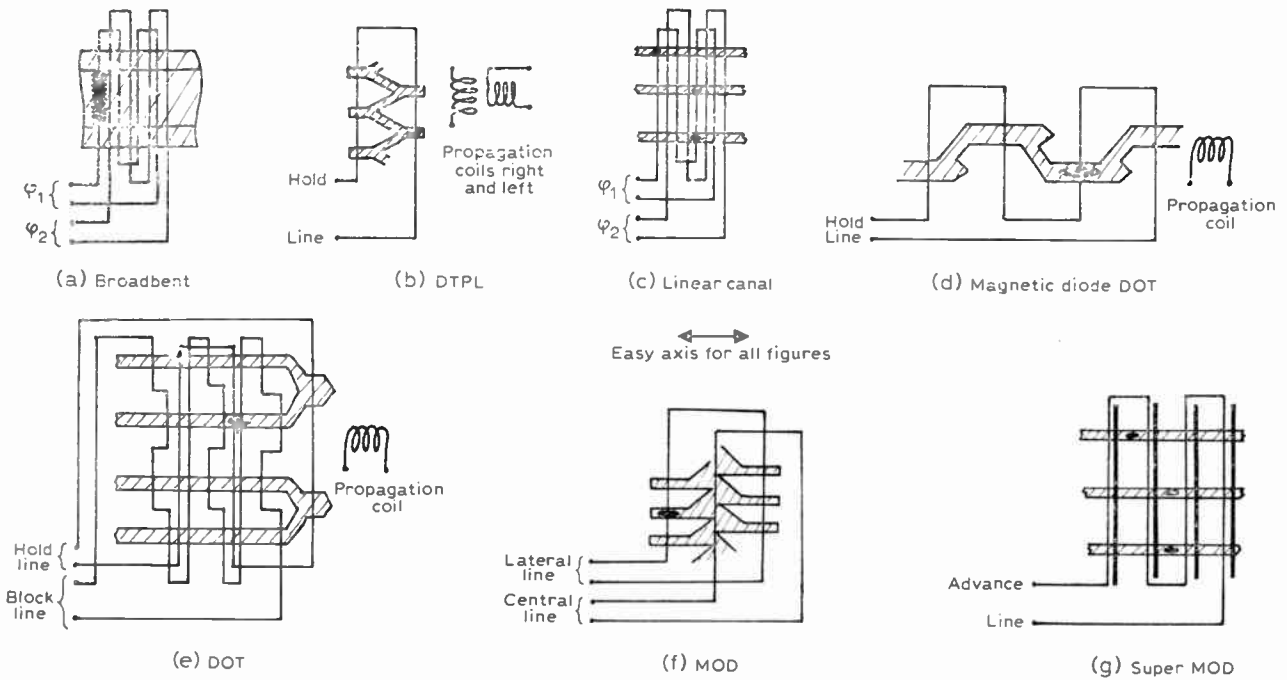


Fig. 3. Domain tip memory structures

of the magnetoresistive effect in a NiFe strip located above the read-out domain. Figure 2(c) illustrates such a scheme where the easy axis of magnetization for the magnetoresistive strip is orthogonal to the easy axis of the domain propagation film. Although direct observation of domains on the strip has not been possible because of edge contrast, it can be assumed that multiple antiparallel domains with transverse magnetization exist in the rest state, corresponding to a lower energy state and magnetization rotation occurs during the domain propagation excitation at a level depending upon the presence or the absence of a domain. For a given read-out channel, the signal can be five times larger in the magnetoresistive station as compared with the flux pick-up station which implies that the magnetoresistive read-out will be preferred with a short register scheme as used in the new super MOD technology where little space is available at each read-out location.

Domain conservation in 1000 Å permalloy type thin film occurs without external means and up to stray field of 1 Oe for domain size larger than 10 × 100 μm; this is the case for most of previous DOT and MOD schemes where stray fields smaller than 1 Oe are obtained with simple substrate shielding. However, higher densities can be obtained only with smaller domains and a static field of a few oersteds must be applied on the domain storage locations. Fortunately the domain magnetization on a super MOD substrate occurs in the plane of the film and this static field is applied by the lines of magnetic charge existing at the edges of hard magnetic film stripes deposited with the advance conductor. Thus, very small domains can be sustained without the need of external coil or magnet. Domain of 5 × 30 μm are stable without external applied field in the present super-MOD design.

### 3 Domain Tip Structures

Quite a few structures have been experimented with, always aiming at higher densities, simplification of the layout to increase manufacturing yields and easier driving currents requirements to minimize the power required and the cost of the associated electronics. All these structures have used nearly the same basic soft magnetic thin film of 1000 Å thickness, either an evaporated NiFeCo or a chemically deposited NiCoP of similar characteristics,  $H_c = 2$  to 4 Oe,  $H_k = 25$  to 30 Oe, where dispersion and skew are not critical,  $\alpha = 90$  and  $\beta \leq 5^\circ$ . Uniaxial anisotropy usually parallel to one edge of the rectangular 0.5 mm thick glass substrate is field induced during film deposition. The most significant structures are shown in Fig. 3 in order of birth in various laboratories. A more detailed description can be found in the literature.<sup>1, 2, 4-7</sup> The main features of these implementations are listed in Table 1 where it can be seen that the DOT technique improvements<sup>8</sup> are directed toward a simplification of the structure with a decrease in clock cycle time and power supply requirements. MOD improvements are seen to be geared toward higher bit densities with a lower power and shorter average access time. Most driving currents are bipolar current pulses of 500 mA to 950 mA amplitudes except in the new designs where it is lowered at least to 250 mA for the 'super MOD'.

### 4 Prototypes and Products

Several prototypes of memories ranging from 0.1 to 2.3 Mbit capacity have been demonstrated and delivered, mainly to government agencies which use the DTPL, the DOT and the MOD techniques.

Figure 4 illustrates a MOD prototype of a television image refresh memory of 2.3 Mbit capacity. The MOD 500 substrate has a 35 000 bits capacity, however a maximum bit rate of 61 Mbit/s is required to refresh the television image and the substrate has only one read-out conductor allowing a maximum bit rate of 0.35 Mbit/s per substrate. Therefore 176 substrates must operate in parallel, meaning that only 13 000 bits per substrate are utilized.

The power requirement is 1600 watts at maximum clock rate, that is  $26 \text{ W}^{-1} \text{ Mbit}^{-1} \text{ s}^{-1}$ , 220 watts at low clock rate and the stored data is non-volatile with power off. The measured error rate in severe configuration is  $10^{-9}$  before correction for the entire 2.3 Mbit memory. The use of a single error correcting code in the controller will reduce this error rate to  $10^{-13}$ . This prototype has been tested in ambient air temperature from 0 to 50°C without increase of the error rate. The MOD memory drawer is on the top of the rack shown in Fig. 4 and houses 22 memory cards. Eight MOD 500 substrates are mounted on each card, potted against a small printed circuit board with interposed heat-conducting plate and a magnetic shield foil; Fig. 4 also shows a memory card.

Another prototype built with MOD 500 substrates is a small disk replacement memory to be used as auxiliary memory for a minicomputer with a controller allowing a sector search, error detection and correction.

A more publicized domain tip memory prototype has been demonstrated recently in Germany, a DOT memory of 2 megabit capacity intended for process control applications.

As we mentioned earlier, domain tip memories have not yet obtained large commercial acceptance and the only product proposed so to speak 'on the shelf' is the DOT-microstore of low performance characteristics and large volume per bit, however with a cost per bit competitive with core memory cost. The measured error rate is of the order of  $10^{-9}$  before correction. Other products may be issued shortly for customer special requirements, very likely with the newer and higher density designs.

## 5 New Domain Tip Memories

Little is yet known of the development of the new DOT memories. Tentative general characteristics are indicated in Table 1,<sup>8</sup> and fabrication costs should be low. We shall report mostly on the super-MOD development.

Fabrication of the super-MOD memory substrate is similar to that of the MOD 500 substrate with the successive deposition on a glass  $6.35 \times 5.72$  cm substrate of the following layers.

- 1000 Å NiCoP electroless
- 1000 Å CoP electroless
- 5 µm polyimide spun and baked
- 2000 Å NiFe electrolytic
- 3 µm copper electrolytic
- 5 µm polyimide spun and baked
- 500 Å Co electrolytic
- 8 µm copper electrolytic.

Table 1. Characteristics of the main domain tip techniques

	Bit density bit/cm <sup>2</sup>	Channel width µm	Soft magnetic film	Number of conductor layers for propagation	Nature of conductors	Number of coils around substrate	Clock cycle time µs	Typical length of registers bits
<i>Previous studies:</i>								
Broadbent <sup>1</sup>	50	2000	1000 Å evaporated NiFeCo	2	flexible printed circuit	0	—	—
DTPL <sup>2</sup>	300	50	1300 Å evaporated NiFeCo	1	flexible printed circuit	2	2	2000
Magnetic diodes	300	50	1300 Å evaporated NiFeCo	1	flexible printed circuit	1	2	—
<i>Available:</i>								
DOT	600	50	1000 Å evaporated NiFeCo	2	flexible printed circuit	1	30	114 recirculating loops
MOD 500	3000	13	1000 Å electroless NiCoP	2	electro-deposit on substrate	0	2.8	4352
<i>New designs:</i>								
Super-MOD	14 000	13	1000 Å electroless NiCoP	1	electro-deposit on substrate	0	1.6	512
New DOT (tentative)	5000	25	1000 Å evaporated NiFeCo	2	flexible printed circuit	0	6	128 to 12 k

Chrome masks are used to define the photoresist patterns to build up the CoP, the NiFe and the copper layers. Edge definition of the resist is of the order of  $\pm 1 \mu\text{m}$  which allows the use of proximity printers, ensuring more than 20 exposures before it is necessary to clean the chrome masks.

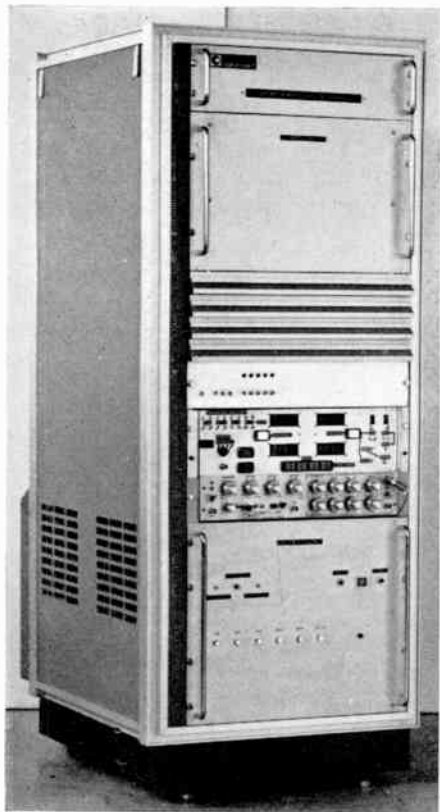
These masks are copies from emulsion master masks generated directly from a programmed light slot. The most critical registration between layers is within  $5 \mu\text{m}$ , easily obtained with standard semiconductor type mask aligners.

The first polyimide layer, the NiFe and first copper layers, can be omitted when the read-out is performed through flux variation rather than magnetoresistance as is possible when fewer read-out stations are implemented on one substrate.

### 5.1 Domain Propagation

The basic propagating structure is illustrated in Fig. 5. The magnetization in a domain is designated by the vector  $M_1$  antiparallel to  $M_0$ , the initial direction of magnetization of the soft magnetic film. Two channels are seen on Fig. 5 with the location of three domains previously propagated and remaining after the end of the current flow in the advance conductor. These domains constitute two characters, 10 and 11, separated by one shifting step. The size of the domains is typically about  $5 \times 20 \mu\text{m}$  and they are prevented from collapsing by a magnetostatic field of 5 Oe issued from the magnetic stripes of high coercive force,  $H'_c \approx 150 \text{ Oe}$ , indicated by the shaded areas of Fig. 5, which are located on top of the insulating layer. The magnetization orientation of the hard magnetic film coupled to the soft film is obtained after fabrication through the application of a 1300 Oe field parallel to  $M_0$ .

The direction of magnetization of the magnetic stripes is obtained by the application of a 300 Oe field antiparallel to  $M_0$ . Consequently alternate lines of magnetic charges + and - occur on the edges of the magnetic stripes, creating a demagnetizing field under the stripes and magnetizing between stripes. This magnetizing field

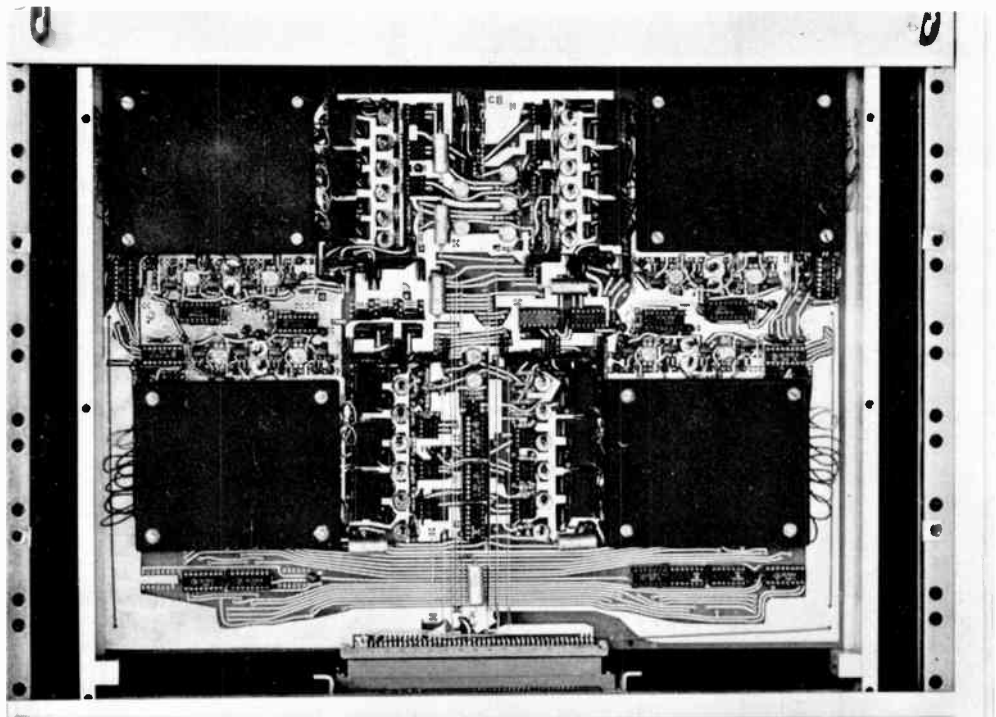


MOD memory  
2.3 M bit.

Test and  
control

Power supply

Fig. 4.  
(above) Prototype for a television image refresh memory using MOD 500 memory cards.  
(right) Prototype MOD 500 memory card.



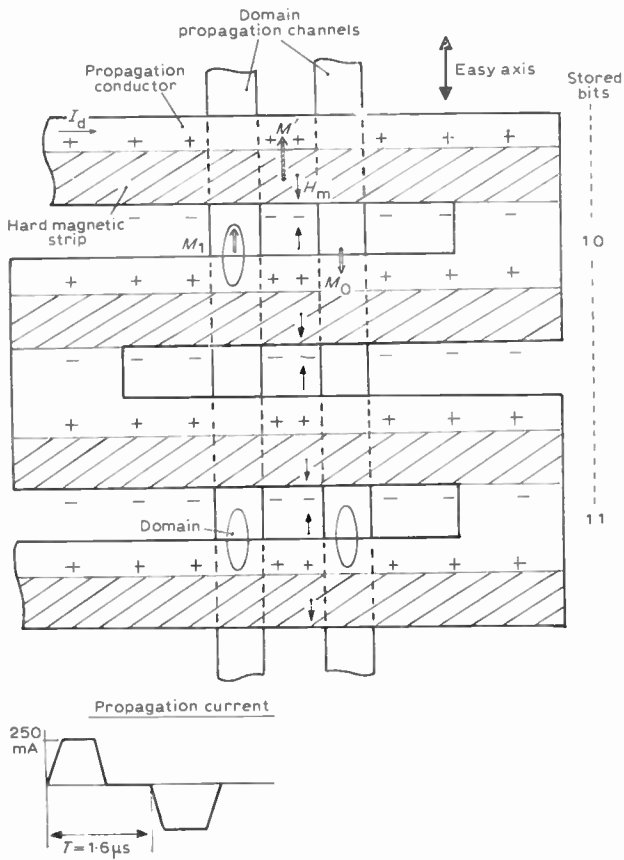


Fig. 5. Domain propagation.

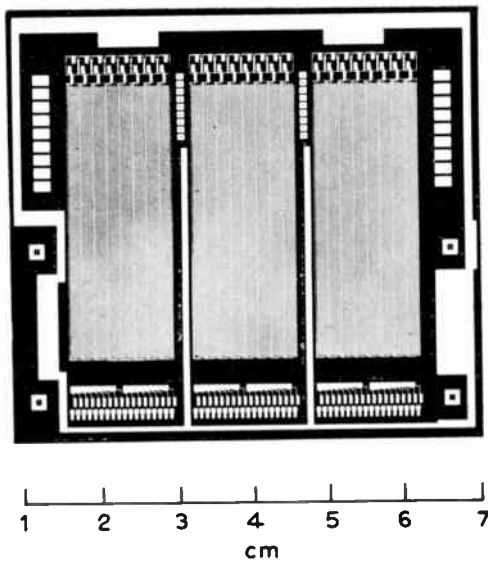
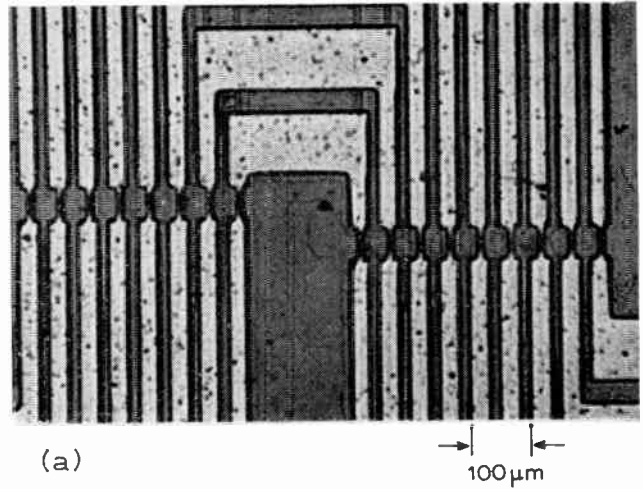
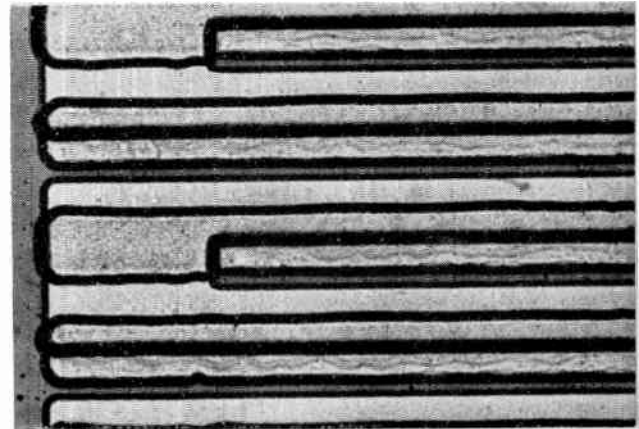


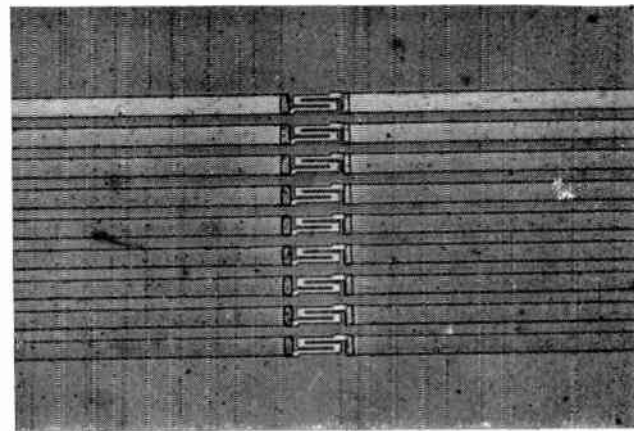
Fig. 6. Super-MOD substrate (Advance conductor level).



(a)



(b)



(c)

Fig. 7.

- (a) Super-MOD substrate. Detail of the 'write' conductors four channels can be seen in the centre area.
- (b) Super-MOD substrate. Detail of the 'advance' conductor.
- (c) Super-MOD substrate. Detail of the magnetoresistive read-out stations.

is offset with respect to the conductor with one tip engaged under the conductor edge in the direction of propagation.

When a current pulse of suitable polarity  $I_d$  is flowing through the advance conductor, the domain grows under the conductor where its tip was engaged until it reaches the next domain conservation location. However, the other end of the domain is erased when the current polarity reverses, and particularly so considering that domain erasure is several times shorter than domain growth. One complete shift step takes two pulses of opposite polarity.

The super-MOD substrate is organized in two-phase registers with one character written and read out at each advance current polarity of 1.6  $\mu$ s. The bit rate on one substrate with a character format of 8 bits corresponding to 16 domain propagation channels under every advance conductor is therefore 5 Mbit/s.

An experimental substrate is illustrated in Fig. 6. It contains 24 full-sized advance conductors or selections of 18 channels of 256 bits, each working in one two-phase register of 512 characters of 9 bits (one redundant). The 9 write conductors are common to the 24 selections. The read-out stations of channels of same rank are chained in 3 groups of 8 selections.

Figure 7 illustrates details of the structure. In Fig. 7(a) the write conductor narrows can be seen and propagate conductors are seen in Fig. 7(b). The small threefold pattern of the magnetoresistive NiFe element is shown in Fig. 7(c); for maximum read-out signal<sup>9</sup> the length is the maximum compatible with the size of the read-out domain, about 100  $\mu$ m long and 40  $\mu$ m wide.

Propagation current margins on experimental full-size registers are typically  $250 \pm 50$  mA on a channel free of defects and when the uniformity of the magnetic layers stays within 10% of the nominal thickness.

On these bases and introducing some redundancy on the substrate, acceptable fabrication yields can be obtained with simple equipment. Nevertheless, careful chemical bath filtration, control of liquid motion, temperature, pH, great care concerning the cleanliness of the photoresist process and controls has proved necessary as for the fabrication of any high level integration device.

## 6 Conclusion

The high density of the super-MOD technique enables 160 000 bits to be integrated on one glass substrate  $6.35 \times 5.72$  cm. The accompanying low power requirement of 2 W/Mbits<sup>-1</sup> and a clock cycle of 1.6  $\mu$ s makes it a serious competitor for bubble memories in the implementations of FAM memories, recorders and other auxiliary memories. Domain tip memories are becoming cost competitive with other techniques while retaining unique features that should allow the definition of new attractive products.

## 7 Acknowledgment

The development of the MOD technology has been supported by the French Government agencies SEFT and DRME.

## 8 References

1. Broadbent, K. D., 'A thin magnetic film shift register', *IRE Trans. on Electronic Computers*, EC-9, No. 3, pp. 321-3, September 1960.
2. Spain, R. J., 'Controlled domain tip propagation', *J. Appl. Phys.*, 37, No. 7, pp. 2572-83, pp. 2584-92, June 1966.
3. Bobeck, A. H., 'Properties and device applications of magnetic domains in orthoferrites', *Bell Syst. Tech. J.*, 46, No. 8, pp. 1901-25, October 1967.
4. Spain, R. and Marino, M., 'Magnetic film domain wall motion devices', *IEEE Trans. on Magnetics*, MAG-6, No. 3, pp. 451-63, September 1970.
5. Spain, R. J. and Jauvtis, H., 'Dot memory technology', INTER-MAG 1974.
6. Battarel, C., 'MOD: a new generation of domain propagation memories with a high performance/cost ratio', Colloque International sur les Mémoires, Paris 1973, pp. 318-28.
7. *Inter-Electronique*, 5th April 1976, p. 2.
8. Henkler, H., BASF, private communication.
9. Bobeck, A. H. and Della Torre, E., 'Magnetic bubbles', 'Selected Topics in Solid State Physics', vol. XIV, p. 191, Gordon & Breach, London.

*Manuscript received by the Institution in final form on 22nd November 1976. (Paper No. 1760/CC269.)*

© The Institution of Electronic and Radio Engineers, 1977

# Microwave diffraction for steel strip detection

R. J. TEPERER, B.Eng., Ph.D., C.Eng., M.I.E.E.\*

and

G. S. HOBSON, B.A., Ph.D., C.Eng., M.I.E.E.†

## SUMMARY

A system has been devised and tested successfully in a laboratory mock-up to tackle the problem of detecting the presence of a metal strip in the particularly hazardous environment of a steel works. This paper briefly outlines the environmental problems, and how they defeated more conventional techniques, before moving on to the basic principles involved with using microwave diffraction for detecting the strip. Modifications are then described to the fundamental concept which are needed to overcome practical problems.

The paper finally outlines how the technique can be installed into the existing bed with very little disruption to the practical set-up and also gives a rough idea of costs involved.

## 1 Introduction

During steel production red-hot strip (still in a plastic state) is taken from rolling mills to a coiling machine along a bed, as depicted in Fig. 1. Some means of identifying its presence is needed in the region of this bed so that the coiling machine can be alerted. Automatic detection of the presence of the strip has not been satisfactorily attained in the past due to severe environmental conditions. Interrupting light beam techniques failed since either the receiving or transmitting lens needed to be situated beneath the moving steel strip and thus the lens became blocked with a mixture of scale (from the red-hot strip) and cooling water (used to prevent heating up of the bed by the continuous passage of red-hot steel strip). Infra-red detectors also proved unreliable because

\* Formerly at the University of Sheffield; now at the Zentrallaboratorium für Nachrichtentechnik, Siemens A.G., München, West Germany.

† Department of Electronic and Electrical Engineering, University of Sheffield, Mappin Street, Sheffield, S1 3JD.

the cooling water tended to produce regions of cooler metal along the length of the red hot steel strip which were often interpreted wrongly as signifying the end of a strip.

Further difficulties imposed on any proposed system includes the limited possibilities for siting any instrumentation. Referring to Fig. 1, instrumentation can only be situated under one or more of the grates set into the bed (where it must withstand a constant trickle of scale-contaminated water) or behind a window in the side wall or in both positions. The remaining side and the area above the bed must be left clear to allow unrestricted access to the bed for overhead cranes.

A suitable system must be able to detect a 15 cm wide steel strip anywhere in the 60 cm width of the bed and allow for possible lifting of the strip by as much as 60 cm above the bed.

This paper offers a laboratory mock-up solution to the problem of detecting the presence of a steel strip on this bed by the use of a microwave diffraction technique which will obviate all of the mentioned environmental hazards.

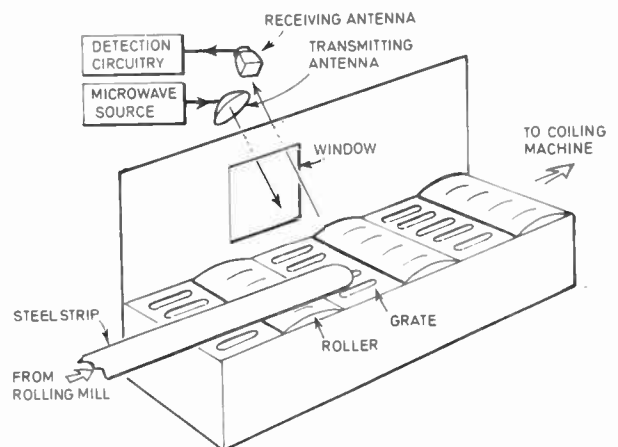


Fig. 1. Sketch of the section of bed with detection equipment installed.

## 2 Principle of the Technique

Consider one of the grates of the bed, shown in Fig. 1, illuminated with microwaves from an antenna mounted behind a window in the side wall. Energy falling on each rung of the grate will be scattered over a wide range of angles above the grate. However, providing the illuminating wave has a plane wave-front then the scattered energy from all the rungs will interfere constructively along directions where path lengths differ by an integral number of wavelengths. Figure 2(a) shows diagrammatically a cross-section of the situation where the wavelength of illumination  $\lambda_R$  is given by

$$\lambda_R = 2d \cos \theta$$

This condition gives rise to a preferred direction which is the exact reverse of the direction of illumination.†

† Jenkins, F. A. and White, H. E., 'Fundamentals of Optics' (McGraw-Hill, New York, 1957).

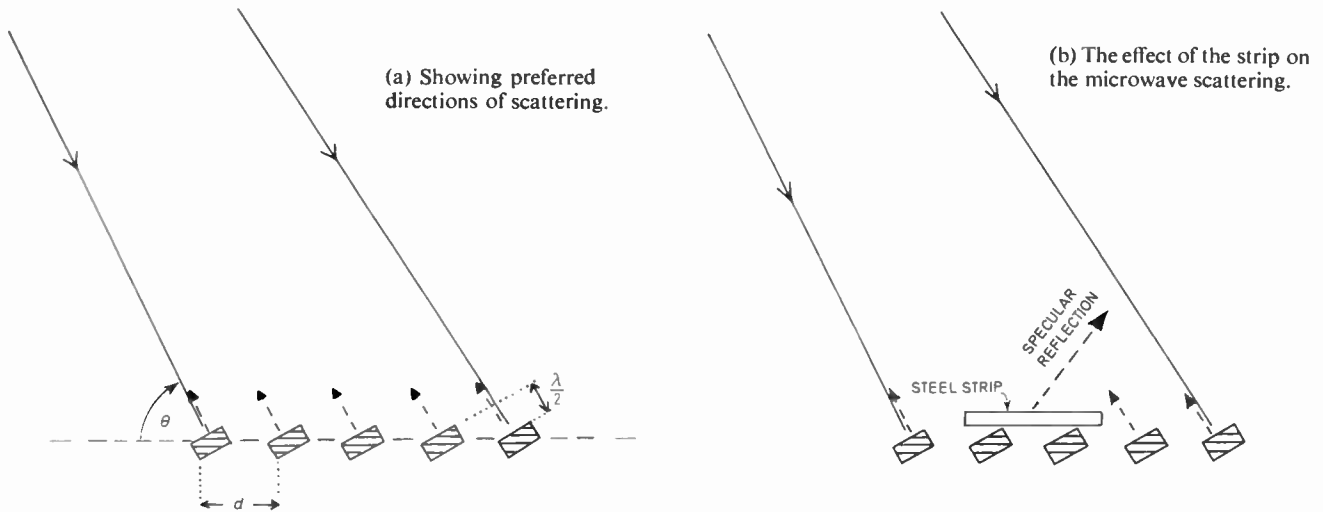


Fig. 2. Cross-section through rungs of a grating illuminated by a plane beam of microwave energy.

Thus a receiving antenna adjacent to the transmitting antenna will detect a strong backscattered energy. Now suppose a metal strip is present over some portion of the grate, as depicted in Fig. 2(b). All the energy incident upon the strip undergoes specular reflection and thus the energy backscattered to the receiving antenna is reduced by an amount dependent upon the number of rungs blocked off by the strip. This reduction in backscatter can then be converted into a signal identifying the presence of a steel strip over the grate by circuitry shown in block diagram form in Fig. 3. Comparison of the backscattered signal with a set ratio of the output of a peak detector rather than a set voltage compensates for long-term changes in the system such as power output from the illuminating antenna and scattering properties of the rungs of the grate.

The envisaged positioning of the individual components is as shown in Fig. 1. In an observed rolling mill (British Steel Corporation's Brinsworth Mill, Rotherham, U.K.),  $d$  is approximately 3.75 cm and a convenient value for  $\theta$  is approximately 60 degrees. This gives a value of  $\lambda_R$  corresponding to a frequency at the lower end of X-band which renders components reasonably cheap and accessible.

### 3 Performance of a Laboratory Simulation of the System

An experimental grate was constructed consisting of flat aluminium reflectors set in a perspex frame measuring 60 cm by 23 cm (the reflectors running parallel to the short side). The length of the reflectors (fifteen in all) was approximately 20 cm, the width was 1.9 cm. The spacing and angle of the reflectors could be independently adjusted. The adjacent antennas used were (i) a 30 cm diameter parabolic dish for transmitting with a beamwidth of approximately  $9^\circ$  at X-band and fed by a signal amplified by a travelling wave tube with a capability of 2 W output, and (ii) a  $30^\circ$  phase angle horn antenna coupled to coaxial crystal detector followed by a d.c. amplifier for a receiver. The separation between grate

and antenna was approximately 2 m so account had to be taken of the spherical wavefront of the illuminating microwaves.

A simple geometrical optics adjustment was adopted. The transmitting dish antenna was considered as a point source at some point, A, behind the dish at distance calculated such that the diameter of the dish would subtend an angle of  $9^\circ$  (the beamwidth) at point A. Point A was assumed to be both the source of illumination and the point of backscatter detection (a simplification that can only be justified by the fact that the experimental tests performed satisfactorily) and was considered to subtend an angle of  $60^\circ$  with the plane of the experimental grate at its centre rung. The position of the remaining rungs of the experimental grate were then adjusted so that, with an illuminating frequency of 8 GHz, the distance between point A and the rung in question differed by only a half wavelength from the distance between point A and either of its neighbours. The angle of the individual rungs was set normal to the wavefront so that the backscattered signal pattern would have a principal maximum in the direction of the receiving antenna. This adjustment is the microwave realization of the blazed diffraction grating in the visible frequency range.† The receiving antenna was again a waveguide horn placed adjacent to the parabolic dish.

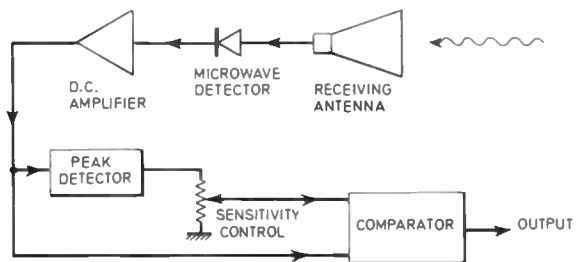


Fig. 3. Block diagram of circuit for detecting presence of steel strip over a grate.

† See previous footnote.

Figure 4 shows plots of received backscatter intensity versus frequency for the experimental set up. It can be seen that at the optimum operating frequency, a decrease in backscatter power of almost 3 dB occurs when 15 cm (worst case) of the 60 cm experimental grate is covered by a steel strip. In this particular case the signal decrease was about 0.5 dB larger if the centre region was covered rather than the edges, but this can be modified by readjustment of the rungs. The comparator circuitry of Fig. 4 was able to detect the presence of the metal strip over the grate under these conditions which are a worst case. Larger strip widths caused a bigger signal decrease in all positions.

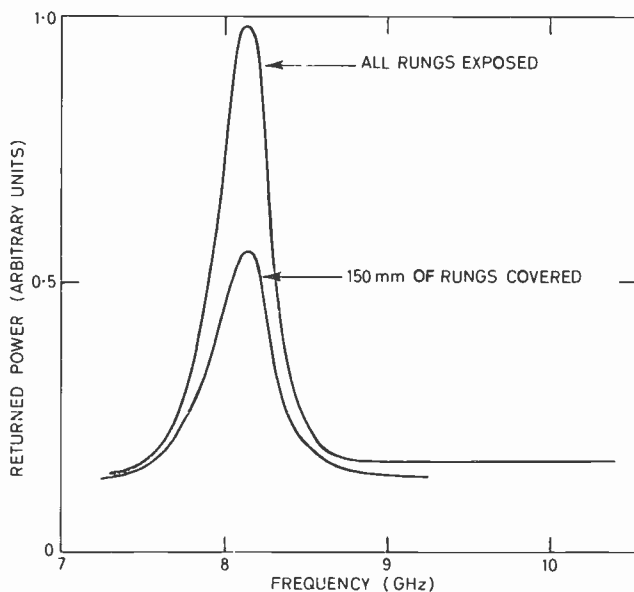


Fig. 4. Plots of received intensity of backscattered microwave power against frequency of illumination for a grate with optimized inter-rung spacing with and without the presence of a steel strip.

The return loss between power leaving the transmitting antenna and power returning to the receiving antenna was found to be approximately 26 dB and hence with a simple crystal detector for a receiver, transmitted power levels of the order of a milliwatt are sufficient to operate the system.

Having successfully set up the grate and dual antenna an equipment simplification was tested using the dish antenna as both transmitter and receiver. This necessitated the use of a circulator and slide screw tuner (to tune out systematic deficiencies giving rise to transmitter power leaking through to the receiving circuitry). The system performance using a single antenna was found to be comparable with the performance obtained using two antennae.

However, when setting up a system from scratch, it has been found necessary to use a separate receiving antenna and a swept frequency source to facilitate final adjustments to the relative positioning of transmitting antenna and grate before changing to single antenna and spot frequency operation.

#### 4 Conclusions

A laboratory mock-up of a microwave diffraction grating has been successfully tested for identification of the presence of steel strip. Experiments were also carried out on a steel grid taken from the bed of a steel strip rolling mill. The rungs were milled to the form of a parallel blazed diffraction grating. The presence of a steel strip caused a signal change approximately half that obtained with the experimental grating in which the grating spacing and angle could be easily modified. The next stage of development would be to build a steel grate to the design information obtained from our laboratory mock-up but we did not have such a facility.

The system is not expected to suffer seriously from the environmental hazards of a steel-works. The large wavelength of the microwave radiation compared with scale and water film thicknesses will not allow significant path length fluctuations and associated modifications of the diffraction pattern during operation. The presence of a mist of water droplets is not expected to produce significant signal attenuation at the short range required for the microwave signal path. All the components are mechanically strong and able to withstand severe misuse in this respect. They are not particularly susceptible to accumulating films of dust, paint and similar contamination—largely owing to the large wavelength of the microwave radiation compared with the thickness of the deposits.

The technique is a non-contact method and it does not need instrumentation to be placed under the bed which would necessitate a hold-up in production during any servicing. The only structural alteration needed to the bed is a specially-designed grate to replace one of the existing grates (which are removable) and a window cut in the side wall of the bed. The cost of the system hardware is estimated to be approximately £500 which is negligible when compared with the loss when incorrect signals are sent to the coiling machine at the end of the bed. Any long-term deterioration of the system is self-compensated as outlined in Section 2 and Fig. 3.

The technique could be used to detect the presence of a strip of any material which significantly reflects or absorbs microwaves.

#### 5 Acknowledgments

The authors wish to acknowledge the valuable help given by Dr. B. Chambers of the University of Sheffield, and also Messrs. E. Fletcher and D. Tuft of The British Steel Corporation Special Steels Division, Swindon Laboratories, Rotherham.

One of the authors (R.J.T.) is indebted to the British Steel Corporation for a Corporation Fellowship under which this work was produced.

A patent is being jointly applied for by the British Steel Corporation and the University of Sheffield to protect the work presented in this paper.

*Manuscript first received by the Institution on 26th July 1976 and in final form on 12th October 1976. (Short Contribution No. 183/ACS 15.)*

# P.a.m.-microwave transmission in coloured Gaussian noise environment

KAMILO FEHER, Ph.D., Eng.\*

and

JOHN HUANG, B.Sc., M.S.\*

## SUMMARY

In the current literature, the theoretical analyses which deal with the problem of additive coloured Gaussian noise (c.g.n.) assume that a pre-whitening filter is built into the receiver. This filter modifies the c.g.n. power spectrum density in such a way that, at the input of the threshold comparator, a bandlimited white Gaussian noise (w.g.n.) is obtained. The assumption of a pre-whitening filter is well justified for the purposes of theoretical analysis. Unfortunately, for practical systems, the design of a pre-whitening filter is not always feasible, as in the case of 1.544 Mbit/s data under voice (d.u.v.) hybrid microwave transmission.

In this paper, the equations for the performance of a multilevel p.a.m. receiver (as is the case in d.u.v.) for a c.g.n. environment are presented and show that, without the insertion of the pre-whitening filter, the same results are obtained as in a w.g.n. environment. The validity of these results is demonstrated by using a number of noise filters to obtain c.g.n. for laboratory measurements and by practical field measurements on an eight-hop 6 GHz microwave system (RCA-MM-600) which employs 4-level p.a.m. transmission in a d.u.v. configuration.

\* Department of Electrical Engineering, Concordia University, Montreal, Quebec H3G 1M8, Canada.

## 1 Introduction

Conventionally, the performance of digital transmission systems is defined by the  $P(e) = f(S/N)$  relation, that is the probability of error is a function of the received signal-to-noise power ratio. This function is well-known<sup>1</sup> for multilevel pulse amplitude modulation (p.a.m.) systems if additive white Gaussian noise (w.g.n.) is assumed. Theoretical analysis for the case of additive coloured noise, power spectrum density and Gaussian probability density function (p.d.f.) assumes a pre-whitening filter.<sup>2</sup>

For a large number of applications and in particular for p.a.m. data transmission on existing f.m. microwave systems the assumption of a pre-whitening filter would require the design of an additional phase linear network. On the other hand, for wide-band f.m. data transmission, such as the 1.544 Mbits/s data under voice (d.u.v.) hybrid microwave transmission, a pre-whitening filter is not assumed.

In the d.u.v. hybrid microwave transmission system,<sup>3</sup> as shown in Fig. 1(a), digital data occupy the lower part of the baseband spectrum by replacing the lower part of the f.d.m. (frequency division multiplexing) channels. This type of hybrid transmission system is widely used in North America. The primary objectives of hybrid transmission techniques include minimal or no modification to existing analogue equipment while simultaneously achieving more efficient digital data transmission. By placing data in the lower f.d.m. channels, we need only one guard band instead of many guard bands necessary if we are to transmit digital data inside the f.d.m. channels (called data in voice), as shown in Fig. 1(b). The guard band is essential to avoid adjacent channel interference. It is worth mentioning here that a new hybrid system called data above voice (d.a.v.)<sup>3</sup> has been developed by placing digital data above the f.d.m. channels (Fig. 1(c)).

Due to the f.m. demodulator employed in the d.u.v. system, the noise power spectrum density difference between the top and bottom frequencies for deep fading is large and can be approximated by additive c.g.n. In other words, in the d.u.v. system, since the data occupy the lower part of the spectrum (Fig. 1(a)) and the noise power spectrum after the f.m. demodulator has a constant slope on a logarithmic scale (point C of Fig. 2), the noise is 'coloured'. On the other hand, this is not so in the d.a.v. system because even though the noise power spectrum after the f.m. demodulator still follows the straight line, the noise spectrum density difference in the d.a.v. data band is relatively small and thus can be approximated by a constant value spectrum density, i.e., white noise. These two situations are shown in Fig. 1(d).

However, we will mathematically demonstrate that under actual working conditions, the model with additive c.g.n. results in the same  $P(e)$  performance as a system in additive w.g.n. and is determined by:

$$P(e) = \left(1 - \frac{1}{L}\right) \cdot P_i[|n| > d] \quad (1)$$

where  $L$  is the number of baseband transmission levels and  $P_i$  stands for probability function.

For a Gaussian noise, this expression results in:

$$P(e) = 2 \left(1 - \frac{1}{L}\right) \cdot Q \left[ \frac{d}{\delta} \right] \tag{2}$$

where

$$Q(x) = \frac{1}{\sqrt{2\pi}} \int_x^\infty \exp(-t^2/2) dt \tag{3}$$

in which

$d$  is the difference between the received nominal level and the nearest decision threshold

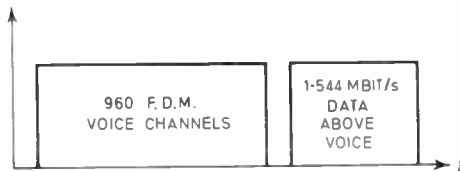
$\delta^2$  is the total mean c.g.n. power at the comparator input

$n$  is the value of the noise at the sampling instant.

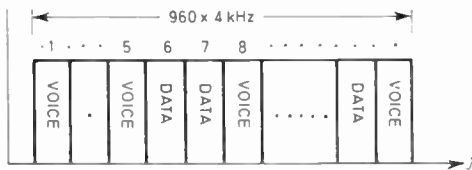
In the following Section, we will demonstrate the validity of equations (1) to (3). Afterwards, experimental results will be presented, with particular application to 1.544 Mbits/s p.a.m.-f.m. transmission. This transmission rate is frequently employed in data under voice (d.u.v.)<sup>3</sup> systems. It is noted, that the primary objective of the presented theory is a better understanding of d.u.v. systems, but is also applicable to other transmission systems.

### 2 The Coloured Gaussian Noise Environment

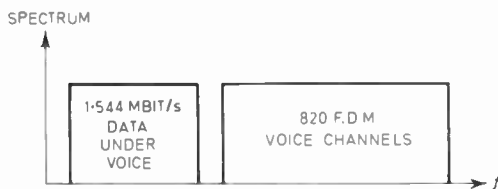
We now proceed with the derivation of the performance of a multilevel baseband, that is, p.a.m. receiver in



(a) Available baseband spectrum for data under voice (d.u.v.).



(b) Voice and narrowband data—data in voice.



(c) Available baseband spectrum for data above voice (d.a.v.).

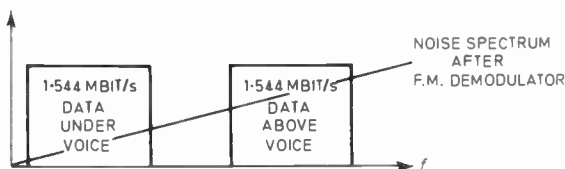


Fig. 1. (d) D.u.v. and d.a.v. corrupted with noise.

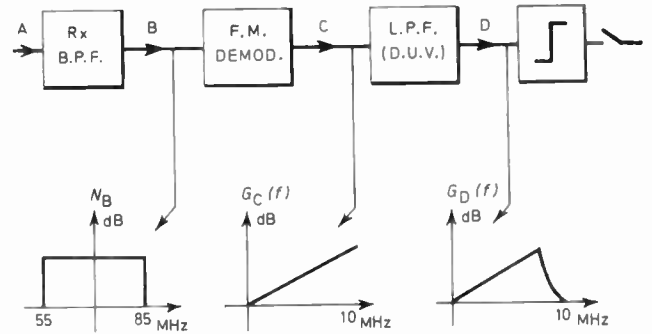


Fig. 2. Data under voice (d.u.v.) noise power spectrum.

c.g.n. environment. In the analysis, it is essential to establish the relationship:

$$P(e) = f(S_D/N, L) \tag{4}$$

where  $S_D/N$  is the mean data-power-to-noise ratio. The term ‘noise’ is used here to mean the total noise power at the comparator (threshold detector) input point. The f.m. receiver baseband output has a noise power spectrum density  $G_c$  such as is shown in Fig. 2 and obeys the law:

$$G_c(f) = Kf^2 \tag{5}$$

where  $K$  is a proportionality constant.

The simplified model for two-level transmission is shown in this figure where it is assumed that at the receiver input (A) the noise is relatively wide, in comparison to the bandwidth of the receiver (Rx) bandpass filter (BPF). Following BPF, (B) within the indicated channel bandwidth this noise has a flat power spectrum. After f.m. demodulation, (C), it has a triangular power spectrum density of 6 dB/octave described in Ref. 5 and is therefore coloured.

The coloured Gaussian noise (c.g.n.) at C is filtered by the Rx low-pass filter (LPF). This filter does not modify the probability density function (p.d.f.) of the Gaussian noise; however, it introduces an additional colouring as depicted by  $G_D(f)$ . The comparator, a threshold detector, receives a signal and added c.g.n. and is followed by a sampling device.

The mathematical model of the system is shown in Fig. 3. The input symbols  $a_n$  are filtered by a transmit filter  $T(\omega)$  and the w.g.n. has a uniform power spectrum density  $N_0$  over all frequencies. The noise colouring filter  $C(\omega)$  modifies  $N_0$  to  $N_c(\omega)$  in the following manner:

$$N_c(\omega) = N_0 |C(\omega)|^2. \tag{6}$$

On the other hand the receive filter  $R(\omega)$  modifies both the signal and the noise spectrum. Clearly the noise spectrum at the input of the comparator,  $N_R(\omega)$  is

$$N_R(\omega) = N_0 |C(\omega)|^2 |R(\omega)|^2. \tag{7}$$

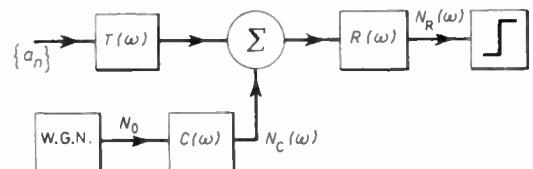


Fig. 3. Model of coloured Gaussian noise p.a.m. system.

Furthermore, it is supposed that the cascade of  $T(w)$  and  $R(w)$  enables data transmission without intersymbol interference; this results in an overall transfer function given by:

$$X(w) = T(w)R(w). \tag{8}$$

The input symbols,  $a_n$ , may assume any of the possible  $L$  equally spaced levels with equal probability and symbols occurring at different times are independent. Based on the above conditions, the  $P(e)$  can be expressed as:

$$P(e) = \left(1 - \frac{1}{L}\right) \cdot P_r[|n| > d] \tag{9}$$

where  $n$  and  $d$  have already been defined. The total noise power at the comparator input is

$$\delta^2 = \frac{1}{2\pi} \int_{-\infty}^{\infty} N_R(w) dw = \frac{N_0}{2\pi} \int_{-\infty}^{\infty} |C(w)|^2 |R(w)|^2 dw. \tag{10}$$

Finally, the  $C(w)$  and  $R(w)$  filters did not modify the Gaussian p.d.f. of the noise and the noise probability distribution of the c.g.n. is still given by the well-known integral

$$Q(x) = \frac{1}{\sqrt{2\pi}} \int_x^{\infty} \exp(-t^2/2) dt. \tag{11}$$

Therefore we conclude that the  $P(e)$  is given by:

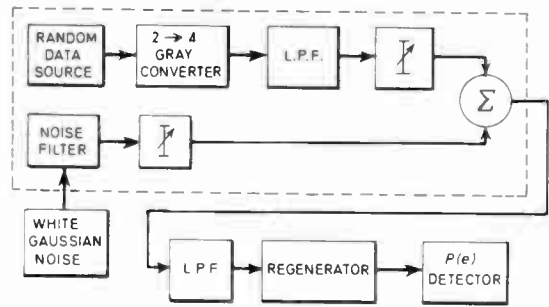
$$P(e) = 2 \left(1 - \frac{1}{L}\right) Q \left[\frac{d}{\delta}\right]. \tag{12}$$

This expression is identical to the equation for w.g.n. given in Ref. 1. The difference in derivation is due to a different determination mode of  $\delta^2$ , the total noise power. As it is seen from (10),  $\delta^2$  is a well-defined quantity once the transfer functions  $C(w)$ ,  $R(w)$  and the w.g.n. spectral density  $N_0$  are known. From the above derivation, we conclude that the performance is determined solely by the signal to total noise power ratio. This terminates our formal proof.

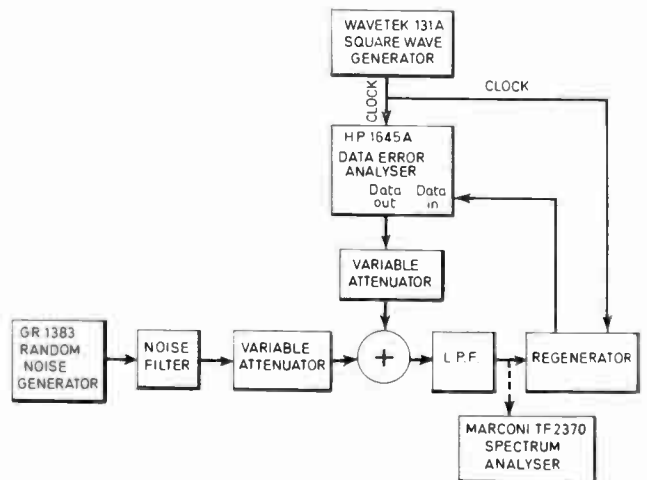
### 3 Measured Results

As a further confirmation, the validity of the above equations was experimentally verified. The block diagram of the coloured measurement set-up in which a binary pseudo-random generator transmits 1.544 Mbits/s non-return-to-zero (n.r.z.) data is illustrated in Fig. 4(a). The dashed box in Fig. 4(a), containing the random data source generator and noise filter, was used to simulate the baseband output corrupted with c.g.n. from the f.m. demodulator (point C in Fig. 2).

A detailed laboratory set-up is described in Fig. 4(b). The Wavetek 131A square pulse generator was used to clock both the Hewlett-Packard HP 1645A data error analyser to generate random data output and the regenerator. The white noise generated by the General Radio GR 1383 instrument has a 20 Hz to 20 MHz bandwidth. The noise filter modifies the flat 'white' source spectrum in accordance with the filter transfer function. At the filter output a coloured Gaussian noise source was obtained. This noise corrupted the random data and simulated the additive channel noise. The composite



(a) Coloured noise measurement set-up for 4-level p.a.m. transmission. The same set-up without the 2 to 4-level Gray converter was used for binary n.r.z. transmission.



(b) Detailed laboratory set-up for n.r.z. data transmission. (A 2- to 4-level Gray converter was added between HP 1645A and the attenuator for 4-level p.a.m. transmission.)

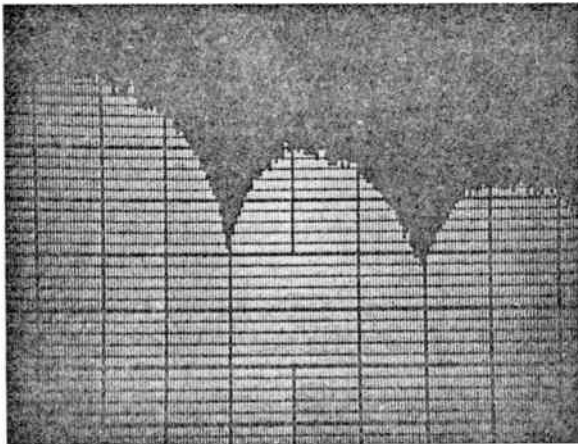
Fig. 4.

signal (data and noise) was then passed through a low pass filter (LPF). The regenerated data (some in error because of the noise corruption) were fed back to the HP 1645A and compared with the transmitted data pattern. Errors were then counted. The spectra shown in Fig. 5 were taken either before or after LPF using a Marconi TF 2370 spectrum analyser. The infinite bandwidth and the band-limited n.r.z. data spectra are shown in Fig. 5(a) and Fig. 5(b) respectively.

Measurements were made first with a two-level n.r.z. transmission. Later, a two-to-four-level Gray converter was added to reduce the transmission rate to 772 kbauds for a four-level p.a.m. measurement. The two low-pass filters in Fig. 4 were used for signal shaping purposes. Results from both measurements agreed very well with our theoretical predictions.

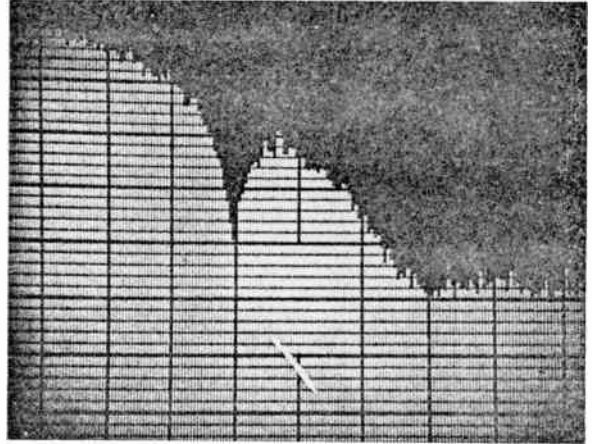
First, spectra of various types of noise filter were analysed. One type of noise filter was obtained by passing the 20 Hz-20 MHz white Gaussian noise from the noise generator through a 2 MHz high-pass filter (HPF). The noise spectrum is shown in Fig. 5(c), and will be called high-pass coloured noise (curve 3) in the measured results presented in Fig. 6. The other was obtained by passing the same noise through a 100 kHz LPF cascaded with a 30 kHz HPF, and its spectrum is

x—d.c. reference



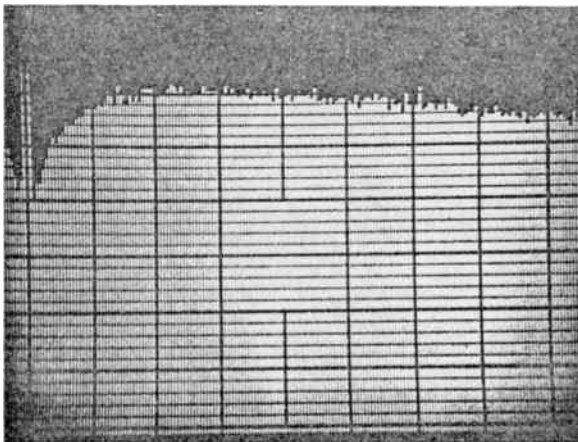
(a) Spectrum of infinite bandwidth n.r.z. random data. Scales: Y 10 dB/div; X 0.5 MHz/div.

x



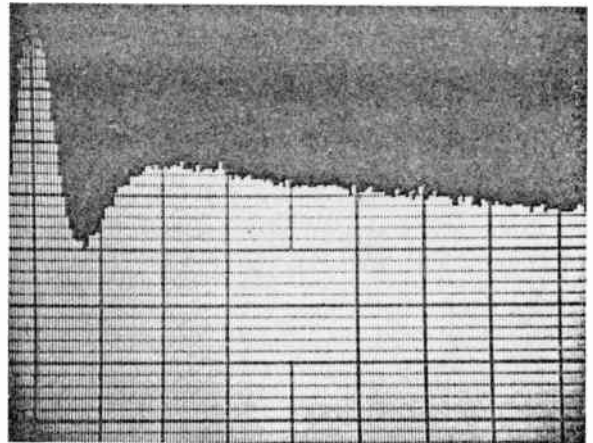
(b) Spectrum of bandwidth limited n.r.z. random data. Scales as for (a).

x



(c) High-pass coloured noise spectrum. Scales: Y 10 dB/div; X 1.0 MHz/div.

x



(d) Narrowband low-pass coloured noise spectrum. Scales: Y 10 dB/div; X 0.02 MHz/div.

Fig. 5. Noise spectra measurements.

shown in Fig. 5(d). We shall call this narrowband low-pass coloured noise in Fig. 6 (curve 4). In Figs. 5(a), 5(b), 5(c) and 5(d), the point marked X is the d.c. reference line of the spectrum analyser. (In Fig. 5(d), the horizontal scale is only 20 kHz/div., and the d.c. reference line is therefore enlarged). As shown in Figs. 5(c) and 5(d), the noise spectrum resembles that depicted in Fig. 2 (point C) from the f.m. demodulator. In other words, the added noise is coloured.

Figure 6 shows the measured results for the two level n.r.z. transmission. Curve 2 is the measured  $P(e) = f(S/N)$  curve with added w.g.n. which has an equivalent noise bandwidth (e.n.b.) of 900 kHz (or  $0.58 B_R$ , where  $B_R$  is the bit rate bandwidth and is equal to 1.544 Mbit/s in our measurement). Curves 3 and 4 are the measured  $P(e)$  curves with the high-pass coloured and narrowband low-pass coloured noises, respectively. It is seen that they are within less than 1 dB of one another, that is, within our measurement accuracy.

Also shown in Fig. 6 is the theoretical  $P(e) = f(S/N)$  curve 1 which has the same e.n.b. as that of curve 2 in our measurement. It was obtained from the optimal

theoretical  $P(e) = f(E_b/N_0)$  curve<sup>4</sup> from the following relationship:<sup>5</sup>

$$E_b/N_0 = S/N + 10 \log \frac{\text{e.n.b.}}{B_R} \quad (13)$$

where  $E_b$  is the signal energy of one bit and  $N_0$  is the noise spectral power density of w.g.n.

Figure 7 gives the same measured results for the four level p.a.m. transmission. Again, curve 1 is the theoretical reference curve with added w.g.n. Curve 2 is the measured  $P(e)$  curve with added w.g.n., while curve 3 is the measured  $P(e)$  curve with a high-pass coloured noise. Curves 2 and 3 are within 0.5 dB of each other. Other colouring filters were also tried out and resulted, within our measurement accuracy, in the same  $P(e) = f(S/N)$  curve.

These laboratory measurements proved experimentally that our mathematical model was well defined and that the derivations in relation to the c.g.n. p.a.m. transmission link were accurate.

Finally, field measurements, on an eight-hop d.u.v. 6 GHz microwave system (RCA-MM-600) between

**Table 1.** D.u.v. field measurements in comparison to w.g.n.

$P(e)$	$S/N$ w.g.n. (dB)	$S/N$ c.g.n. (dB)
$10^{-4}$	18.6	18.5
$10^{-8}$	24	23.7

Montreal and Spencerville and operated by the Canadian National and Canadian Pacific Telecommunications companies, compared favourably to our theoretical predictions which were based on c.g.n. assumptions. These results are shown in Table 1.

In the second column, results for additive w.g.n. are given for the corresponding  $P(e)$  values listed in the first column. In the third column, (c.g.n.), the 8-hop system field measurements are given. These results agreed favourably to our theoretical prediction.

At this point, it might be interesting to note, that in contrast to the d.u.v. model, in the case of 1.544 Mbit/s data above voice or data above video (DAVID) transmission the noise power spectrum density difference between the top and bottom d.a.v. frequencies is not significant enough to merit a separate analysis.<sup>6,7</sup>

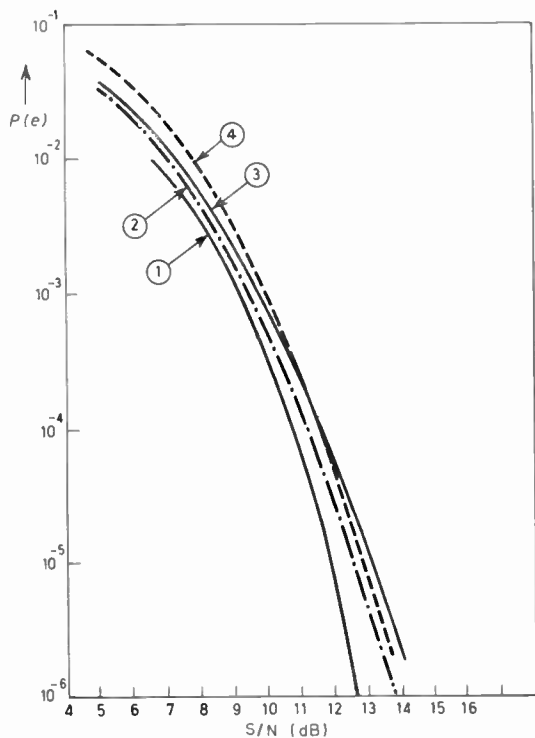


**Fig. 6.** Coloured Gaussian noise evaluation (Two-level n.r.z. transmission).

- (1) Theory—added white Gaussian noise equivalent noise bandwidth (e.n.b.) = 900 kHz (or  $0.58 B_R$ ).
- (2) Measured with added w.g.n. having an e.n.b. = 900 kHz ( $0.58 B_R$ ).
- (3) Measured with added high-pass coloured noise.
- (4) Measured with added narrowband low-pass coloured noise.

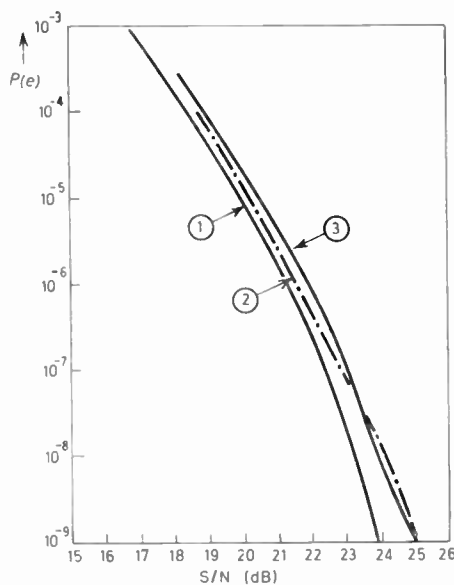


**Fig. 7.** Coloured Gaussian noise evaluation (Four-level p.a.m. transmission).

- (1) Added white Gaussian noise—theory (theoretical curve).
- (2) White noise—measured in laboratory.
- (3) High-pass coloured noise—measured in laboratory.

#### 4 Conclusion

The performance of a multilevel baseband p.a.m. receiver in additive coloured Gaussian noise environment has been derived. The validity of the presented theory has been demonstrated by various laboratory measurements and also field measurements on a 6 GHz f.m. microwave system, which carried 1.544 Mbit/s data under voice traffic.

#### 5 References

1. Lucky, R. W., Salz, J. and Weldon, E., 'Principles of Data Communication' (McGraw-Hill, New York, 1968).
2. Van Trees, H. L., 'Detection Estimation and Modulation Theory', Part 1 (Wiley, New York, 1968).
3. Feher, K., Goulet, R. and Morissette, S., '1.544 Mbit/s data above f.d.m. voice and data under f.d.m. voice microwave transmission', *IEEE Trans. on Communications*, COM-23, No. 11, pp. 1321-7, November 1975.
4. Taub, H. and Schilling, D. L., 'Principles of Communication Systems' (McGraw-Hill, New York, 1971).
5. Milstein, L. B. and Austin, M. C., 'Performance of non-coherent fsk and am-fsk systems with postdetection filtering', *IEEE Trans. on Communications*, COM-23, No. 11, pp. 1300-6, November 1975.
6. Feher, K. and Chan, D., 'Psk combiners for fading microwave channels', *IEEE Trans. on Communications*, COM-23, No. 5, pp. 554-8, May 1975.
7. Feher, K. and Morris, M., 'Simultaneous transmission of digital phase-shift keying and of analog television signals', *IEEE Trans. on Communications*, COM-23, No. 12, pp. 1509-14, December 1975.

*Manuscript first received by the Institution on 15th February 1976, in revised form on 28th July 1976 and in final form on 13th December 1976. (Paper No. 1761/Com. 144).*

# Optimal codes for digital magnetic recording

J. C. MALLINSON, M.A., M.Inst.P.\*

and

J. W. MILLER, B.S.\*

*Based on a paper presented at the Conference on Video and Data Recording held in Birmingham from 20th to 22nd July 1976*

## SUMMARY

Channel coding is universally employed in digital magnetic recording to match certain properties of the coded data to the characteristics of the recorder channel. In this paper, attention is focused primarily on the digital sum variation and d.c. content of various codes. The older, more familiar examples, such as NRZ, Manchester, enhanced-NRZ and Miller are compared with the more recently developed group, zero modulation and  $M^2$  codes.

\* Ampex Corporation, 401 Broadway, Redwood City, California 94063.

## 1 Introduction

Three distinct classes of binary digital coding are discussed frequently in connection with magnetic recording. *Source coding* is used to reduce the quantity of data to be recorded, as in differential p.c.m. or delta modulation, or to render recorder defects less significant, as in Fourier, Hadamard or other transformations. Conversely, in *error detection and correction coding* the quantity of data is increased by the inclusion of redundant information which permits a purely logical determination and treatment of error conditions; examples range from simple parity checking schemes to Hamming and other highly complex cyclic codes. In *channel coding*, the principal subject of this paper, the data to be recorded are modified to obtain the highest density permitted by the limiting characteristics of the magnetic recording channel.<sup>1</sup>

Whilst it is clear that many differing criteria could be used in the design of such channel codes, two points of view are most prevalent. Using well-founded tenets of communication theory, it is argued that in order to maximize, on the average, the storage or transfer of information in the recorder channel, the power spectral density of the channel code, for random input data, should match the transfer function of the recorder.<sup>2</sup> Unfortunately, however, a code based upon statistical considerations alone remains vulnerable to specific worst case or so-called 'pathological' data sequences for which the error rates may be greatly in excess of the average. This fact, which is of particular concern in the recording of digital data for computers, has led increasingly to an alternative approach which may be termed worst case design of channel codes.

Upon recalling that magnetic recorders are absolutely incapable of reproducing very low frequency or d.c. waveforms, it is perhaps not surprising that most of the important advances in worst case channel code design have involved modification to the low frequency or d.c. spectral content. Indeed the evolution of channel codes for magnetic recording may be regarded rather logically as a gradual process of reduction of the d.c. content without concomitant increases in bandwidth.

After reviewing the magnetic recording channel limitations and certain definitions concerning codes, in this paper we follow the evolution of the following codes: NRZ, Manchester, ENRZ, GC, Miller, ZM and  $M^2$ . Attention is directed primarily at the digital sum variation and maximum d.c. content.

## 2 Magnetic Recording Channel Limitations

A magnetic recorder is a band-pass, highly non-linear communication channel which suffers both amplitude instability and timing errors. Each of these factors constrains the selection of channel codes.

As a band-pass channel the recorder will reproduce neither very low frequency, long wavelength nor very high frequency, short wavelength waveforms. Transmission of d.c. is precluded for several reasons; no magnetic field emanates from d.c. magnetized media and, therefore, no read-head flux is induced; the read-

head output voltage is due to time domain differentiation of the head flux and the possible use of either coupling (rotary) transformers or capacitors. The absence of read-head d.c. flux is absolute in all current designs and will only be changed by the unlikely advent of designs in which the recording medium actually threads the head coil.<sup>3</sup> As a practical matter, the long wavelength limit in current recorders is directly related to the overall physical dimensions of the read head. Short wavelength response may be limited by the read-head gap null and the existence of extreme spacing losses. Practical limits in current precision recorders are long and short wavelengths of 1–2 cm and 0.5–1.0  $\mu\text{m}$  respectively. The band-pass characteristic favours codes with small or zero d.c. content and a high density ratio.

At long and medium wavelengths a recording channel may be rendered linear by the use of a.c. bias. However, at short wavelengths this technique is no longer effective and both a.c. biased and unbiased recording yield identical non-linear responses.<sup>4</sup> On the other hand, when binary symmetric levels are recorded on erased media with proper pre-equalization the output becomes a linear transform of the input and linear post-equalization is then effective in correcting the channel distortions. The channel non-linearity and the output amplitude instability, due principally to variations in head-medium spacing, operate against the use of multi-level or partial response coding.

Timing errors arise for two main reasons: improper corrections, or equalization of the channel distortions and variations in the head-medium relative velocity. This necessitates run length controlled channel codes which are self-clocking.

### 3 Code Parameter Definitions

It is useful to define several parameters of the channel codes; in general our definitions follow those of Patel.<sup>5</sup>

Suppose that, on average,  $x$  data bits are encoded into  $y$  binary digits; the ratio  $x/y$  is called the rate of the code. All codes considered below have rates between one half

and unity; lower rate codes require higher frequency clock and detection circuits.

Following conventional practice we assume that the ones and zeroes in the coded sequence are recorded on the medium by the presence and absence of magnetic polarity transitions respectively. The shortest run length of zeroes between consecutive ones is  $d$  digits; this determines the minimum distance  $(d+1)$  between transitions and hence the highest transition density. The longest run of zeroes between consecutive ones is  $k$  digits; the greater  $k$ , the worse become the self-clocking properties of the code.

The digital sum variation (d.s.v.) is the running integral of the area beneath the coded sequence; in computing the d.s.v. the binary levels are assumed to be  $\pm 1$ . If the d.s.v. of the code can grow indefinitely the code has d.c. content; if the d.s.v. is bounded the code is d.c. free.

A convenient measure of code efficiency is the density ratio,  $DR$ , which is given by

$$DR = \frac{\text{data density}}{\text{highest transition density}} = \frac{x}{y}(d+1)$$

For data bits arriving at time intervals of  $T$ , the minimum time interval between media transitions is  $DR.T$ . The density ratios of all the codes treated below fall between one half and unity. As a general rule, the high frequency response of the channel must extend somewhat above the Nyquist frequency corresponding to the maximum transition density. This frequency is  $(2DR.T)^{-1}$ ; the larger the  $DR$ , the lower the bandwidth of the code.

## 4 The Codes

Seven distinct channel codes are in current use in magnetic recording. In Fig. 1 we show typical waveforms corresponding to all the codes. In Table 1 we give the values of all the code parameters defined in the previous Section.

### 4.1 Non-return to Zero

NRZ is the archetypal code in which data are generally supplied to the recorder. Two main classes exist; in NRZ (mark), ones in the data stream are recorded (i.e. marked) as magnetic transitions in the middle of the data bit interval and zeroes are ignored.<sup>6</sup> In NRZ (level), zeroes and ones are recorded as positive and negative

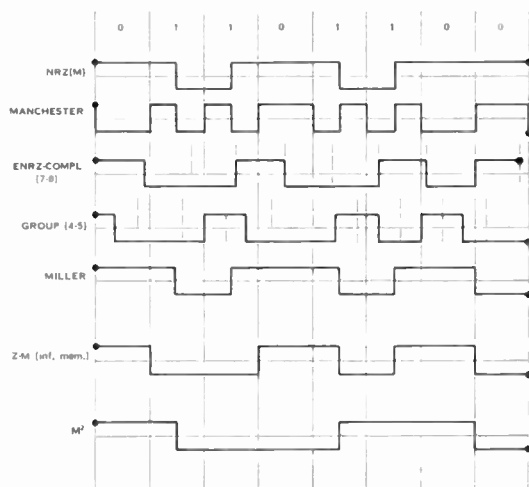


Fig. 1. Code waveforms.

Table 1. Code parameters

	Rate	$d$	$k$	$DR$	Maximum d.s.v.	Maximum d.c. content
NRZ(M)	1	0	$\infty$	1	$\pm \infty$	$\pm 1$
Manchester	1/2	0	1	1/2	$\pm T$	0
ENRZ-C	7/8	0	7	7/8	$\pm \infty$	$\pm 3/4$
Group	4/5	0	2	4/5	$\pm \infty$	$\pm 2/5$
Miller	1/2	1	3	1	$\pm \infty$	$\pm 1/3$
Z-M (INF.)	1/2	1	3	1	$\pm 3/2T$	0
$M^2$	1/2	1	5	1	$\pm 3/2T$	0

levels so that transitions only occur whenever the data bits change. NRZ is not a run-length-limited code. For long strings of zeroes the d.s.v. is unbounded and the maximum d.c. content is unity; in consequence the 'eye' pattern† can become completely closed rendering simple binary threshold detection impossible. NRZ(M) is used in 800 bits/in IBM compatible longitudinal recorders.

#### 4.2 Manchester

Manchester coding and its variants are known by many names: bi-phase, double-frequency, phase-encoding, frequency-shift-keying and, quite inaccurately, frequency-modulation.<sup>7</sup> Here the coding rules are identical to NRZ(M) with the addition of extra transitions at the beginning of every data bit interval. The resultant half-rate code is run-length limited and was the first known code with bounded d.s.v. and zero d.c. content. Unfortunately these advantages are achieved at the cost of a DR of one half. The Nyquist frequency is accordingly twice that of NRZ and this excessive bandwidth requirement has limited Manchester coding to low density applications. Manchester coding has not led to significant evolutionary developments. Manchester coding is used in 1600 bits/in IBM compatible data recorders.

#### 4.3 Enhanced-NRZ

Two variations of ENRZ have been described; both may be regarded as simple, but mainly ineffective, modifications of NRZ(L).<sup>8</sup> The basic idea is to add extra transitions to NRZ(L) in order to make it run-length limited (i.e.  $k$  bounded); this assures clock extraction for any input data. In both versions an extra interval is inserted after seven code bits. In ENRZ-parity, the eighth bit is odd parity on the previous seven code bits; in ENRZ-complement the eighth bit is the complement of the seventh code bit. A single bit memory is required to implement both codes. In both cases the d.s.v. remains unbounded and the maximum value of d.c. is 3/4. For worst case input data the eye pattern amplitude can close to 1/4; this corresponds to a loss in effective signal-to-noise ratio of 12 dB, which is incompatible with high density recording. Whilst it is clear that the d.c. content could be reduced by introducing the extra bit more frequently; this would reduce the DR and increase the bandwidth excessively. ENRZ has been used in, for example, certain high density recorders for instrumentation applications.

#### 4.4 Group Coding

Group coding, which is also called run-length-coded-NRZ, is a generic term identifying the technique of slicing the incoming data into blocks or groups and transforming these data groups into longer code words which are then recorded as NRZ(M). The transformation may be performed according to algebraic rules or by using a look-up table or dictionary. These alternatives should strictly be called group (after group theory) and block coding respectively but this distinction is not always

honoured. The advantage of transforming the data words into larger code words is that undesirable code words may be rejected and only favourable ones retained. For example, in the only known application of group coding, in 6250 bits/in IBM compatible longitudinal recorders, four-bit data words become five-bit code words; a four-data-bit memory is thus required.<sup>9</sup> The 16 (out of 32) chosen code words are shown in Table 2, wherein it will be seen that the possibilities with long strings of zeroes (large  $k$ ) have been rejected; this makes clock extraction more certain and keeps the d.s.v. of each code word within the limits  $\pm 2T$ . When concatenating five-bit code words, the maximum d.s.v. value can grow indefinitely and the maximum d.c. content is 2/5. It is obvious that, by selecting a code word length sufficiently greater than the data word, only code words with a d.s.v. value of zero need be used; this possibility would be accompanied, of course, by significant increases in the bandwidth necessary.

#### 4.5 Miller

Miller code is known by two other names: delay-modulation and (even more confusingly) modified-frequency-modulation (MFM).<sup>10</sup> The coding rules are: data ones are coded, as in NRZ(M), with transitions in the middle of the bit cell, isolated data zeroes are ignored (or delayed) and transitions are inserted at the beginning of the bit cell between pairs of data zeroes. The great virtue of Miller code is that, since isolated zeroes are ignored, the DR remains unity as in NRZ; the bandwidth requirements of Miller code are, consequently, little greater than in NRZ. The penalties include a rate of one half which necessitates a double frequency clock, the inability to recover clocking until a 101 data pattern occurs, a loss of effective signal-to-noise ratio of 3 dB since transitions have to be identified both at the beginning and the middle of bit cells and the requirement

Table 2. Four-five group code

Data words	Code words	d.s.v.†
0000	11001	-2T
0001	11011	-1T
0010	10010	+1T
0011	10011	+2T
0100	11101	+1T
0101	10101	0
0110	10110	+2T
0111	10111	+1T
1000	11010	0
1001	01001	+1T
1010	01010	-1T
1011	01011	0
1100	11110	-1T
1101	01101	-2T
1110	01110	0
1111	01111	-1T

† Eye pattern: a time synchronized oscilloscope display of the coded waveform recovered from the recorder which is frequently used in assessing the subsequent detectability of the data.

† Assuming starting conditions of zero d.s.v. and a negative level.

for a single bit memory for encoding. That these difficulties are not considered too severe may be judged from the widespread application of Miller code; it is used in all recent IBM disk recorders and until recently in all Ampex high density digital longitudinal recorders. An examination of Miller code leads to the conclusion that the maximum d.c. content is  $1/3$ ; the eye pattern is thus constricted by 3.5 dB on this account. When comparing ENRZ with Miller we may, therefore, expect a difference in effective signal-to-noise ratio of  $12 - (3 + 3.5) = 5.5$  dB. This value is in close accord with the experimental determination of the difference in 'recording margin' reported in a companion paper.<sup>11</sup> Several minor variations of the Miller theme are employed (they include the even more confusingly styled modified-modified-frequency-modulation (MMFM) or Wood codes) but the minor changes involved do not render them d.c. free.

#### 4.6 Zero-Modulation

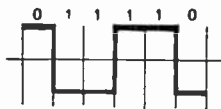
ZM codes were first described in 1975 by Patel who states, 'Zero-modulation was designed for, and is used in, magnetic recording'.<sup>5</sup> The crucial idea in ZM is to modify Miller code so that it becomes d.c. free and yet retains unambiguous code patterns which allow non-error-propagating decoding. Any data stream may be considered a series of sequences of two types:

(a) 011110;  $n$  ones bounded by zeroes,  $n \geq 0$

and (b) 111111;  $m$  ones.

Under Miller coding rules, sequences of type (a) with  $n$  even and non-zero have a non-zero d.s.v. which, upon concatenation with interleaving type (b),  $m$  even sequences, can grow indefinitely. All other sequences, type (a) with  $n$  odd or zero or type (b) have zero d.s.v. In the sequences with non-zero d.s.v., ZM encodes the zeroes in the Miller manner; the ones, however, are encoded as though they were zeroes but with alternate transitions deleted. The example in Fig. 2 makes the d.s.v. of the sequence zero. The omission of alternate transitions between pairs of 'ones coded as zeroes' makes this pattern distinct for decoding. Note that since

Fig. 2. Zero-modulation coding.



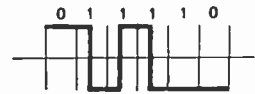
the d.s.v. returns to zero at the very end of the sequence, the final data zero must not be counted again for the next sequence; an example appears in Fig. 1. All other data sequences are, of course, coded by the normal Miller rules. Unfortunately this coding change is rather difficult to implement because complete sequences have to be altered. In principle, therefore, infinite look-forward and look-backward memories are required to identify the sequence boundaries and to provide the ZM modified code sequence if, indeed,  $n$  turns out even. Patel recognized this difficulty and suggested that the necessary memory could be limited by blocking the data into groups of  $f$  bits followed by a zeroes parity bit. This guarantees that all modified sequences fall within

an  $(f+1)$  bit block. Naturally, however, the addition of extra code bits reduces the density ratio,  $DR$ , and increases the bandwidth requirements of the code.

#### 4.7 $M^2$

$M^2$  is another recent modification, invented by one of the authors (J. W. Miller), of the Miller code. This proprietary Ampex code is used in the current high density longitudinal recorders discussed in a companion paper.<sup>11</sup>  $M^2$  is also used in the recently announced Electronic-Still-Store, the world's first commercial digital video recorder. In  $M^2$ , as in ZM, the basic Miller code is modified so that it becomes d.c. free. Again, this is achieved by modifying the sequences which have non-zero d.s.v. To limit the memory required, however, the changes are introduced only at the end of the sequences. In the sequences with non-zero d.s.v.,  $M^2$  encodes all the ones, excepting the last, in the normal Miller manner; the final one is simply ignored. For example, in Fig. 3 the d.s.v. returns to zero after the final data one and consequently, in contrast to the situation prevailing in ZM, the final data zero is to be counted again for the next

Fig. 3.  $M^2$  coding.



sequence. All other sequences are coded by standard Miller rules.  $M^2$  coding produces characteristic transition free runs of  $2\frac{1}{2}$  and 3 data intervals which do not occur in Miller code; this ensures unique decoding. The most significant advantages of  $M^2$  over ZM are that only 3 bits of memory are needed and that a density ratio,  $DR$ , of unity is maintained. The bandwidth requirements of this d.c. free code are, in consequence, very little greater than in NRZ. Negligible base-line wander or eye-pattern closure occurs with  $M^2$ . The effective worst-pattern signal-to-noise ratio expected is 3.5 dB better than in Miller; in high density digital recording this difference becomes extremely significant.

## 5 Conclusions

Driven by the continuing requirement for higher recording densities, a steady improvement in channel codes for digital magnetic recording has taken place. The most important developments have been guided by a philosophy of 'worst-case' design and have been reviewed in this paper. Particular emphasis has been placed in reducing or eliminating the d.c. content of codes without incurring appreciable increases in the bandwidths necessary. Whereas group coding has the potential to be d.c. free, its present realizations are not. On the other hand, the most recently announced codes, ZM and  $M^2$ , appear to have achieved the goals completely. Both are d.c. free and need little more bandwidth than NRZ. Even though  $M^2$  is scarcely more difficult to implement than Miller, it is expected that the current pace of intense channel code development will continue. More refined and complicated codes will most probably be discovered; for example, by encoding

longer sequences it may be possible to increase the code rate ( $x/y$ ) or to match the code spectrum more closely to the magnetic recorder channel. The ultimate viability of such developments will depend largely upon the cost and complexity of the associated encoder-decoder circuitry.

## 6 References

1. Kiwimagi, R. G. *et al.*, 'Channel coding for digital recording', *IEEE Trans. on Magnetics*, MAG-10, No. 3, pp. 515-8, September 1974.
2. Knoll, A. L., 'Spectrum analysis of digital magnetic recording waveforms', *IEEE Trans. on Electronic Computers*, EC-16, No. 6, pp. 732-43, December 1967.
3. Mallinson, J. C., 'On recording head field theory', *IEEE Trans.*, MAG-10, No. 3, pp. 773-5, September 1974.
4. Mallinson, J. C. and Bertram, H. N., 'Write processes in high density recording', *IEEE Trans.*, MAG-9, No. 3, pp. 329-31, September 1973.
5. Patel, A. M., 'Zero-modulation encoding in magnetic recording', *IBM J. Res. Dev.*, 19, No. 4, pp. 366-78, July 1975.

6. A.N.S.I. Standard X 3.22-1973, 'Recorded Magnetic Tape for Information Interchange' (800 char/in, NRZI).
7. A.N.S.I. Standard X 3.39-1973, 'Recorded Magnetic Tape for Information Interchange' (1600 char/in, PE).
8. Wells, J. B., 'High density digital magnetic tape recording using enhanced-NRZ coding', Conf. on Video and Data Recording, July 1973, pp. 113-8 (IERE Conference Proceedings No. 26.)
9. A.N.S.I. Standard X 3.54 (Proposed), 'Recorded Magnetic Tape for Information Interchange' (6250 char/in, group coded recording).
10. Cullum, C. D., 'Encoding and signal processing', in 'Advances in Magnetic Recording', Annals New York Acad. Sciences, Vol. 189, pp. 52-62, 1972.
11. Spitzer, C. F., Jensen, T. A. and Utschig, J. M., 'High bit-rate, high density magnetic tape recording', Conf. on Video and Data Recording, July 1976, pp. 147-60. (IERE Conference Proceedings No. 35.)

*Manuscript first received by the Institution on 29th March 1976 and in final form on 19th November 1976. (Paper No. 1762/Com. 145.)*

© The Institution of Electronic and Radio Engineers, 1977

## The Authors



John Mallinson read natural philosophy at University College, Oxford, graduating in 1953. He joined Amp, Inc., Harrisburg, Pennsylvania, in 1956 to work on the theory and design of all-magnetic logic elements and six years later moved to Ampex Corporation, Redwood City, California, to investigate fundamental considerations in magnetic tape recording. As manager of the Basic Technology Section of the

Research Department, he directed the activities of a group working on magnetic recording theory, micro-magnetics, communication theory, and the exploration of advanced concepts in various areas of recording. He holds several patents as a result of his work. Mr. Mallinson is currently managing a High Bit Rate Recording Group in the Data Products Division of Ampex, which is investigating several



Jerry Miller received the B.S. degree in electrical engineering from Heald College, San Francisco in 1959, where he remained until the end of 1960, lecturing in a variety of engineering subjects. He joined Ampex in 1961 and worked for the next seven years on the development of instrumentation tape recorder systems of both longitudinal and rotary-head designs. He then took part in the development of the TBM

memory system, first as system engineer and subsequently as engineering manager. Since 1974 he has been with Company's Research Department studying high density magnetic recording channel noise and signal characteristics. Mr. Miller is the holder of several issued and pending design patents and has published three previous papers dealing with recording methods and systems.



# Marine Radar Today—A Review

A. HARRISON, B.Sc., F.R.I.N., C.Eng., F.I.E.R.E.

*The different units making up a marine radar installation are first described, with particular emphasis on the display, where the greatest variety of design has recently appeared. System aspects are then discussed, especially the clutter problem, as well as reliability and maintenance.*

## Introduction

The International Meeting on Radio Aids to Marine Navigation in May 1946<sup>1</sup> set out the first specification for a civil marine navigational radar, and a radar set has now become a mandatory fitting<sup>2</sup> for UK ships over 1600 tons, and in ships registered in some other countries. Today's UK specification<sup>3</sup> differs only in detail from the original, mainly in the accuracy of range and bearing measurement, and the ability to withstand a more arduous environment: the required target detection ranges are unaltered. Better engineering of individual units has been evolved from operational experience, but much of the basic design shows little change. There have however, been advances in display techniques and in system design and these will be reviewed after the individual units have been discussed.

## UNITS

### The Aerial

This has to form a beam no more than 2 deg wide in the horizontal plane, but between 1.5 and 0.75 deg is usual. The aerial rotates about an axis perpendicular to the deck, i.e. not stabilized against ship motion, so a wide vertical beam is used, about  $\pm 10$  deg. The rotation rate of at least 20 rev/min must be maintained in wind speeds up to 100 knots.<sup>3</sup>

The early reflector types are now almost entirely superseded by slotted waveguide designs (see Fig. 1) which have the advantage of close control of the power distribution across the aperture. This allows the best compromise between the narrow main beam and the sidelobes, presents a better match to the transmitter-receiver, and eases the difficulty of maintaining these in production. The slim shape minimizes wind resistance.

Horizontal polarization is usual. Circular polarization is known to reduce rain clutter by about 15 dB, but it is also blind to a corner reflector used to enhance the echo of a

buoy or small vessel. One manufacturer provides two arrays back-to-back in a common assembly, so that circular or horizontal polarization may be selected as required.

Ships which have to operate in ice-forming conditions (e.g. deep-sea trawlers) may also have a de-icing boot, which can be pulsed to expand by compressed air. The sequence of photographs in Fig. 2 shows it in dramatic action.

### The Transmitter-Receiver

All current designs use a multi-cavity magnetron as r.f. generator, with peak transmitted powers from 75 down to 3 kW, about the lowest which will safely meet the requirement. A variety of modulators is used. A charged line, discharged by a thyratron, was an early design which still has some advantages. Hard valve types, in which a power amplifier tetrode driven by a low power pulse has the magnetron as its anode load, are very flexible for pulse length and recurrence frequency changes—see Table 1. A choice of valves is available for the lower, but not for the higher powers where 15 A at 15 kV may be needed. Magnetic modulators are also used, in which a long pulse is narrowed in successive stages. Exact control of the magnetic properties of the cores is required to produce pulses much shorter than 100 ns, but the performance, power capability, and reliability of this design are excellent for longer pulses.

The use of the same aerial for transmission and reception makes a duplexer necessary. This has the magnetron on one arm of a waveguide T-junction with the aerial coupled to the 'stem' of the T. The other side arm leads to the receiver, protected by a T-R cell, which ionizes to short-circuit that arm when the transmitter pulse is being radiated, ensuring that all the power goes to the aerial and none to the receiver. To prevent receiver damage from signals transmitted by nearby radars, the T-R cell may be backed by a primerless type which needs no ionizing current, or a shutter may be inserted automatically when the radar is switched off. The distance of the magnetron from the T-junction is chosen so that its cold (i.e. non-oscillating) impedance, which is nearly a short-circuit, effectively disconnects that arm from the junction for signal reception. This is an elegant and economic design, since the waveguide assembly provides mounting facilities for all the microwave components—magnetron, T-R cell, and mixer crystals, in the necessary rigid relationship with each other.

The receiver noise figure is about 10 dB. This could be improved by a microwave preamplifier before the mixer, but would produce little operational advantage since all small targets are clutter-limited, not noise limited. The silicon crystal mixer, which may be single-ended or balanced, is also fed with the output of a local oscillator to heterodyne the microwave frequency signals down to an intermediate frequency. Klystrons are in the process of being superseded by Gunn diodes for this purpose. Tuning is usually by manual

---

Alban Harrison (Fellow 1964, Member 1959) is a graduate of London University and during the war worked on military radar at ADRDE Malvern (now part of the Royal Signals and Radar Establishment). In 1947 he was appointed Deputy Chief Engineer of the newly-formed radar development department of Henry Hughes and Son, now the Kelvin Hughes Division of Smiths Industries Limited; his present position is Chief Scientist (Radar) with the company. He has numerous published papers and patents concerned with radar and radar beacons to his credit and he received the Institution's Brabazon Premium in 1974 for a paper on a new radar situation display. Mr. Harrison has served on the IERE Aerospace, Maritime and Military Systems Group Committee since its formation in 1960 as well on organizing committees of joint conferences in the fields of ocean technology and marine navigational aids. He has been a member of various UK Government committees and working groups for marine radar and of working groups of IMCO Sub-committee on Safety of Navigation.

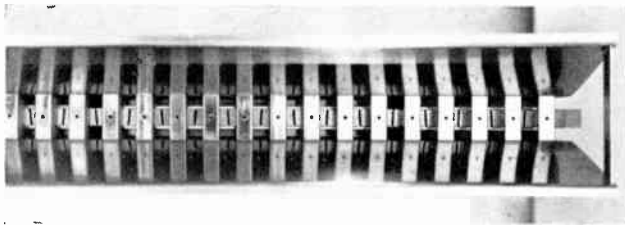


Fig. 1. Detail of horizontally polarized slotted waveguide aerial. The angle of the resonant slot determines the power it radiates. Blocks between the slots ('throttles') form waveguides below cut-off to attenuate the unwanted vertically polarized component from each slot. The assembly is in the throat of a horn which shapes the vertical beam.

control with some form of indicator; a.f.c. is rarely used. The i.f. signal is fed to an amplifier (30–80 MHz), with its bandwidth switched as far as practical to suit the pulse length in use. Typical parameters are shown in Table 1. This is followed by a detector, sometimes a push-pull or emitter follower type for higher efficiency, since a 60 ns pulse will comprise only four cycles of a 60 MHz i.f. The video output stage is hard limited or clipped to avoid overdriving the c.r.t.

**Displays—Raw Radar**

The cathode-ray tube is in universal use as a plan-position indicator easily understood by the mariner. The spot, deflected radially to indicate range, in the direction the aerial is pointing, is brightened when a signal echo is received from a surface object. This builds up in polar co-ordinates, a picture on the screen looking like a chart, with own ship at the origin and other ships, buoys and coastlines all displayed. This can be 'ship's head up', or can be compass stabilized to be 'North up'. Either a rotating coil driven by a servo or a synchronous motor in step with the aerial, with one time-base; or orthogonal fixed coils with component time-bases, may be used to deflect the spot, and the deflection rate can be switched to change the scale of the picture to display different ranges of view. An accurate oscillator supplies range calibration rings (as in Table 1). This may be supplemented by a scaled variable range marker. If the most accurate range measurement is desirable, e.g. for fishing near national limits, a precision crystal-controlled v.r.m. is available as an extra. The accuracy is limited only by the observer's ability to superimpose a variable ring on the displayed target.

Figure 3 shows the excellent definition achieved. The coasts of Essex (top) and of Kent stand out clearly, as do the pairs of buoys marking the deep channel into Sheerness. To distinguish immediately between moving ships and buoys in the main channel requires experience and knowledge of the chart. Marking the position of a target, perhaps on a reflection plotter superimposed on the display, discloses the buoys and stationary ships, and shows the relative track of other ships. A ship on a collision course will approach on a constant compass bearing, despite the movement of both ships. A cursor, a rotatable radial line above the c.r.t., can be

Table 1. Typical related parameters

Display range (naut. miles)	$\frac{3}{4}$	$1\frac{1}{2}$	3	6	12	24	48	60
Cal. interval (naut. miles)	$\frac{1}{4}$	$\frac{1}{2}$	$\frac{1}{2}$	1	2	4	8	8
Pulse length (microseconds)	0.05	0.25		0.75				
P.R.F. ( $\times 1000$ per second)	3.2	1.6		0.8				
Receiver bandwidth (MHz)	25	15		5				

set to check this. It can also be used to measure the compass bearing of a headland or seamark for position fixing.

The choice of a safe action to avoid collision can be best evaluated if the other ship's true course and speed are known. Drawing the triangle of velocities to find it is tedious, and the so-called 'True Motion' (1956) or ground-stabilized display (developed for airborne ground-mapping radar about 1942), in which own ship is moved across the screen proportionally to its true movement, allows direct plotting of the true course. Own ship's movement now makes the 'mechanical' bearing cursor unusable, since it rotates about the centre of the screen, so an electronic cursor must be used. One manufacturer has also provided six short electronic cursors, each of which may be set on a target, so that its bearing may be checked easily during its approach.

Figure 3 conveys quite a wrong impression of the brightness of the actual display. In reality, the radial time-base line rotates in synchronism with the aerial, refreshing the bright-

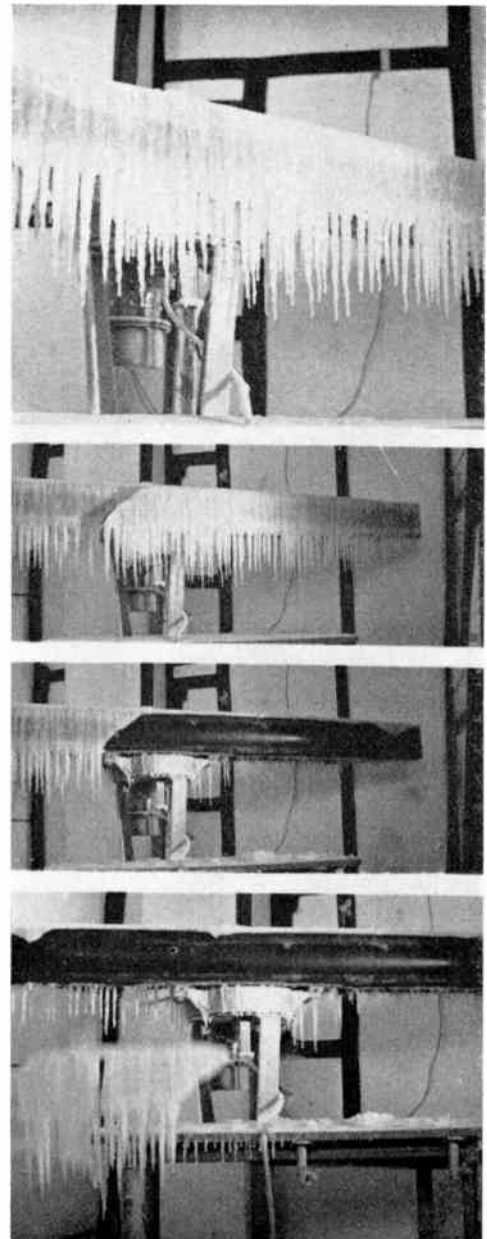


Fig. 2. De-icing boot: sequence of operation'

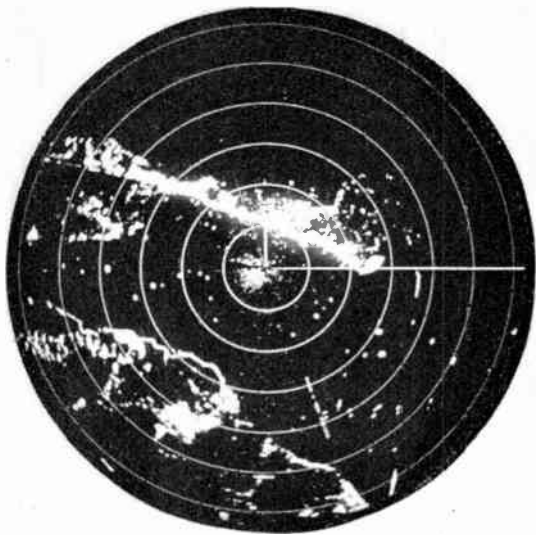


Fig. 3. Cathode-ray tube as plan position indicator. Range 6 miles. Entrance to Port of London.

ness of each displayed target, which then fades for 2½ seconds until again refreshed. The light output from the yellow (fluoride phosphor) screen is so low that a visor must be used in daylight.

#### Displays—Stored History

Moving targets can be made to plot their own tracks by the automatic storage and recall of successive p.p.i. pictures, and memory c.r.t.s<sup>4,5</sup> have been used. Pictures have been transferred from one 'Tenicon' memory tube to another<sup>6</sup> using destructive read-out and addition of the up-to-date picture, but none of these proposals survived the demonstration stage. A marine display in which the radar picture on a c.r.t. is photographed on cine film, which is processed and dried in 3 seconds, so that the radar picture can be projected as a

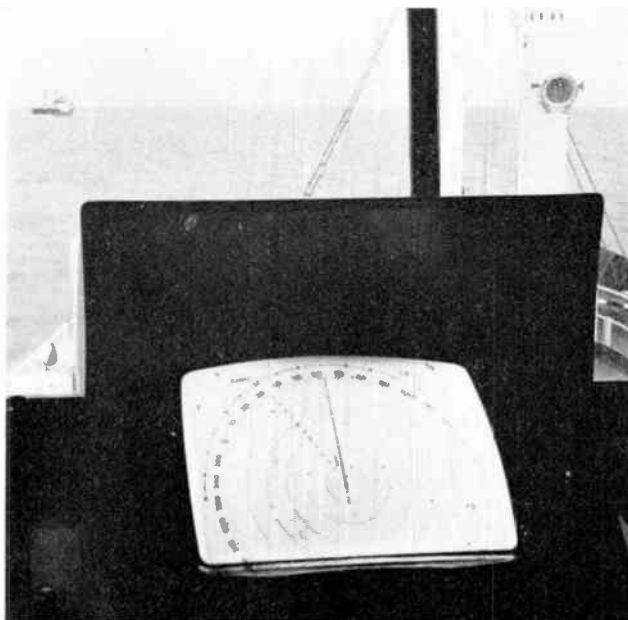


Fig. 4. Situation display on board ship.

600 mm diameter daylight-bright picture,<sup>7</sup> has been used to record ship's tracks. Unfortunately the data renewal rate had to be the same as the track duration, 3 or 6 min, which was unacceptable in many operational situations.

The first successful system used bandwidth compression techniques to record the raw radar data on an endless loop of magnetic recording video tape.<sup>8</sup> Every ten seconds a six-minute-old picture was erased and replaced by the up-to-date one, the pictures being so interlaced on the tape that on replay the screen showed the 6-minute-old picture, the 4-minute, 2-minute, and the up-to-date picture in cyclic sequence. Each ship's track is shown as a sequence of four spots, having the brightness refreshed in turn, which indicates direction. An apparent movement directly towards own ship on a constant bearing indicates a collision risk. Shifting the older pictures as they are displayed by a distance corresponding to own ship's movement in the elapsed time, converts the display to true motion, so that the true course and speed of the other ships are indicated. Alternatively, a shift corresponding to the difference between own ship's actual course and speed, and a proposed change to avoid collision, shows what the situation would be after the change, and allows examination of the effect prior to action—it is a 'trial manoeuvre' facility.

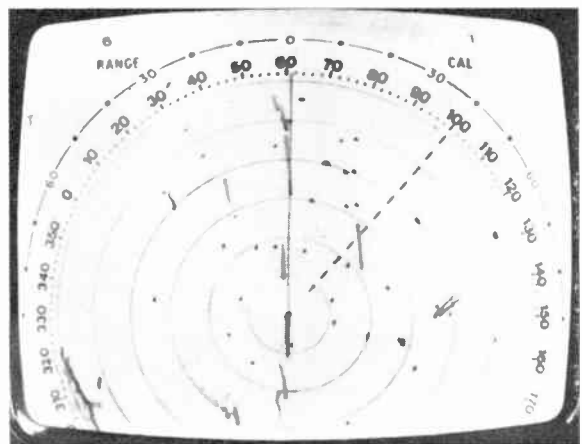


Fig. 5. Fishing vessels at anchor and tracks of moving ships, off Clacton. Shown on a 'stored history' display.

A new history system which also has the advantage of a daylight-bright picture<sup>9</sup> uses a light-storage panel,<sup>10</sup> which when polarized by d.c. will store the projected radar picture. This is viewed by a television camera and presented on a large bright screen, as seen at sea in Fig. 4, where the track of the ship seen through the window is clearly shown at half-mile range on the screen of the television display. Another example of the advantage of this display appears in Fig. 5, which conveys the essential information at a glance in a crowded traffic situation. Disregarding the scrap of Essex coastline and Clacton Pier at the bottom left, there are over 50 objects displayed. Twelve are moving and only two of these will come near us in the next 10 minutes if we maintain our course of 61°.

#### Displays—Processed

The storage and calculating facilities of an electronic computer have led to displays (full or limited vector) in which targets are automatically tracked. The data can be recalled for presentation as history tracks, relative or true, or predicted future tracks, and the effect of a trial manoeuvre can

be studied, all on a screen of adequate brightness. The amount of information which can be extracted and presented at the touch of a button appears limitless—some items have been criticized as being redundant. For example, knowing that a ship is steaming 14.72 knots on a course of  $314.2^\circ$  is considered by many seamen to be of little use until it is translated into a line on the display, actually or mentally.

A different form of presentation (p.a.d.) uses a selected minimum closest approach, and computes and displays ellipses which surround the future predicted positions of other ships to define 'predicted areas of danger', which own ship must be manoeuvred to avoid. The immediate indication of areas free for own ship's safe passage may be considered better than the facility for a trial manoeuvre, since successive trials may be required to discover a safe manoeuvre.

Errors in the raw radar data and in the gyro compass, particularly the slow cyclic bearing errors caused by ship motion, can falsify the predicted future data in these systems, but this is a negligible error if the tracking time before prediction is not unduly restricted. They have been fully discussed elsewhere.<sup>11-17</sup> Some systems require a higher signal-to-noise ratio because of their need for a high probability of detection and a low false alarm rate; small targets may be lost.

### Displays—General Comment

On a cost basis, particularly on small ships, the raw radar c.r.t. display will continue in use, despite its disadvantages. The variety of displays available to the shipowner, who will purchase expensive equipment if he can be convinced of its utility, leaves him a difficult choice. To acquire information on this, Shell International Marine commissioned a research project at the Department of Maritime Studies, Liverpool Polytechnic, in which simulated displays, of the different types available, were observed by each of a large number of subjects while recorded traffic situations were replayed and the subject's performance assessed.<sup>18</sup>

All the systems were found to be 'well ahead of raw radar'. The work-load factor, accuracy of interpretation of the displayed situation, and identification of target types (e.g. stationary, a buoy or anchored ship) were assessed for each subject and the results collated. The full vector system scored highest, closely followed by the stored history system, then the p.a.d. system, the limited vector system, and finally, well behind, came raw radar. The head of the Communication and Navigation Department at Shell I.M. concludes his commentary with the words:<sup>18</sup>

'... the storage systems provide the optimum solution at present. They achieve a large part of what the seafarer needs, they are simple, reliable, and readily understood. The predicted vector systems with automatic acquisition clearly provide somewhat more information but only, we suggest, at the expense of integrity and generally unwarranted higher capital outlay.'

### Inverter

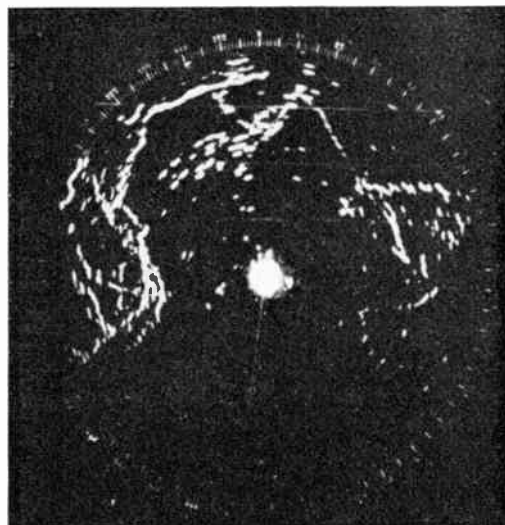
The inverter performs the useful function of taking power from a variety of ships' main supplies, usually 'dirty' and perhaps not well regulated, and converting it to clean, stabilized a.c. at a standard voltage and frequency. The use of a high frequency (say 800 Hz) reduces the size of all power transformers, smoothing chokes and capacitors leading to a smaller compass safe distance, and may simplify the design of the modulator. Rotary machines are in the majority, but some static invertors are in use.

Some radars, particularly those of American design, may take power directly from ships' a.c. mains at 60 Hz.

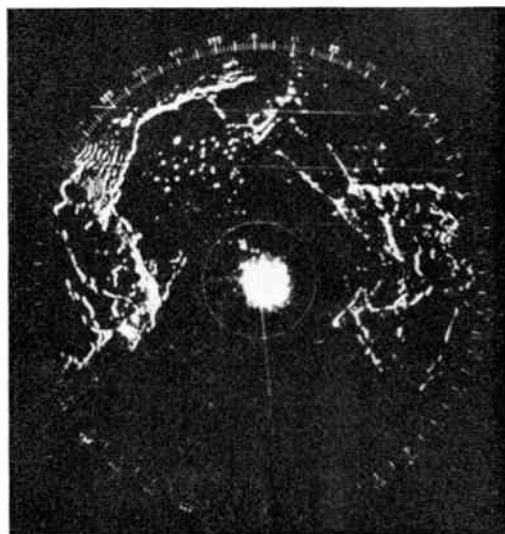
### Performance Monitor

In the UK Specification<sup>3</sup> a performance monitor is mandatory. The usual type is a small microwave cavity of high  $Q$  (30,000 is typical) coupled to the aerial waveguide. When brought into tune by a plunger moved by an electromagnet, the cavity resonates to produce a solid disk of signals in the middle of the display (the 'sun') whose radius is a measure of overall performance of the transmitter and the receiver. This is supplemented by a signal detector attached to the aerial mount, which produces a lobe of solid signal (the 'plume') as the aerial beam passes. This indicates the radiated power level by its length.

Proposals have been made for an automatic alarm as a malfunction warning. There are difficulties in the way of a perfect solution; warning of some failures, such as the loss of video signals to the c.r.t. base (but not the screen) or non-rotation of the aerial, and so on, would be possible but the present small demand is insufficient to justify production.



(a) 10 cm.



(b) 3 cm.

Fig. 6. Suez Bay. Display range 8 miles.

## SYSTEM FEATURES

### Choice of Wavelength

The arguments about 10 cm and 3 cm still continue, but Fig. 6 presents most of the differences. The better definition of 3 cm is clearly shown by the ships at anchor, and particularly by the entrance to the Suez Canal with a ship in it at 12 o'clock—remember the navigator wants to see not the piers but the entrance between them. 3 cm detects low small targets better—note the coastline at 9 o'clock, and also extending from the Canal entrance round to 3 o'clock. This sensitivity can become a disadvantage, as it also ensures the detection of sea clutter to a greater range, as seen in the middle of the picture, and also rain clutter (not shown). 10 cm penetrates rain, etc. better than 3 cm.

### Interswitching

System availability despite unit faults can be improved by duplication, but even more by interswitching units. This can achieve with two radars the reliability of three independent radars (as shown in Appendix) and this, of course, at lower cost.

### Clutter

Unwanted echoes from the sea, rain, etc., are called clutter.<sup>19</sup> Sea clutter can be removed from the display by 'swept gain'—a reduction of gain at short range, by as much as 80 dB, with a progressive recovery to full gain at a rate corresponding to the fall of sea clutter signals with range. This is inversely proportional to range cubed, out to a range of  $8Hh/3\lambda$ , after which it becomes an inverse seventh power law.<sup>20</sup> ( $H$  is the height of the radar aerial,  $h$  the wave height from peak to trough, and  $\lambda$  the radar wavelength in use.) Slightly different figures are quoted by some observers.<sup>21</sup> Rain clutter can be reduced by 'differentiation'—video a.c. coupling, which removes its d.c. level—and further suppressed by 'gain' reduction. The disadvantage of these techniques, the loss of other signals, is obvious, and all three controls must be used with discretion.

There have been many attempts, without much success, to suppress clutter automatically, such as passing video signals through a tapped delay line, combining the outputs from the taps to form an average of the signal in the area, then subtracting this from the video signal at the middle tap.<sup>22</sup> The most successful is the use of a logarithmic receiver<sup>23</sup> which uses the fact that clutter is random, with variance proportional to mean amplitude, as with white noise. Clutter signals automatically occupy that part of the logarithmic gain characteristic (set by their mean amplitude) which will amplify them (the variance) to the same mean level as noise. Good design is not easy, problems arise, e.g. with noise and clutter frequency components on the edge of the pass band.

Clutter has the same characteristics as other signals except that its instantaneous amplitude is random (approximately Rayleigh distribution).<sup>23, 30</sup> Integration of signals from successive transmitter pulses will therefore reinforce a steady target signal more than the local clutter, though ship movement limits the integration time available to a few seconds only. Unlike rain clutter, sea clutter is auto-correlated for about 20 ms, that is, the signal from one pulse length-beamwidth element of sea surface being illuminated by the radar does not change in the time the aerial beam sweeps across it. This makes the sea-clutter signal look like a collection of small, real targets, changing on each aerial revolution. The correlation can be avoided by rotating the aerial at several hundred rev/min, to have the same number of pulse echoes from the target in the integration time, but uniformly

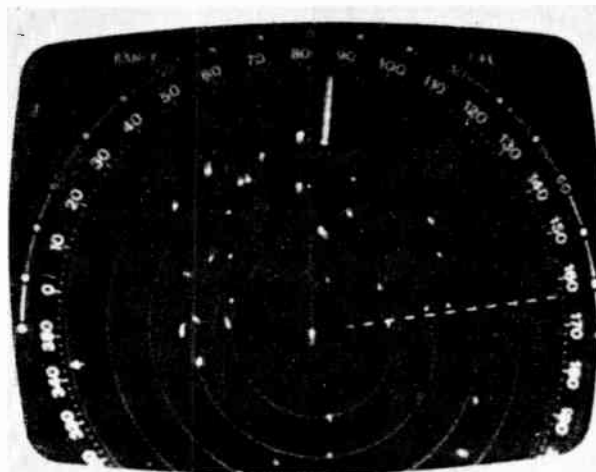


Fig. 7. Responder beacon on Goeree Light Tower, at 9 miles.

distributed, instead of in two or three groups of identical echoes, and therefore showing a wide range of random changes. Experimental equipment has shown that the signal-clutter ratio can be improved up to 6 dB by the fast aerial, and a further 6 dB max can then be obtained by integration.<sup>22, 24, 30, 31</sup>

The advantage of integration can be seen in Fig. 7 where the track of a small helicopter, speed about 80 knots, is visible at 0° 5 miles (2½ rings)—excellent sensitivity for such a small fast target—and also in the line of buoys, the first on 10° at 4 miles (2 rings), and three more in line at 2-mile intervals, parallel to the ship's head marker, and indicating the northern boundary of the channel the ship is entering. The integration occurs here in the picture storage.<sup>9</sup>

Pulse compression techniques, which can provide valuable discrimination against clutter on military radars (Ref. 19, Fig. 16), cannot be applied here, since the usual shortest pulse length is less than 100 ns. (See Table 1.)

### B.I.T.E.

The extent of built-in test equipment has varied from time to time, but is currently quite small. On some radars a tuning indicator is fitted, perhaps two neon lamps controlled by a discriminator. Usually a small meter is mounted in the transmitter-receiver to check that the current in the mixer crystals is correct, providing a first check on the crystal serviceability and a verification of local oscillator power. This meter is often connected through a switch so that the magnetron current, the supply voltage, etc., may be checked. The meter scale may be merely a green sector for a 'satisfactory' reading.

Although not test equipment in the normal sense, the display c.r.t. shows a picture which gives much information about the operation of the time-base, deflector coils, receiver, etc. In conjunction with a logical fault-finding chart, it serves as test equipment.

### Maintenance Philosophy

The use of a soldering iron for on-board maintenance is hardly needed today, and is usually restricted to a properly qualified maintenance technician. The advent of transistors and printed circuits has resulted in a design where small units require little skill to exchange to cure a fault. Repair is largely displaced by replacement. Faulty units may be repairable at a well-equipped shore base.

## CO-OPERATIVE EQUIPMENT

## Corner Reflectors

The response from a small object such as a buoy can be enhanced by adding a corner reflector, an assembly of three mutually perpendicular planes which gives a specular reflection back instead of scattering the incident energy. A reflecting cross-section of one square foot returns a signal equivalent to that from a 144-ft wooden minesweeper.<sup>25, 26</sup> In Fig. 3, No. 1 Sea Reach Buoy carries a reflector, which makes it clearly visible, exactly on the 6-mile ring at the right.

The commonly used octahedral cluster of eight corners is often mounted in the wrong attitude on a small boat. This is the 'point up' position, which leaves about 100° of the horizon with virtually no signal. Each triangular corner faces 35° above or below the horizon, but is fully effective only over a cone of 30° half angle. With one triangular face looking up (aircraft?) and one down (submarines!), the other six are equally spaced round the horizon, facing alternately 20° above and below it. This gives fairly uniform all-round reflection, being within 6 dB of the maximum except for very small arcs of -12 dB (maximum range halved).<sup>27</sup>

An assembly of a number of small corner reflectors, marketed as a 'convenient' design to hoist in the rigging of a small boat, is in fact a very bad design. Reflections from the separate elements cannot be in phase over more than a very small vertical angle, so they interfere destructively in most directions.

The 'face-up' attitude is unsuitable for a small sailing vessel, which is rarely on an even keel. In this case the best compromise is probably to mount the reflector with two points transverse to the fore-and-aft axis, and one edge parallel to it. With the vessel upright, the performance of the reflector is not optimum, but is much better than the 'point up' attitude. This improves as the vessel heels on either tack; at 36° of heel, the reflector is in the 'face-up' attitude.<sup>32</sup>

## Responder Beacons

A low-power transmitter-receiver system, which can be 'interrogated' by the marine radar transmission to 'respond' with a characteristic signal which will appear on the radar display, is used to identify certain seamarks. In Fig. 7 the Goeree Light Tower off the entrance to the Hook of Holland (at 12 o'clock in the photograph) is easily distinguished from the anchored ships by the periodic appearance of a long (4 mile) tail extending behind it. The frequency of the small transmitter (200 mW with 6 dB aerial gain) is swept across the marine frequency band of 9320-9500 MHz, co-operating sequentially with ships on all available frequencies. The signal appears on the display for about ten seconds every two minutes. In Fig. 3 a beacon undergoing trials, temporarily mounted in a launch, is responding with an identifying morse letter at 5 o'clock, 3 miles. The range performance of these devices is only limited by the radar horizon.<sup>28, 29</sup>

Other responder beacons have been developed and are in limited use, in which the response is on a frequency  $9310 \pm 10$  MHz. A separate receiver, or the radar receiver retuned, is needed to receive these signals, but there are advantages, such as the capacity for more information transfer without obscuring the radar picture.<sup>33</sup>

## References

1. 'International Meeting on Radio Aids to Marine Navigation', pp. 104-7 (H.M.S.O., London, 1946).
2. 'The Merchant Shipping (Radar) Rules 1976', issued by the Dept. of Trade. (H.M.S.O., London, 1976).
3. 'Marine Radar Performance Specification 1968', issued by the Dept. of Trade and Industry. (H.M.S.O., London, 1968).
4. Haeff, A. V., 'A memory tube', *Electronics*, 20, pp. 80-9, September 1947.
5. Kelly, T. J., 'Improvement in radar presentation', International Meeting on the Use of Radar at Sea, Genoa, Italy, 1957.
6. Manley, B. W., 'True motion in relative displays', *J. Inst. Navigation (G.B.)*, 15, No. 2, pp. 172-8, June 1962.
7. Parsons, S. R., 'The application of rapid access photographic techniques to radar display systems', *J. Brit. Instn Radio Engrs*, 24, No. 3, pp. 213-20, September 1962.
8. Watt, J. and Piercy, B. C., 'A new marine radar display system', *J. Inst. Navigation (G.B.)*, 22, No. 1, pp. 205-28, April 1969.
9. Harrison, A., 'A novel radar situation display', *The Radio and Electronic Engineer*, 44, No. 10, pp. 537-44, October 1974.
10. Ranby, P. W., 'An electro-luminescent image retaining panel', *Electrical Review*, 174, No. 13, pp. 474-8, 27th March 1964.
11. Shuffleton, W. N. and Evans, N. G., 'A critical evaluation of an experimental collision avoidance system', International Conference on Advances in Marine Navigational Aids. 1972. (IEE Conference Publication No. 87, pp. 117-23.)
12. Gasparini, O., Grassot, G. and Pardini, S., 'A smoothing logic with high precision in velocity for naval collision avoidance', *ibid.*, pp. 81-6.
13. Harrison, A., 'The risk of error in predicted c.p.a.', *ibid.*, pp. 75-80.
14. Gustafson, B. G. and As, B. O., 'System Properties of Jumping Frequency Radars', Svenska A. B. Philips, Stockholm, 1965.
15. Whipps, S. L., 'The Advantages to be Gained by Positioning the Master Gyro Compass Unit at the Roll Centre of a V.L.C.C.' Unpublished internal memorandum. Kelvin Hughes, 1971.
16. Harrison, A., Herther, J. C. and Wylie, F. J. Correspondence on 'Automatic plotting radars' in *J. Inst. Navigation (G.B.)*, 27, Nos. 1, 2, 3, pp. 111-5, 218-70, 298-304, 1974; 28, No. 3, pp. 363-8, 1975; 29, No. 1, pp. 94-5, 1976.
17. Riggs, R. F., 'The effects of sensor errors in certain marine collision avoidance and threat assessment systems', *Navigation (J.U.S. Inst. Navigation)*, 21, No. 1, pp. 16-34, 1974.
18. Jones, K. D., Perkins, C. S. and Butt, J. A., 'Automatic plotting radars', *J. Inst. Navigation*, 29, pp. 232-53, 1976.
19. Harrison, A., 'Methods of distinguishing sea targets from clutter on a civil marine radar', *The Radio and Electronic Engineer*, 27, No. 4, pp. 261-75, April 1964.
20. Schönfeld, W. H., Müller, V. and Schwarz, K. O., 'Stand der Möglichkeiten zur Verminderung der durch Seegangechos bedingten Störung des Radarschirmbildes von Schiffsradaranlagen', *Ortung und Navigation*, 100, No. 11, p. A2, 1968.
21. Shearston, C. R. and Croney, J., 'Measurements of Sea Clutter Amplitude on an X-Band Civil Marine Radar by a Statistical Method', A.S.R.E. Technical Note IX-53-2. 1953.
22. Rivers, W. K., *et al.*, 'Airborne Search Radar Design Study', p. 137. Institute of Technology. Atlanta, Georgia, U.S.A. 1969.
23. Croney, J., 'Clutter on radar displays', *Wireless Engineer*, 83, No. 4, pp. 81-91, April 1956.
24. Croney, J., 'Improved radar visibility of small targets in clutter', *The Radio and Electronic Engineer*, 32, No. 3, pp. 135-48, September 1966.
25. Wylie, F. J., 'The Use of Radar at Sea', p. 64 (Hollis and Carter, London, 1952).
26. Nathanson, F. E., 'Radar Design Principles', p. 167 (McGraw-Hill, New York, 1969).
27. Hogben, H. E., *et al.*, 'Radar Reflectors for Marine Navigation', Fig. 11. ASRE Monograph No. 833, 1948.
28. Harrison, A., 'Radar beacons for use with civil marine radar', *I.A.L.A. Bull.*, 26, p. 11, October 1965.

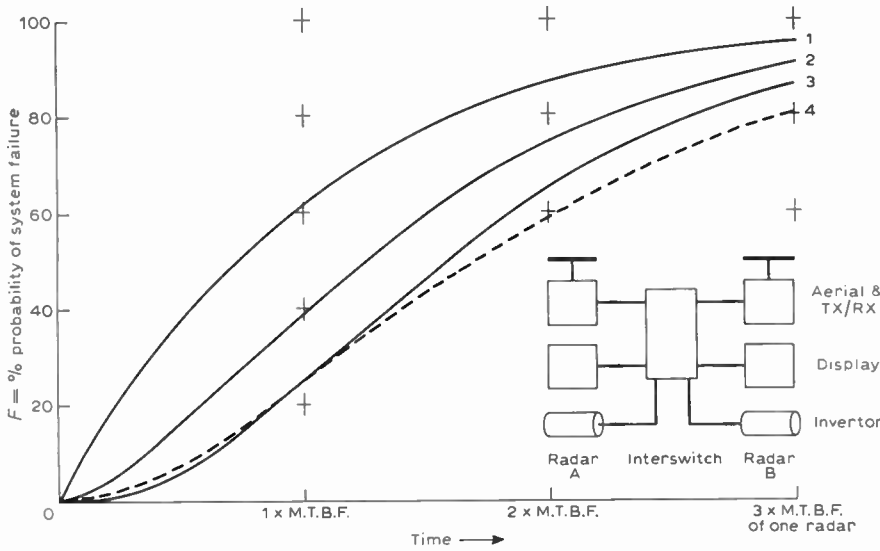


Fig. 8. Relative reliability of multiple and interswitched radars. See Appendix for calculation.

- Graph 1. One independent radar.
- Graph 2. Two independent radars.
- Graph 3. Three independent radars.
- Graph 4. Two interswitched radars.

29. Harrison, A., 'Responder beacons for marine use'. International Marine and Shipping Conference, Group 6, p. 12, 1973.
30. Croney, J., Woroncow, A. and Gladman, B. R., 'Further observations of small targets in sea clutter', *The Radio and Electronic Engineer*, 43, No. 3, pp. 105-15, March 1975.
31. Croney, J. and Woroncow, A., 'Dependence of sea clutter decorrelation improvements upon wave height', IEE Conference Publication No. 87, 'Advances in Marine Navigational Aids', London, July 1972.
32. Harrison, A., 'The use of radar reflectors and transponders by sailing craft', *J. Inst. Navigation (G.B.)*, 30, No. 3, 1977. (To be published.)
33. 'Marine s.s.b. for rescue service', *The Radio and Electronic Engineer*, 46, No. 1, p. 47, January 1976.

**APPENDIX**

**Reliability comparison of multiple independent versus interswitched radars**

Let the unit of time be the m.t.b.f. for one radar. (See Fig. 8).

Let  $S$  = probability of success,  $F$  = probability of failure.  
 $F + S = 1$ .

At time  $t$  units:

For ONE independent radar

$S_1 = e^{-t}$     $F_1 = 1 - e^{-t}$    Graph 1

For TWO independent radars

$F_2 = F_1^2$    Graph 2

For THREE independent radars

$F_3 = F_1^3$    Graph 3

The maintenance records for one particular radar set are typical, and show that faults are distributed between the units in the proportion:

Transmitter-receiver and aerial	0.5
Display	0.4
Invertor	0.1
Interswitch unit	almost 0

For the interswitch unit

probability of success =  $e^{-0}$  approx. = 1

For the transmitter-receiver and aerial

probability of success of one unit =  $e^{-0.5t}$   
 probability of failure of one unit =  $1 - e^{-0.5t}$   
 probability of failure of two units =  $(1 - e^{-0.5t})^2$   
 probability of success of two units (one or both) =  $[1 - (1 - e^{-0.5t})^2]$

A similar expression can be obtained for the display and the invertor.

The probability of success of the complete system is equal to the product of the probabilities of success of its separate sections.

Hence for two interswitched radars:

$S_4 = [1 - (1 - e^{-0.5t})^2]. [1 - (1 - e^{-0.4t})^2]. [1 - (1 - e^{-0.1t})^2]. [1]$

and  $F_4 = 1 - S_4$    Graph 4

Manuscript received by the Institution on 1st November 1976. (Paper No. 1763/AMMS 79).

# IERE News and Commentary

## World Energy Lecture

The Fellowship of Engineering has arranged a Joint Meeting with The Royal Society on Wednesday, 25th May 1977, at 5.30 p.m., at 6 Carlton House Terrace, London S.W.1, when a Review Lecture on 'World energy prospects to the year 2000' will be given by Professor C. L. Wilson. Professor Wilson is Director of the Workshop on Alternative Energy Strategies at the Massachusetts Institute of Technology. Members wishing to attend are asked to inform the Executive Secretary of The Royal Society at 6 Carlton House Terrace (Telephone 01-839 5561, ext. 278).

## Queen's Silver Jubilee Prize

The Council of the Institution has founded a Prize to commemorate the Silver Jubilee of Her Majesty Queen Elizabeth II. It will be given for an outstanding innovation or development in electronic engineering which has provided economic and social benefit.

The prize will take the form of a silver plaque and an illuminated citation and it will be restricted to United Kingdom and Commonwealth individuals or organizations.

Members of the Institution are invited by the Council to apply on their own account or to make recommendations of individuals or organizations for the prize. All nominations should be accompanied by a brief description (up to 200 words) of the work which is being put forward for consideration. Please send nominations by not later than 31st May 1977 to the Institution, marked for the attention of the Secretary of the Silver Jubilee Prize Committee (Mr. F. W. Sharp), from whom further details may be obtained. It is intended to make the announcement of the first Prize at the Annual General Meeting in London on 5th October 1977.

## Personal Services for Engineers

Professional engineers may take advantage of a range of services including trade buying and personal discounts through an organization sponsored by the United Kingdom Association of Professional Engineers and approved by CEI. Known as Professional Engineers Services, it also gives assistance with UK and World patent applications, provides industrial purchasing information and arranges preferential mortgages and car insurance, as well as holiday home exchanges. An insurance scheme for engineer's defence costs in the event of prosecution under the Health and Safety at Work Act is a further facility. Further details may be obtained from: Mr. M. Cleary, C.Eng., Secretary, Profes-

sional Engineers Services, 100-104 King Street, Maidstone, Kent.

## New Section in Hong Kong

Approval has been given by Council to the formation of a Local Section of the Institution in Hong Kong. An enthusiastic group of Corporate Members petitioned Council under the guidance of Mr. John Powell (Vice President) who has visited the Colony on business several times recently and was able to assure Council of the need and measure of support for a Local Section. Members are currently meeting under the provisional chairmanship of Mr. Norman Wheatley (Fellow). Information on the Section and its proposed activities may be obtained from Mr. Wheatley whose address is: Cable & Wireless Ltd., P.O. Box 597, Hong Kong (business), or 49 Deepwater Bay Road, Hong Kong (home).

## Professional Engineers' Contribution to Industry

A project aimed at assisting Britain's industrial performance by investigating the contribution made by professional level engineers to manufacturing industry is to be undertaken under the auspices of the British Association for the Advancement of Science, with full backing from the government, industry and the scientific world. The objective of the project is to recommend action to be taken in the education, recruitment and deployment of engineers to improve the performance of the British manufacturing industry and, in particular, the effectiveness of production management.

The inquiry will be conducted by a specially recruited, full-time team based at the University of Aston in Birmingham. The theme has arisen out of discussions between the British Association, the Royal Society and the National Economic Development Office during which it was emphasized that the engineer plays a leading part in determining the technical competitiveness of manufacturing industry. Consultations with senior officials in government departments, including the Central Policy Review Staff, as well as industry, the Council of Engineering Institutions and other interested parties, have ensured the widest possible backing from all quarters.

Extensive information relevant to the project is already held by government departments, industry, the CBI, joint bodies such as the Engineering Industry Training Board and the engineering profession itself. This knowledge will be made available to the project team, together with informed comment and suggestions for action. Co-operation has already been confirmed from the Departments of Industry and Education and Science as well as the Manpower Services Commission, the National Economic Development Office, the Council of Engineering Institutions, the Schools Council, the TUC, the CBI and a number of individual companies.

A British Association Co-ordinating Group has been formed to launch and monitor the project; it consists of representatives of all the above bodies and substantial representation of the major British companies and nationalized industry. Detailed control will be exercised by a Management Committee under the chairmanship of Sir Ieuan Maddock of the Department of Industry. The total cost of the project is expected to be approximately £36,000 of which £18,000 has been provided by three government departments—Industry, Education and Science, and the Manpower Services Commission. The remainder has been raised by contributions from industry and private enterprise.

The project team itself will operate under the direction of the Vice-Chancellor of Aston University, Dr. J. A. Pope, who, as well as having interests in industry, is also the General

Treasurer of the British Association. The resulting report will be published in July 1977 so that public discussion of the findings can culminate in an informed debate at the British Association Annual Meeting which is being held at the University of Aston in Birmingham in September.

### Practice 'Slow Morse' Transmissions

In the belief that even in these days of high speed typewriters there are members who have an interest, professional or otherwise, in sending and receiving Morse code, we published in the November Journal details of proficiency tests broadcast by the Royal Naval Amateur Radio Society. These lead to proficiency certificates for speeds between 15 and 40 words per minute.

The Royal Air Force Amateur Radio Society has now provided details of practice 'Slow Morse' transmissions every Monday to Friday evening, which should enable the RNARS tests to be embarked upon with confidence! Transmissions commence at 5 words/min, followed by a practice at 12 words/min over a total period of approximately half an hour. The callsign is G3RAF on frequencies 1920 kHz and 145.225 MHz, all on mode A2.

Further information about the Royal Air Force Amateur Radio Society and 'Slow Morse' transmissions may be obtained by writing to the Admin. Secretary, RAFARS Headquarters, No. 1 Radio School, Royal Air Force Locking, Avon BS24 7AA. (Telephone Banwell 2131, ext. 218.)

### New CEI Statement on Academic Requirements

CEI has published a new statement (No. 12), which defines its future policy in respect of the Academic Requirements for Registration as a Chartered Engineer. Statement No. 7 which was the first comprehensive statement of this policy is now withdrawn. Unfortunately, this leaves a temporarily untidy situation, since Statement No. 10, which duplicates some of the information given in Statement No. 7, will remain in circulation until the Part 2 examination syllabus has been revised. Revision was due in 1978 but seems likely to be at least a year late.

The major change resulting from the introduction of the new Statement is that recognition of degrees in the disciplines specified in Statement No. 7 will no longer be automatic. This will not materially change the situation in respect of recognition of the degrees in engineering awarded by UK universities and the CNAA, but may lead to the taking of a somewhat harder line in respect of degrees in what the Statement calls 'allied disciplines'. Where degrees awarded by Universities overseas are concerned, there will be no general recognition in future: every application involving such degrees will be assessed individually. This again will make no significant difference to the applicants' chances of acceptance: the main reason for the change is to put an end to the anomalies existing at present.

Copies of CEI Statement No. 12 can be obtained either from the Institution or from CEI, 2 Little Smith Street, London SW1P 3DL, price 35p post free.

### Association of Learned and Professional Society Publishers

At the General Assembly of the Association of Learned and Professional Society Publishers held in London on 19th January 1977, Mr. F. W. Sharp, IERE Editor, was elected as one of the four ordinary members of the ALPSP Council for a two-year term. Also elected at the Assembly were Mr. W. G. Askew, IEE Director of Publishing, as Chairman and

Dr. K. Paulus of the Institute of Physics as a member of Council; other officers and members were representatives of societies in the chemical and medical fields.

ALPSP was formed in 1972 and has at present 50 members, including 11 Institutions who belong to CEI and several belonging to other Sections of the Engineers Registration Board. Its objectives are to protect the collective and individual publishing interest of member organizations; to further the development of the publishing activities of British professional and learned societies and the flow of their publications both within and without the United Kingdom; to provide a facility for the exchange of ideas relating to professional and learned societies' publishing activities; and to represent the collective views of member organizations to appropriate bodies within the publishing field, to related trading bodies and to Government Departments and Agencies. Membership is open to learned or professional bodies which publish journals, books or similar publications.

### Channel Islands Group of Professional Engineers

The Institution supports the Channel Islands Group of Professional Engineers and any member resident there or visiting who wishes to attend meetings of the Group should contact the Honorary Secretary, Mr. S. A. Gothard, Tudor Lodge, Bagatelle, St. Saviour, Jersey, C.I.

### Standard Frequency Transmissions—February 1977

(Communication from the National Physical Laboratory)

February 1977	Relative Phase Readings in Microseconds NPL—Station (Readings at 1500 UT)		
	MSF 60 kHz	GBR 16 kHz	Droitwich 200 kHz
1	8.8	11.1	6.1
2	8.6	6.4	5.9
3	8.5	7.5	5.7
4	8.3	7.8	5.5
5	8.4	9.3	—
6	8.3	9.9	—
7	8.4	7.8	5.3
8	8.2	7.0	4.9
9	8.1	7.3	4.8
10	8.1	6.6	4.7
11	7.9	7.3	4.7
12	8.2	—	4.6
13	8.1	8.7	4.5
14	8.0	6.6	4.4
15	8.1	7.2	4.2
16	7.9	7.1	4.2
17	7.9	7.0	4.0
18	7.7	7.7	3.9
19	7.9	7.4	3.8
20	7.9	8.1	3.8
21	7.7	7.5	3.8
22	7.7	9.4	3.6
23	7.7	9.8	3.2
24	7.7	10.2	3.0
25	7.7	10.1	2.5
26	7.4	10.0	2.3
27	7.5	10.7	2.1
28	7.1	10.2	1.8

Notes: (a) Relative to UTC scale ( $UTC_{NPL-Station} = +10$  at 1500 UT, 1st January 1977).

(b) The convention followed is that a decrease in phase reading represents an increase in frequency.

(c) Phase differences may be converted to frequency differences by using fact that  $1 \mu s$  represents a frequency change of 1 part in  $10^{11}$  per day.

# Testability and Testing Technology

*Organized jointly by the Aerospace Maritime and Military Systems, and Electronics Production Technology Groups, and held in London on 7th December 1976,*

The Chairman, Brigadier R. Knowles introduced Sir Leonard Atkinson, a past President of the Institution, who in his opening address referred to the need for seeking improvements in testability in the interests of life-cycle costing, or terotechnology. To do this he suggested that Test Technology should be treated as a fundamental subject which provides specialist support to equipment designers by allowing the optimization of test facilities for production, in-use and maintenance purposes. The past practice of separating test and test equipment considerations from the main equipment design had often led to appreciable inadequacies in meeting overall testability requirements.

The first paper, entitled 'Philosophy of Maintenance', was presented by Col W. Baker (MOD). In this he stressed the Service customer's interest in testability and the contribution it could make in achieving the best compromise between equipment availability and life cycle costs. He reviewed the test criteria needed to support the various lines of servicing, ranging from replacement of major assemblies at unit level down to detail repairs at base workshops and stressed the need for consultation between customer and designers in translating the Service Staff Requirement in the early stages of design. He emphasized the importance of identifying and catering for both the user aspects of testability and these required for production purposes. This dichotomy of interest between producer and user was highlighted during the discussion period.

The second paper 'Design for Testing' by Mr P. Thompson (Ferranti) looked at how attempts had been made to improve testability in equipments by considering this feature from the outset of product design. Although built-in-test was now a fairly common requisite of performance criteria, the general application of testability still had low priority. He went on to describe how test development engineers with specialist knowledge of test techniques and equipment, including ATE, could be brought into a design team so that circuits could be vetted and re-configured before finalization of the design if necessary to allow activation and interfacing for test purposes. There was understandably considerable reluctance to alter circuits to assist in testing after they had been proved to function adequately.

Penalties in terms of cost, weight, complexity and reliability that might offset the benefits of improved testability were discussed briefly. A final re-emphasis of the importance of the calibre of the test development engineer in successful

design involvement led to several questions on this point and others on design technique and management.

The next paper 'Testability and Testing Techniques', by F. Slater (Plessey), continued the theme of design for testability. He reiterated the need to design accessibility for test and diagnosis into products and to avoid allowing higher priority design criteria such as performance, size and reliability to crowd out consideration of testability.

Mr. Slater reviewed the hierarchy of product specification required design, acceptance and field testing and pointed out the need for a clear understanding in the allocation of limits which took account of performance required at the various phases, the related measurement uncertainties, and equipment ageing.

Looking at the role that training has to play, Mr. L. Hale (BAC) introduced the term 'programmed experience situations' in his paper entitled 'Training for Design and Testing'. He explained that by this means an attempt was made to speed up the experience process by placing staff in specific environments which force them to appreciate results of their own efforts that much quicker. Taking the chain of events on an engineering project from customer requirement through innovation, design and development, modelling, production engineering test, customer use and maintenance, an examination was made of the way improved efficiency could result from staff acquiring better knowledge of stages other than their own prime work areas. From these examples in implementing programmed experience situations were given, which when supplemented by organized 'state of the art' instruction sessions could be seen to go a long way towards providing the practical training requirements.

The training theme was continued in the next paper, 'Training and Technical Writing' by Mr. J. H. Brooks (BBC). However, here the emphasis was put on the need to consider testing and testability as part of a much broader picture. Options that had to be considered such as redundancy, centralized maintenance, acceptance of loss of service, automation, standardization, training for versatility or specialization all had an effect on testability requirements.

Other facets of training and providing information as influenced by staff skills and site criteria (ranging from a large resident complement with specialist terms down to unattended sites) were reviewed in the context of testability.

The final paper 'Achievement of Testability' by Mr. J. W. Anstead (Smiths Industries) looked initially at his company's approach to planning and the allocation of responsibilities within the design groups. He illustrated how organizational arrangements assisted in the preparations for meeting customer needs and the formulation of realistic cost estimates. He described how the allocation of test engineers to project teams enabled circuit lay-outs to be improved for test purposes and assistance could be given in documenting specifications.

Mr. Anstead finally referred to three documents which were being prepared by government and industry committees.

- (1) 'The Achievement of Testability in Electronic and Allied Equipment'—this is expected to be published by MOD (PE) in the near future.
- (2) A draft syllabus for teaching testability, under preparation by the Testing Education and Training Sub-group of the Electronic Engineering Association's ATE Working Party.
- (3) An explanatory brochure on Abbreviated Test Language for All Systems (ATLAS) also being prepared by the same sub-groups.

R. W. HILL

# Technical News

## **New Advanced Training College for IAL**

International Aeradio Limited (IAL) has purchased Bailbrook House, London Road West, Bath, and is to establish an advanced technical training college in the house and grounds. The new College will provide courses in a range of aviation and communications technical subjects such as air traffic control, radio navigation aids and communications systems. Students from the UK and overseas will attend and the company expects to open the College on October 1st.

There are currently two training establishments operated by IAL in England—the College of Air Traffic Services at Oxford Airport and the College of Radio Engineering at its Southall Headquarters. It is intended to transfer both of these colleges to the new establishment—the College of Radio Engineering in October next and the College of Air Traffic Services in 1978.

IAL is owned by thirty-two international airlines including British Airways and British Caledonian Airways. There are twenty subsidiaries and associates in the IAL Group which provide aviation and communication services in over fifty countries worldwide. The provision of technical training is an integral part of many of the company's contracts.

## **NPL Takes Over BCS Management**

Since the Department of Industry took over responsibility for the British Calibration Service from the Department of Prices and Consumer Protection on 1st November 1976, BCS has been brought under the management of the National Physical Laboratory, Teddington. The BCS is a national service which the British Government set up in 1966 to provide authenticated calibration of scientific instruments and other measuring devices.

Mr. A. E. Bailey, Superintendent, Division of Electrical Science at the Laboratory, has been appointed BCS Superintendent in addition to his present duties. This move is designed to strengthen links between NPL's measurement standards work and industry through BCS.

The Advisory Council on Calibration and Measurement, under its Chairman, Mr. R. H. C. Foxwell, advises the Secretary of State for Industry on the operation of the British Calibration Service and other matters. The following have been appointed members of the Council: Mr. D. H. Mallinson, Director, National Engineering Laboratory, East Kilbride, Glasgow; Dr. E. N. Eden, Head/Metrology, Quality Assurance and Standards Division, Department of Prices and Consumer Protection; Mr. D. G. Spickernell, Director (Technical), British Standards Institution.

New assessors to the Council are: Mr. P. Dean, Head of the D. of I. Research & Development Contractors Division and Mr. Bailey, replacing respectively Dr. Eden and Mr. J. D. Platt, former Director BCS.

## **Hewlett Packard Progress**

The UK subsidiary, Hewlett-Packard Ltd., of the well-known American electronics company reported a 49% increase in exports and a 32% increase in home sales for its

financial year ending in October 1976. Total sales for the year were over £36M. Largely as a result of the export achievements, after tax profits more than doubled to £2,651,000.

Announcing the results, Managing Director Dennis Taylor (Fellow) said that the export success was particularly pleasing with over 80% of the output of the South Queensferry plant going overseas. The main reason for the increased sales was strong demand for the specialized communications test instruments designed by the Company's R. & D. department. He pointed out that Hewlett-Packard's Scottish division was now at the top of the profitability league among the Company's 27 manufacturing plants throughout the world. Besides the USA and the UK there are HP plants in Brazil, France, Germany, Japan, Malaysia and Singapore. Working within HP's 'centre of excellence' policy, South Queensferry had established itself as the Corporation's chief source of communications test equipment.

The total sales of the American parent company for 1976 totalled \$1,111M and its overall expenditure on R. & D. was about 8% of this figure. While its UK subsidiary concentrates on instrumentation for communications, other parts of the Company cover products in the broad divisions of computer systems, composites, medical, calculators and analytical.

Established in Bedford in 1961, Hewlett-Packard Ltd. moved its main manufacturing plant to South Queensferry in 1972 and the Company's total work force has grown to a total of 1100. In 1969 the Microwave Link Analyser designed in the Scottish laboratories gained a Queen's Award for Technical Innovation.

## **Safety of Electrically Operated Laboratory Equipment**

The safety of electrically-operated laboratory equipment is a matter of vital importance to both users and manufacturers and the increasing use in all countries of imported apparatus makes it imperative that there should be internationally recognized standards. A special working party has been set up by the Scientific Instrument Manufacturers' Association of Great Britain (SIMA) and has been considering equipment used in all types of laboratories—industrial, research, educational and medical (but not those for use either attached to or in the environment of a patient).

The SIMA text was submitted for consideration by Working Group 5 (Laboratory Equipment) of the International Electrotechnical Commission (IEC) SC 62D and the IEC Central Office in Geneva recently agreed to issue the draft to national standards committees with a view to obtaining early comments. The BSI now have this document available for public comment and consideration by the national committee before subsequent submissions to the IEC. Copies are available from the British Standards Institution, 101 Pentonville Road, London N1 9ND and applications should quote Ref: 77/21060 DC. (£1 to Members of the BSI; £1.50 to non-members. Addressed labels must be included).

With the growing complexity of contemporary laboratory equipment and the increasing extent to which apparatus is used outside its country of origin, the safe operation of electrically operated units has become a matter of urgent importance; additionally, of course, it is now necessary to consider the implications of the Health and Safety at Work etc. Act (1974) and other similar laws on the subject in many countries. The issue of this draft document for comment is therefore extremely significant and all those who may have a valid contribution to make are requested to avail themselves of the opportunity offered before final agreement is reached and an International Standard is issued. Designers, manufacturers and users alike are equally concerned at this stage and comments will be welcomed.

**Mr. R. L. Heather** (Graduate 1969) who was previously Service Manager with Micro Consultants Ltd., Reading, is now Senior Systems Engineer with EASAMS Ltd., Camberley.

**Mr. C. D. Hinds, B.Sc.** (Graduate 1969) has been appointed Production Manager of Avel-Lindberg Ltd. and Cotswold Electronics Ltd., and will be mainly concerned with the reorganization of the manufacture of toroidal transformers. Mr. Hinds has served for most of his professional career with the RAF, which he joined in 1963 as an engineering cadet, retiring last year in the rank of Squadron Leader.

**Major R. M. A. Jay, B.Sc. (Eng.) REME** (Graduate 1971) has transferred from 7 Maintenance Advisory Group REME, where he was Officer Commanding, to become Force Electrical and Mechanical Engineer with 6 Field Force, at Aldershot, Hants.

**Mr. H. A. Johnson** (Graduate 1974) who is with Post Office Communications, Cardiff, has been promoted to Assistant Executive Engineer.

**W.O. N. W. S. Maddex, RAF** (Graduate 1971) has been posted from ACE COMSEC, CANDE, where he was N.C.O. in charge of Radiation Survey, to be W.O. in charge of Support Flight, RAF North Coates, Grimsby.

**Mr. D. F. Mason** (Graduate 1971) is now Chief Industrial Engineer with Tannoy Products Ltd., High Wycombe.

**Mr. U. K. Munasinghe** (Graduate 1973) is now a Regional Telecommunication Engineer with the Post and Telecommunication Department in Kandy, Sri Lanka.

**M. F. U. Ogu** (Graduate 1970) is a Telecommunications Supervisory Engineer with Shell-BP in Port Harcourt, Nigeria, and has responsibility for all the flow-stations' telecommunications in the swamp area of the Company's Eastern Nigeria operation.

**Mr. H. J. Revell, B.A.** (Graduate 1967) has left the UK and taken up an appointment in Australia as Project Engineer with Delairco ML Engineering Pty. Ltd. in Sydney. He was previously Assistant, Design and Test (Signalling) with the Leeds Divisional Signal and Telecommunication Engineer's Office, British Rail.

**Mrs. S. R. Roome, B.Sc.** (Graduate 1975) who joined Hawker Siddeley Ltd. in 1976 as Assistant Avionics Engineer at Dunsfold Aerodrome, has been appointed Systems Programmer with Real Time Developments Ltd., Odiham, Hants.

**Mr. B. M. Stephens** (Graduate 1967) has moved from Plessey Radar, Weybridge, where he has been a Senior Technical Author since 1966, to EMI Electronics, Feltham, where he has taken up a post as Engineer/Author.

**Major D. P. Herring, R. Sigs.** (Associate Member 1973, Associate 1958) has been appointed to the position of Staff Officer responsible for Telecommunications and Signal Works Services on the Joint Service Signal Staff, Hong Kong. During the last six years he has been serving with the 30th Signal Regiment at Blandford Camp, Dorset, with responsibility for the project engineering, design and specifications for civilian type microwave systems for use by the armed forces.

**Mr. M. Jamil** (Associate Member 1973, Associate 1971) is now an Inspector in the Standard Calibration Laboratory of Saudi Arabian Airlines, which he joined in 1973.

**Sgt. A. H. Lee, RMAF** (Associate Member 1974) has been promoted from NCO in charge, Air Radio Servicing Flight, RMAF Base, Kuala Lumpur, to be Senior NCO in charge, Research and Investigation Project Team, Ministry of Defence, Kuala Lumpur, Malaysia.

**Mr. G. J. Rees** (Associate Member 1976) has completed his service with the Royal Navy as Electronics Technician and is now an Electronics Engineer with Seer TV Surveys Ltd., Old Woking, Surrey.

**Mr. B. A. Shoemith** (Associate Member 1974), previously an Instructor with the Advanced Electronic Squadron at RAF Cosford, has been transferred on promotion to be Production and Planning Supervisor for Service Radio Installation Modifications at RAF Wyton, Huntingdon.

**Mr. Avtar Singh** (Associate Member 1973, Associate 1970) has been appointed Managing Director of Sangtronic, Staines, Middlesex.

**Flt. Lt. G. S. Clark, RAF** (Associate 1970) who was previously Officer Commanding Supply Control and Accounting Flight, RAF Uxbridge, is now Supply 4B2, Headquarters Strike Command, RAF High Wycombe.

**Mr. H. D. Read** (Associate 1965) who was previously an Electronic Design Engineer with Westland Aircraft Ltd., Yeovil, has taken up a post as Electronic Installation Engineer with the Molins Machine Company, London.

## Obituary

The Institution has learned with regret of the deaths during recent months of the following members:

**Philip Herbert Francis George** (Fellow 1944, Member 1926) died in Durban on 10th November 1976, four weeks before his 81st birthday. He leaves a widow.

Born and educated in London at Alleyn's School, Philip George studied at the Regent Street Polytechnic School of Engineering, obtaining the Polytechnic's Diploma with distinctions in five subjects in 1913. He worked for two years with the General Electric Company as a Technical Assistant and in 1915 joined the Royal Flying Corps and was subsequently commissioned in the Royal Air Force. In 1920 he returned to GEC at the Osram Valve Works, but in 1921 he took up an appointment as Radio Engineer with the Brunei Government.

He was to spend nearly all his working life in the Far East, first in Borneo until 1926, and then in the Malaya Post and Telegraphs Administration. He served this body

as a Radio Engineer, rising to the rank of Director of the Telecommunications Department. In this post he was responsible for the development and maintenance of all radio services of the Department, including broadcasting stations, for the telecommunication services in control of civil aviation, the meteorological services, and the police radio services. He escaped from Singapore in 1942 and during the next two years worked first in Johannesburg and then in London, before being recalled to Malaya in 1944 to take charge of the planning of telecommunications for the reoccupation of Malaya. He retired to live in South Africa in 1948.

**Edwin John Godfrey Lewis** (Fellow 1942) died on 15th February 1977, aged 73 years. He leaves a widow, and a son and two daughters from his first marriage.

'Ted' Lewis was born and educated in Ealing, Middlesex, and after studying radio communications and gaining experience in

radio servicing, joined the Gramophone Company, Hayes, in 1929. For the next two years he prepared technical information on radio production, and later gave demonstrations of equipment throughout the country. From 1931 to 1932 he was a senior service engineer with EMI Service Ltd., and he then transferred to the Technical Information Division, being appointed Manager in 1934. Subsequently he became Manager of the Technical Information and Publications Division of EMI Sales and Service Ltd., and held a similar position within EMI following its reorganization, until ill-health caused his retirement in 1967.

Throughout his professional life Ted Lewis had a close interest and indeed involvement in technical education, particularly for the technician. He was for many years following its inception associated with Radio Trades Examination Board, both as a member of the Board as an IERE representative and of its Examina-

tions Committee, serving as chairman of the latter for several years, and he was himself an examiner. His work ideally equipped him to write, in 1935, a pioneer British book, 'Radio Receiver Servicing and Maintenance', which went into four editions and helped many thousands of technicians, both in the Services and in the radio industry and trade, through examination tests, and in their work. It was followed by the almost equally well-known 'Television Terms and Definitions' and 'Radio Servicing Equipment'.

His other major contribution to the Institution was active membership of the Programme and Papers Committee from 1951 to 1958.

**Gnanapragasam Manuelpillai Rajkumar** (Fellow 1973, Member 1966, Graduate 1952, Student 1945) has died in his 56th year.

Mr. Rajkumar joined the Post and Telecommunication Department of the Government of Ceylon in 1944 as a Technician working on carrier telephony, and during the years 1947 to 1951 he obtained City and Guilds Certificates and passed the Institution's Examination while working as an Inspector of Telecommunications. In 1963 he was promoted to Engineer, Radio and Transmission, subsequently being concerned with planning cable networks. Since 1968 he had been a Superintending Engineer, and latterly was Head of the Division concerned with maintenance, development and planning for radio, transmission and telegraphs. Among the more recent projects for which he was responsible was a police radio network for the whole of Sri Lanka covering 273 police stations and numerous mobiles in major towns using h.f., v.h.f. and u.h.f. and including teleprinter communication.

**John Whinfrey Ridgeway** (Fellow 1943) died on 13th February 1977, his 74th birthday. He leaves a widow.

Born in Sheffield, John Ridgeway studied metallurgy at Sheffield University and from 1919 to 1924 worked in the Electro-Metallurgical Research Department. He then joined the Sheffield Office of the Metropolitan Vickers Electrical Company as a radio engineer and in 1929 moved to London to become Assistant to the Chief Radio Engineer. When regrouping of the interests of companies with Associated Electrical Industries took place he was

appointed Assistant Manager of the Radio Division which was under the Edison Swan name. In 1940 he was appointed Manager of this Division and joined the Board of the Edison Swan Electric Company.

John Ridgeway took an active part in the industry's trade associations, serving the British Radio Valve Manufacturers' Association as chairman for 18 years – from 1942 to 1947 and 1949 to 1962. He was also a member of the Council of the Radio Manufacturers' Association (now BREMA) and of the Radio Industry Council. He was appointed an O.B.E. in 1946.

This Institution too has reason to recall the services of John Ridgeway. He was a member of the Professional Purposes Committee (now known as the Executive Committee) for several years and he was on the Finance Committee from 1944 to 1955, from 1945 to 1950 as chairman. He also served on the Membership Committee for a time and represented the Institution on the Radio Trades Examination Board in 1947. He was appointed for three complete terms as a member of the Council and was a Vice-President in 1950-51.

On the reorganization of AEI in 1962, Mr. Ridgeway took an early retirement and left the industry to farm very successfully some 350 acres at Buckfastleigh in Devon, until 1974 when he went to live in a village near Taunton, Somerset.

**Robert Richard Clark** (Member 1959, Associate 1946) died on 24th October 1976, at the age of 57. He leaves a widow and one daughter.

Mr. Clark was a Director on the main Board of the Brocks Group of Companies, and of its marine navigational aid company, Astaron Electronics Ltd., of Poole, Dorset; since 1968 he had been Managing and Technical Director of Electronic Laboratories Ltd., also at Poole.

**Lawrence George Frakes** (Member 1971) died in November 1976 at the age of 42. He leaves a widow.

Mr. Frakes began his career in 1953 as an NCO aircraft instrument fitter, and in 1956 joined the English Electric Company as an instrumentation technician. From 1959 to 1970 he was with Handley Page Ltd., latterly as Senior Development Engineer concerned with aircraft navigation aid instruments and automatic flight control system. In 1970 he moved to Hawker Siddeley Aviation Ltd., Manchester, as

Senior Avionics Engineer with similar responsibilities.

**Victor Ernest Plant** (Member 1964, Graduate 1963, Associate 1958) died on 29th October 1976 at the age of 61. He leaves a widow.

Mr. Plant had been a lecturer in mathematics and electrical subjects, including telecommunications, at Willesden Technical College, London, since 1957. During the war he served in the Royal Air Force Signals Branch, and on demobilization in 1946 started a small radio components company. It was during this time that he published a handbook on the home construction of radio receivers by the amateur.

**Leslie Nield Whitehead** (Member 1942, Associate 1941) died on 25th February 1977 at the age of 66, leaving a widow.

Mr. Whitehead obtained his training and early experience with Ferranti Ltd., Manchester, between 1925 and 1936, when he joined the British Broadcasting Corporation as a transmitter engineer at Moorside Edge, Yorkshire. He remained with the BBC until his retirement in 1971, having held posts as a senior engineer at various stations including Daventry and Brookman's Park, and the Holme Moss television transmitter.

**Robert Michael Wood** (Graduate 1963) died suddenly on 21st October 1976. He was 43 years old, and leaves a widow. After National Service in the Royal Corps of Signals, he joined the National Coal Board in 1955 as a Scientific Technical Officer.

**Henry Roy Parnell** (Associate 1960) died on 7th February 1977, aged 57, leaving a widow.

Mr. Parnell enlisted in the Royal Air Force in 1935 as apprentice wireless operator mechanic, and from the earliest days was concerned with radar development and calibration. After leaving the RAF he was for two years with BOAC as a radar engineer, and in 1948 he joined International Aeradio Ltd. Mr. Parnell held many instructor posts with IAL, working at Nairobi Civil Airport, Sharjah on the Persian Gulf, and as Chief Instructor to the Royal Pakistani Air Force in 1953. He was from 1956 to 1967 Technical Training Officer at the Company's school in London, and he then went abroad once more to Perth, Western Australia, and Bahrain, from where he returned to the United Kingdom shortly before his death.

*Members are invited to advise the Institution's Membership Department of new appointments whether or not these involve changes in postal address; it is helpful if these details are sent in using the form which is included at the back of most issues of the Journal. The information can then be considered for inclusion under the heading of 'Members' Appointments' unless it is stated that this is definitely not desired.*

*The co-operation of members in letting the Membership Department know of the deaths of colleagues who belong to the Institution would be appreciated in order that the despatch of journals and other communications can be stopped without delay and thus avoid further distress to their families.*

## Market Survey on the Integrated Circuit Industry

With the world market for Integrated Circuits likely to reach 9.7 billion dollars by 1985, an increasing number of Original Equipment Manufacturers will be tempted to start up their own i.s.i. production facilities. From the outset, states a new report from Mackintosh, these manufacturers must 'recognize clearly and unequivocally that, in purely financial terms, the move is very probably uneconomic'.

Another controversial recommendation from the report, entitled 'The Integrated Circuit Industry to 1985', insists that the new semiconductor subsidiary (or an OEM) 'should have an entirely independent management team... with an absolute right to decide in favour of the special interests of its division and against the general corporate needs if these are in conflict'.

Elsewhere the report goes on to define imminent areas of conflict between computer companies, minicomputer manufacturers and traditional i.c. suppliers, caused by the introduction of the revolutionary microprocessor.

The report, now available to all interested organizations,

is an abridged summary of the general conclusions reached in the major Semiconductor Survey recently completed by Mackintosh for the German Ministry of Research and Technology and co-sponsored by the European Commission and the governments of France, The Netherlands and the United Kingdom, to advise on their future support strategy for what is certain to be 'one of the most fundamental and important industrial technologies of the 1980s'.

The report identifies likely future trends in integrated circuit technologies, production methods, applications and markets. It also assesses the key strategic factors influencing success in the international i.c. industry, with evaluation of the importance of government support, industrial structure, vertical integration (upwards and downwards), market availability, entrepreneurial freedom and basic research programmes.

The report is available, price £295, from Mackintosh Publications Ltd., Victoria House, Victoria Street, Luton, England LU1 5DH.

## Applicants for Election and Transfer

THE MEMBERSHIP COMMITTEE at its meeting on 15th March 1977 recommended to the Council the election and transfer of the following candidates. In accordance with Bye-law 23, the Council has directed that the names of the following candidates shall be published under the grade of membership to which election or transfer is proposed by the Council. Any communication from Corporate Members concerning the proposed elections must be addressed by letter to the Secretary within twenty-eight days after publication of these details.

*Meeting: 15th March 1977 (Membership Approval List No. 232)*

### GREAT BRITAIN AND IRELAND

#### CORPORATE MEMBERS

##### Transfer from Graduate to Member

OWENS, David John. *Ipswich, Suffolk.*  
RAYMAN, Nanu. *London.*  
WATSON, Brian Richard. *Bracknell, Berkshire.*

##### Transfer from Student to Member

KOURRA, Louis. *London.*

##### Direct Election to Member

GARRETT, John. *Ipswich, Suffolk.*  
LORDAN, Frank Graham, *Tewkesbury, Gloucestershire.*

#### NON-CORPORATE MEMBERS

##### Transfer from Graduate to Associate Member

BURNS, John. *West Bromwich, West Midlands.*

##### Direct Election to Associate Member

GREEN, William Gerald. *Gosport, Hampshire.*  
HAMBLY, Anthony Patrick. *Plymouth, Devon.*

LINDFIELD, Terence James. *Mitcham, Surrey.*  
OIKU, Festus John. *Leeds, Yorkshire.*

#### STUDENTS REGISTERED

CHAN, Eddie Kam Hon. *Plymouth, Devon.*  
GEORGE, John Oladapo. *London.*  
ROSS, Ian Michael. *Southend-on-Sea, Essex.*

### OVERSEAS

#### CORPORATE MEMBERS

##### Transfer from Graduate to Member

STICKELLS, Nigel Brian. *St. Helena.*  
THYAGARAJAN, V. *Tiruchirappalli, India.*

##### Direct Election to Member

ARAWOLE, Roland Oladimeji. *Oshogbo, Nigeria.*  
LAU, Song Hee. *Penang, Malaysia.*  
MUIR, Donald Ross. *Auckland, New Zealand.*  
SALMASSI, Hartoun Grigorian. *Tehran, Iran.*  
TSE, Chun Cheong. *Hong Kong.*

#### NON-CORPORATE MEMBERS

##### Transfer from Student to Graduate

LIM, Pang Kit. *Gadong, Brunei.*

LUK, Leung Ping. *Hong Kong.*  
PAPADOPOULOS, Aristodemos. *Athens, Greece.*  
YIP, Wai Leung. *Hong Kong.*

##### Direct Election to Associate Member

ANG, Ban Sher. *Singapore.*  
JAMES, Walter Philip Mansel. *Salisbury, Rhodesia.*  
JOCELYN, Vance John. *Labatse, Botswana.*  
LEE, Kim Long. *Kuala Lumpur, Malaysia.*  
LEE, Sung Wah. *Singapore.*  
LOW, Hien Kiah. *Batu Pahat, Johore, Malaysia.*  
ODUMAH, Stephen Charles. *Benin City, Nigeria.*  
QUEK, Kok Ann. *Singapore.*

##### Transfer from Student to Associate

VAISHNAV, Pradyumna M. *Ahmedabad, India.*

#### STUDENTS REGISTERED

CHIN, Kuan Heong. *Penang, Malaysia.*  
LEE, Kah Leong. *Singapore.*  
LEE, Kuan Sin. *Singapore.*  
NG, Yan Yap. *Singapore.*

## FORTHCOMING INSTITUTION MEETINGS

*Tuesday, 10th May*

JOINT IEE/IERE/BES MEDICAL AND BIOLOGICAL  
ELECTRONICS GROUP

Physiology for Engineers—The Visual  
Cortex

By Dr. S. Zeki

Botany Lecture Theatre, University College  
London, 6 p.m.

*Tuesday, 24th May*

COMPONENTS AND CIRCUITS GROUP

Colloquium on PRINTED CIRCUIT  
WIRING

Royal Institution, Albemarle Street,  
London W1, 2 p.m.

Advance registration necessary. For  
further details and registration forms apply  
to Meetings Officer, IERE.

*Thursday, 26th May*

COMMUNICATIONS GROUP

A null steering antenna for mobile com-  
munications

By Professor D. E. N. Davies and Mrs. M.  
Rizk (*University College London*)

Manson Theatre, London School of  
Hygiene and Tropical Medicine, 6 p.m.